## ResearchOnline@JCU



This is the author-created version of the following work:

Levchenko, Igor, Mandhakini, Mohandas, Prasad, Karthika, Bazaka, Olha, Ivanova, Elena P., Jacob, Mohan V., Baranov, Oleg, Riccardi, Claudia, Roman, H. Eduardo, Xu, Shuyan, and Bazaka, Kateryna (2022) Functional Nanomaterials from Waste and Low-Value Natural Products: A Technological Approach Level. Advanced Materials Technologies, 7 (11).

Access to this file is available from:

https://researchonline.jcu.edu.au/75472/

© 2022 Wiley-VCH GmbH.

Please refer to the original source for the final version of this work:

https://doi.org/10.1002/admt.202101471

#### **REVIEW**

# Functional Nanomaterials from Waste and Low-Value Natural Products: A Technological Approach Level

Igor Levchenko<sup>1</sup>, M. Mandhakini<sup>2</sup>, Karthika Prasad<sup>3</sup>, Olha Bazaka<sup>4</sup>, Elena P. Ivanova<sup>4</sup>, Mohan V. Jacob<sup>5</sup>, Oleg Baranov<sup>6</sup>, Claudia Riccardi<sup>7</sup>, H. Eduardo Roman<sup>7</sup>, Shuyan Xu<sup>1</sup>, and Kateryna Bazaka<sup>3,5,8</sup>

- <sup>1</sup> Plasma Sources and Application Centre, NIE, Nanyang Technological University, 637616, Singapore
- <sup>2</sup> Center for Nanoscience and Technology, Anna University, Chennai, 600 025, India
- <sup>3</sup> School of Engineering, The Australian National University, Canberra, ACT 2601, Australia
- <sup>4</sup> School of Science, RMIT University, PO Box 2476, Melbourne, VIC 3001, Australia
- <sup>5</sup> Electronics Materials Lab, College of Science and Engineering, James Cook University, Townsville, QLD 4811, Australia
- <sup>6</sup> Jožef Stefan Institute, Ljubljana, Slovenia
- <sup>7</sup> Dipartimento di Fisica "Giuseppe Occhialini", Università degli Studi di Milano-Bicocca, Piazza della Scienza 3, I20126 Milan, Italy
- <sup>8</sup> Faculty of Engineering, Queensland University of Technology, Brisbane, QLD 4000, Australia

#### **Abstract**

Low and negative value (waste) products represent a valuable resource. Its use as an input source for the fabrication of high value materials represents a lucrative pathway to increase sustainability and decrease the economic cost for a wide range of industries. Thermochemical methods for the valorization of biowaste and low-value natural products are simple and cheap yet sufficiently efficient to deliver significant economic benefits to the biotechnological and agricultural sectors. High-value products that can be realised using thermochemical methods include carbon aerogels for energy storage, graphene oxide-based supercapacitors, keratin-urea nanocomposite fertilizers, and graphene-based nanomaterials for the photocatalytic dye degradation and environmental remediation. Plasma-based methods represent another family of technologies for waste-to-value conversion. Unlike thermal technologies that rely primarily on the surface processes, the nanostructure nucleation and growth in plasmas involve a complex set of physical and chemical processes that occur in bulk plasma and on substrate/nanostructure surfaces. Sustaining this set of processes requires the use of more complex pieces of equipment, and in return offer a greater level of control and complexity of materials that can be produced. The choice between these two types of technology should be done on the basis of a complex optimization that takes into account a whole set of factors, including (i) cost and availability of precursors for production at scale; (ii) initial outlay and operating cost of equipment, which, in case of plasmas, may be higher initially yet lower in the long run due to the absence of large hot furnaces and ability to initiate the process virtually immediately when the system is on; (iii) cost of labour that is typically higher for the plasma-based systems; (iv) cost of production engineering including the R&D efforts for designing the industrial technology, which is typically higher for the plasma-based systems, and so on. In this article, we present a technological level comparison of thermochemical and plasma-based techniques for valorization of raw and waste biomass, where the intent is to use the resulting products for the environmental remediation, energy storage, optoelectronics and biomedical applications.

#### 1. Introduction

Advanced functional nanocomposites, nanomaterials and complex hierarchical material systems  $^{[1-5]}$  are currently considered as the means to advance and in some instances even revolutionize energy conversion,  $^{[6-9]}$  sensors,  $^{[10-13]}$  biosensors,  $^{[14]}$  catalysis  $^{[15-18]}$  and photocatalysis,  $^{[19]}$  biotechnology,  $^{[20-23]}$  water purification,  $^{[24,25]}$  space exploration  $^{[26-29]}$  and nanomedicine.  $^{[30-33]}$  Various methods and techniques are currently under exploration to design cheap, environmentally friendly technologies for the mass production of functional nanocomposites and nanomaterials, with the total yield for e.g. silica reaching 1.5 million tons (**Table 1**) and rapidly growing.  $^{[34,35]}$  The

production of complex nanomaterials usually assumes the consumption of high quality feedstock materials and precursors and complex multi-step processing, both generally quite expensive. This considerably increases the retail price of nanomaterials, which can reach, *e.g.* 500 USD per 1 gram for graphene oxides, which are potential candidates for the supercapacitor production (see *e.g.* Sigma Aldrich<sup>[36]</sup>).

✓ Conversion of biowastes and low-value natural products into useful, high value nanomaterials and nanocomposites could potentially significantly reduce the price of these nanomaterials.

Many types of biowaste and low-value natural products are generated in vast amounts and thus represent a truly unlimited source of raw input material for nanotechnology. For example, close to 200 million tons of rice husk was produced in 2018 alone, and the production of valuable nanomaterials from the husk has already been demonstrated. The global yearly waste of food accounts for 1.3 billion tons which could be a practically unlimited supply of raw material for nanomaterial production. Virtually any biowaste and plant material could be successfully used for nanomaterial production and the type of nanostructures are not limited to carbon-based materials. For example, waste thyme (*Thymus vulgaris L.*) was used for the production of ZnO nanoparticles.

✓ Conversion of biowastes en masse to desirable nanocomposites could also significantly reduce the ecological load of many industries and could contribute to environmental remediation by reducing waste that goes into landfill. Indeed, "waste is not waste until we waste it".

**Table 1.** Global consumption of several types of engineered nanomaterials of high importance. Data from *Waste Manag.* **2018.**<sup>[45]</sup> With the consumption reaching significant numbers, production of nanomaterials from waste and low-value materials becomes a very important avenue to reduce their cost and impact on the environment. \* Mass production of fullerenes 60 was estimated from global fullerene market estimation of USD 487.9 Million in 2020, <sup>[46]</sup> and price of about USD 280 per 1 gram.

Engineered nanomaterial	Global consumption, t/a
Silica (SiO <sub>2</sub> )	1.5 million
Other oxide nanomaterials	>15,000
Titania (TiO <sub>2</sub> )	10 million
Zirconium dioxide (ZrO <sub>2</sub> )	2500–3000
Carbon panetubos	Tubes: 200–250,
Carbon nanotubes	Fibers: 300–350
Fullerenes*	≈ 2
Zinc oxides	>1000
$CeO_2$	10
Alumina (Al <sub>2</sub> O <sub>3</sub> )	0.2 million
Iron oxides and zerovalent iron	100
Silver (Ag)	22
Gold (Au)	0.004
Global demand in nanomaterials, 2013	\$3.6 billion <sup>[47]</sup>
Global demand in nanomaterials, 2025	\$34 billion <sup>[47]</sup>

However, the success of this waste-to-value concept relies heavily on the availability of conversion techniques capable of taking a multi-component, chemically variable bulk source and transforming it into a high-quality material with controlled structure and properties at nano-, micro- and macro-scales. Importantly, to be viable, these conversion techniques should be able to achieve this goal without consuming significant energy or labour resources, or using processes that are too complex or difficult to integrate. Some waste materials are particularly difficult to valorise. For instance, feather and bone waste represent a rich source of microelements, such as sulphur and of nitrogen. At the same time, they are difficult to degrade in the landfill, remaining in the environment for a considerable period of time. As such, they are ideal candidates for the waste-to-value valorisation. However, the disulphide bond present in the structure of feathers makes their break-down into keratin a challenge. Similarly challenging is the efficient fractionation and extraction of the usable forms of cellulose, hemicellulose, lignin and extractives from *e.g.* saw dust and sugarcane bagasse, and their subsequent conversion into value-added products. While there exist many examples of successful application of existing technologies for the synthesis of functional nanomaterials from a broad range of naturally derived precursors, [48,49] many of these methods may not necessarily be viable at scale given their complexity, and considerable energy, time and resource consumption [50,51] (Figure 1).

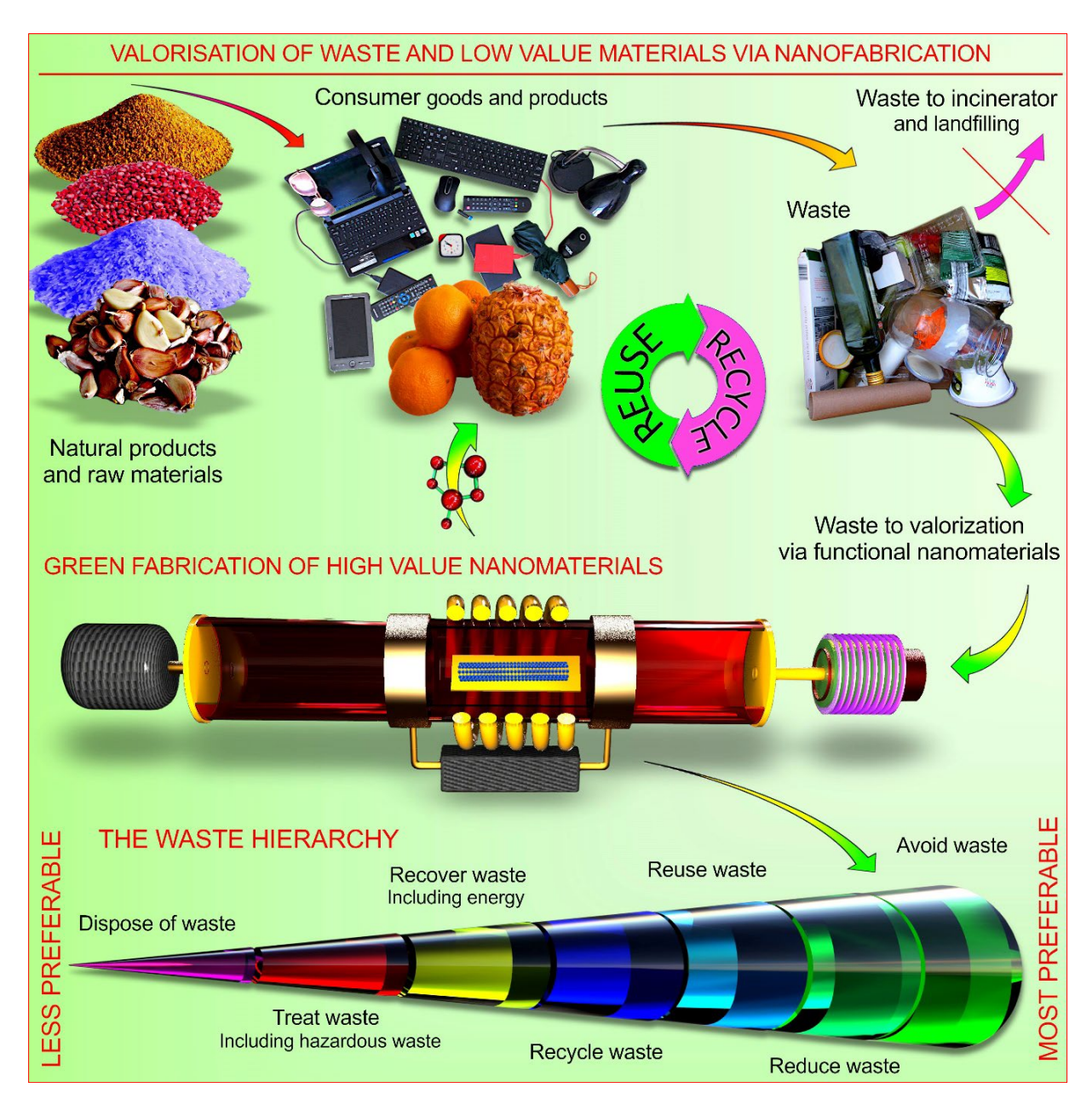


**Figure 1**. Valorisation of waste and low value materials via nanofabrication. Waste from numerous industrial processes, as well as from electric, electronic and plastic consumer industries can be viewed as valuable input materials that can be transformed into high value engineered nanomaterials. By consuming waste products, and producing materials that could directly (*e.g.* adsorption of oil spills or photodegradation of dyes) or indirectly (*e.g.* light-driven energy generation and storage) aid environmental remediation, the waste-to-value paradigm can substantially reduce the environmental impact of our society while preserving its quality of life. Disruption of the traditional end-of-life waste management by means of introducing innovative nanofabrication processes that prevent waste from ever reaching the landfill will bring us one step closer towards closing the sustainable life-cycle loop.

Among currently available technological approaches that could be implemented in biowaste valorization, two groups that feature quite different physical and chemical processes stand out: thermochemical techniques <sup>[48,52]</sup> and plasma-based techniques. <sup>[53-55]</sup> While thermochemical techniques utilize high temperatures as the main process driver, the plasma technology utilizes electricity-driven processes. <sup>[56-58]</sup>

Taking these two features into account, it appears quite natural to consider in detail and with practically applicable examples the traditional thermal (thermochemical) and the plasma-based approaches. Both of them feature a common denominator managing the nanomaterial synthesis process, that is, the *precursors in the gas or liquid phase*. In fact, both thermal and plasma synthesis processes are conducted via precursors either in the liquid or in the gas phase. Along with this common feature, these two approaches are different in the term of the principal process environment, i.e. plasma-based techniques in a large extent are based on bulk processes while thermochemical techniques are mostly surface-based (**Figure 2**).

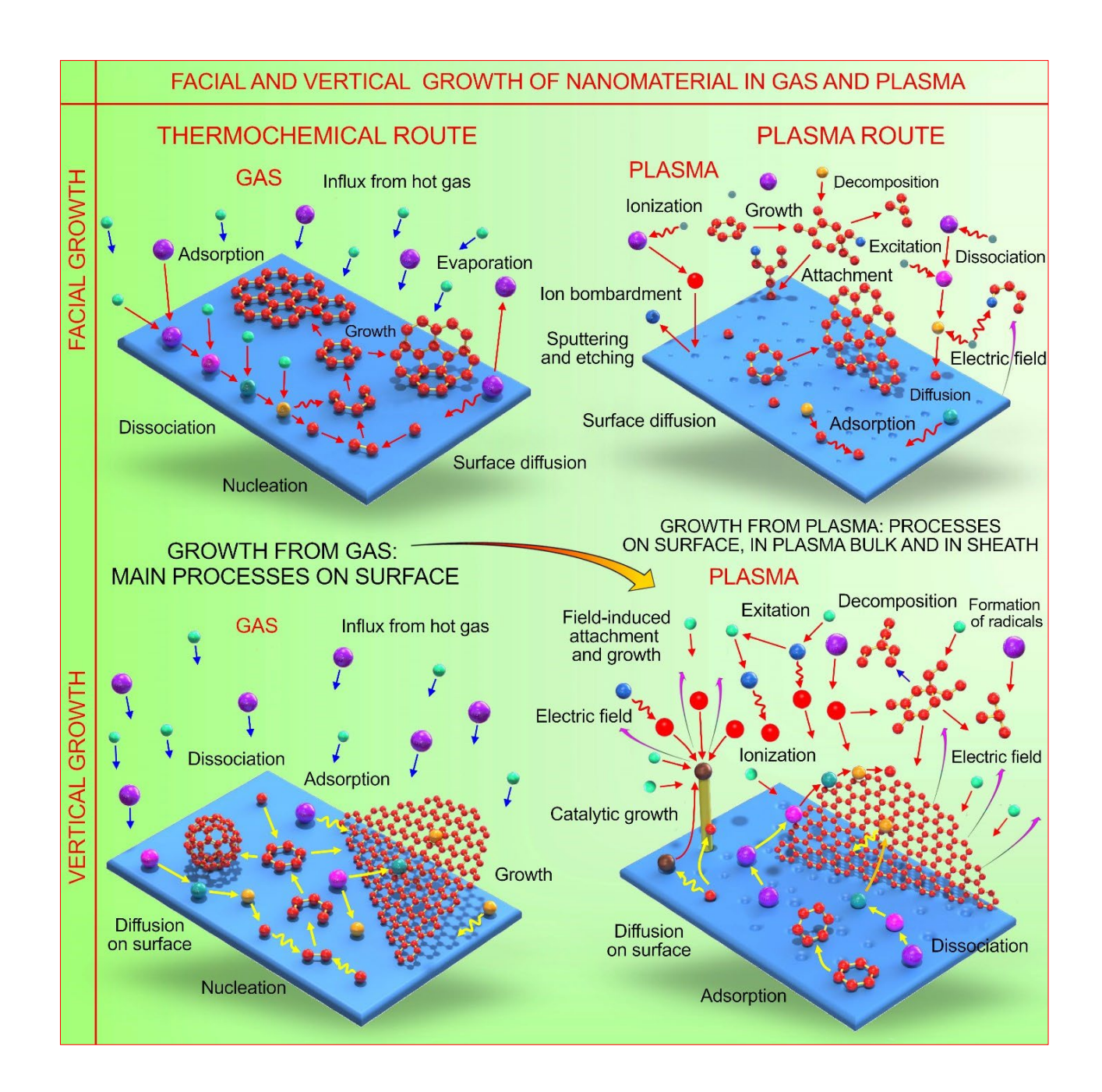


**Figure 2**. A comparison of processes that take place in the proximity of and on the surface of the substrate during thermal and plasma-based surface growth of nanostructures. Processes during the growth of nanostructures on surface and growth of vertical nanoflake in thermochemical (a,b) and plasma (c,d) environments. Thermal route involves mainly surface-localized chemical and physical processes and reactions, while the plasma-based technology includes a very complex set of processes in plasma such as ionization, ion acceleration by electric field, re-distribution of ion fluxes by near-surface electric field in plasma-surface sheath, charging the plasma-immersed surfaces and many others.

✓ In this article, we present a technological approach level overview and comparison of thermochemical and plasma-based techniques and methods for valorization of natural wastes and low-value natural products where the use of waste minimises the impact from conventional industries and achieves environmental remediation by reducing waste that enters the ecosystem.

The remainder of this paper is organized as follows. In **Section 2** we briefly compare the processes that occur in plasma-based and thermal methods used for nanosynthesis; in **Section 3** we outline several typical thermal methods for biowaste-nanomaterial conversion, and in **Section 4** we outline the several typical plasma-based methods for biowaste-nanomaterial conversion; then, in **Section 5** we discuss the challenge of selecting the right tool for the task; and finally, outlook and perspectives are outlined in **Section 6**.

#### 2. Plasma and thermal methods for nanosynthesis – a general comparison

Biowaste and natural resource valorization through their conversion to functional nanostructures and nanomaterials entails a complex set of requirements and the use of processes that at times may be difficult to realise within a single processing environment due to their vastly differing characteristics and needs. [59-61] Fabrication of nanomaterials usually presumes a complex set of physical and chemical reactions which are difficult to realize within the framework of relatively simple, cheap technologies.

✓ This is why it is important to examine and compare some representative examples of successful processes that are flexible and have the capacity to be upscaled in the future to enable valorization of biowaste and low value natural products en masse, particularly where the quality and performance of the resulting nanomaterials is high.

To ensure large-scale low-cost production of value-add nanomaterials from low- and negative-value precursors, two parameters are of particular importance: *flexibility and adaptivity, i.e.* the ease with which the process can evolve to accommodate scale up production of high-quality products from different input sources, and *energy consumption* which directly relates to the final cost of the product.

Flexibility and adaptivity. When compared to other techniques, plasma-based methods are characterised by a very high flexibility and adaptivity of the process, [62] while thermochemical methods may be simpler and cheaper, requiring less complex equipment and control means. [63,64] In general, thermal processes involve mainly surface-localized chemical and physical processes and reactions while the plasma-based technology includes also a very complex set of processes in plasma [65,66] (ionization, [67] acceleration of ions by electric fields, [68] re-distribution of ion fluxes by near-surface electric fields, [69] charging the plasma-immersed surfaces via electron fluxes [70] and many others [71]). Figure 2 presents a comparison of the processes near the surface during material synthesis using thermal and plasma-based technologies. As a result of the presence of both surface and bulk processes in plasma, the plasma-based environment ensures higher flexibility and controllability, as compared to the thermochemical surface-based techniques. Figure 2 illustrates the principal processes occurring during the growth of flat and vertically-aligned nanostructures under thermochemical (neutral gas) and plasma-based process conditions.

Energy consumption during the biowaste-to-nanomaterials conversion is the second critical consideration to be taken into account. While the plasma-based techniques are usually more intricate and require significantly more complex equipment as compared with the often simpler thermal methods, the thermochemical approaches could have greater energy consumption. This is because in thermal methods, materials need to be heated to initiate bond dissociation in the precursor material, and this high temperature often needs to be sustained over a considerable period of time to achieve desirable yields. Furthermore, higher temperatures are often needed for the synthesis of nanomaterials with higher quality. In contrast, in plasmas, it is possible to initiate bond dissociation virtually instantaneously by subjecting the precursor material to bombardment with energetic plasma-generated particles. The synthesis is also significantly faster. **Table 2** presents an example of a comparison of energy cost per atom incorporated for a nanoscale structure grown using thermal and plasma-based methods. It should be noted that there exists a wide range of thermochemical systems and approaches and hence this value would vary significantly. Nevertheless, these results show that the minimum possible  $e_{atom}$  expressed as  $e_{atom} = P/m$ is notably lower for atmospheric pressure plasma systems in the absence of external substrate heating. Here, P denotes the discharge power and m is the mass production rate for the nanomaterial. Interestingly, while the instantaneous power consumption during pulses can exceed 100 kW for e.g. NRP spark plasma systems, the short pulse length of tens of nanoseconds mean that the overall  $e_{atom}$  power budget is relatively low when compared to continuous mode plasma systems, and especially when compared to the thermochemical system. This holds true even for relatively short thermal growth cycles, as the one used in this study where carbon nanotube synthesis took place on a Fe-catalyzed silicon substrate, with the heating-up time of 5 min (6 kW) followed by the growth time of 10 min (500 W) in a conventional furnace OTF-1200X (MTI Corporation). It should be noted that m was assumed to comprise all of the material collected or evaporated from electrodes, with the data on the bases of which the calculations were performed available in Ref. 72. To compare  $e_{atom}$  for plasma processing to conventional non-plasma synthesis, a carbon nanotube growth experiment was also performed using a typical thermal furnace process. [73] The rightmost column lists the energy cost of nanomaterials calculated from the  $\varepsilon_{atom}$ values, E (J/kg). This numbers are rather indicative, since they were calcilated for small experimental samples without optimization of the use of equipment operational space and capacities.

**Table 2.** Energy cost of incorporating each atom into the nanostructure  $\varepsilon_{atom} = P/m$  using different atmospheric-pressure synthesis processes, where P is the average power coupled into the system and  $\dot{m}$  is the average mass production rate. In all cases, no external heating was used. Quantities marked by (\*) have been calculated in Ref. [72] based on data given in the listed references. Reprinted from *Sci. Rep.*<sup>[73]</sup> The rightmost column lists the energy cost of nanomaterials calculated from the  $\varepsilon_{atom}$  values, E (J/kg).

Source	Carries gas	Excitation	Nanomaterial	P [W]	Max. <i>ṁ</i> [μg/s]	Min. $arepsilon_{atom}$	Ref.	E, J/g
Thermal furnace	Ar	-	Carbon nanotubes	5,000	1	$1.2 \times 10^{8}$	73	10 <sup>12</sup>
Microplasma	Ar	144 MHz	Si nanocrystals	35	0.017	600000*	74,75	5×10 <sup>9</sup>
Microplasma	Ar	450 MHz	MoO <sub>3</sub> nanosheets	31	1*	42000*	76	5×10 <sup>7</sup>
Microplasma	Ar	450 MHz	WO₃ nanoparticles	20	35*	1400*	77	5×10 <sup>5</sup>
Microsecond	Ar	2-μs spark following	Au nanoparticles	1.5*	2*	1500*	78	7×10 <sup>5</sup>
spark		voltage ramp						
mw torch	Ar	2.45 GHz	Graphene	250	33	1000*	79	8×10 <sup>6</sup>
mw torch	Ar	2.45 GHz	Carbon nanotubes	400	7	7200*	80	6×10 <sup>7</sup>
DC arc	Ar	DC	Ag nanoparticles	120*	3	50000*	81	5×10 <sup>7</sup>
NRP spark	Air	40-ns pulse at	MoO₃ nanofalkes /	0.5-4	1.6	75	73	5×10 <sup>4</sup>
		PRF = 30 kHz	nanowalls					

**Table 2** shows that the energy consumption is an important characteristic that significantly depends on the process and its underpinning set of physical and chemical processes. The simplest thermal furnace-based technology features the highest energy consumption per atom, while plasma torches which are relatively simple in technical realization exhibit lower levels of energy consumption. The lowest levels of energy consumption are reported for the nanosecond plasma systems that feature low production yield and require more complex and hence expensive equipment.

Along with the energy cost per atom, the energetical efficiency of thermal and plasma-based methods are also strongly dependant on the equipment configuration. The thermal systems usually incorporate bulky heaters to heat the reaction zone (e.g., tubular quartz chamber located directly in the heater), the heat is dissipating into the ambient environment during the conversion process which could be quite long. This is an apparent consequence of thermophysics, since the neat could be conducted by heat transfer only to the material being processed. As a result, the heating requires significant time and moreover, heat is dissipating in the entire structure of the equipment, yet this process is moderated by the thermal shields and heat insulation. In plasma-based processes, the processed matter could be activated directly from plasma (indeed, external heating is not needed in many plasma nanosynthesis techniques<sup>[82,83]</sup>) due to the involvement of electric processes that are able to sustain plasma without contacts with chamber walls and hence, without excessive dissipation of energy.

**Figure 3** illustrates the comparison of heated reaction zone and plasma reaction zone assembled in a single reactor designed for the synthesis of various nanomaterials. Both systems provide similar output when operating in heating and plasma modes, but apparently the large heater (OTF-1200X, 6 kW) requires more power than the localized plasma discharge.<sup>[84]</sup> Large size of heating assembly and very compact plasma bulk with the discharge power much lower than the power of heating elements apparently illustrate energy efficiency of plasma-based approach. Note that the power level of 5 to 10 kW is still intrinsic to the most advanced furnaces of similar size, e.g. the furnace with a tubular heating zone of 660 mm features 10 kW (Protech Technology Co.).<sup>[85]</sup>

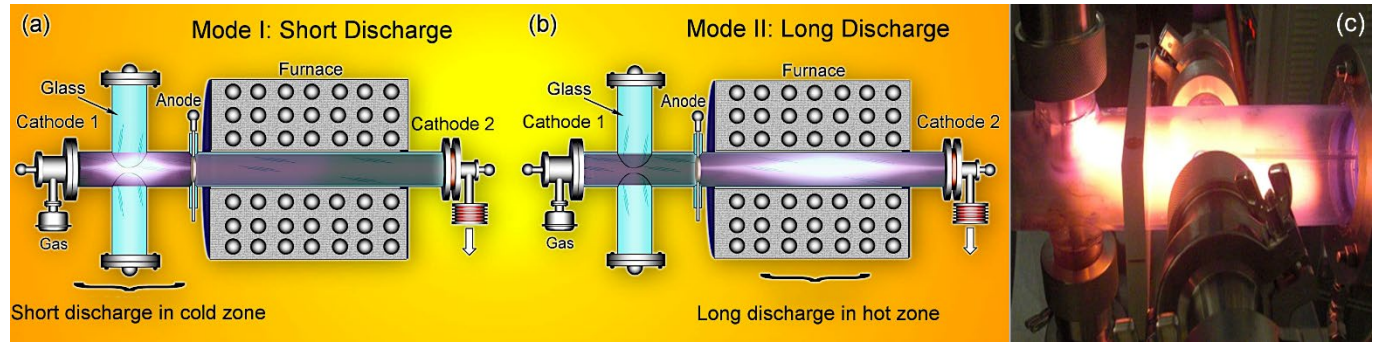


**Figure 3.** (a,b) Two variants of the modified thermal furnace for the advanced nanosynthesis, and (c) photograph of the localised plasma in cold zone shown in (a). The systems provide similar output when operating in heating and plasma modes, but apparently the large heater (OTF-1200X, 6 kW) requires more power than the localized plasma discharge. Reprinted with permission from IEEE Trans. Plasma Sci. 2014.

✓ The methods for biowaste valorization via production of functional nanomaterials require careful selection of the process, taking into account the flexibility and adaptivity of the technology to upscaling, and energy consumption that can vary over a very wide range.

It is worth noting that any comparison between these technologies, be it plasma-assisted or driven by thermochemical reactions, is limited by the fact that this area is still rapidly evolving and is not sufficiently consolidated to allow a definitive comparison.

#### 3. Thermal methods for biowaste-nanomaterial conversion

We will examine some examples of thermal techniques first, mainly because of their relative simplicity and lower costs. While some thermal approaches are very simple and are mainly based on combustion, they are still capable of synthesising quite complex and valuable nanomaterials such as graphene, graphene oxides and even complex catalysts.<sup>[86,87,88]</sup>

✓ Since for graphene and graphene oxide, their application in the field of energy generation and storage is highly promising and a strong focus of academic research globally, the examples we will review emphasise the synthesis of graphene for supercapacitors.

#### 3.1. Graphene oxide and reduced graphene oxide preparation from agricultural and plant wastes

Graphene and graphene oxide are currently considered among prime candidates for energy applications, including in supercapacitors and batteries. [89,90] Simple thermal methods allow for the conversion of low-value products and wastes directly into high-quality graphene materials. [91,92] Biomass wastes are nearly unlimited negative-value resource, this the development of simple, cheap techniques for the production of graphenes from biowastes is a very important problem. [93,94,95]

Tamilselvi *et al.* has recently demonstrated the conversion of coconut coir, a natural fibre that can be extracted from the outer husk of the coconut and is an abundant, difficult to degrade by-product of coconut industry, into reduced graphene oxide via a simple reaction of catalytic oxidation, where ferrocene was used as a low-cost yet efficient catalytic platform.<sup>[96]</sup> Thus-produced reduced graphene oxide was of high quality, and, when used as an electrode material for an electric double layer supercapacitor, shows high performance and excellent stability during cycling. Considering the simplicity and relative sustainability of the processes coupled with high quality of the reduced graphene oxide material, the proposed approach is a promising pathway for the conversion of fibrous agricultural waste into high-value supercapacitor electrodes.

This study also explored the flexibility of the process by using two types of agricultural waste, specifically the coconut coir and coconut shell. The process of direct waste-to-nanomaterial conversion is illustrated in **Figure 4a**, and is based on the simple catalytic oxidation of the fibre. It should be noted that it was necessary to first mechanically grind both the coconut shell and coconut coir into a relatively fine powder to increase its surface-to-volume ratio. This fibre-rich powder was then mixed with ferrocene catalytic particles, and placed in a muffle furnace for 15 min at 300 °C under atmospheric (air) conditions. Both the quality of graphene oxide and the conversion yield were confirmed to be high. Subsequent thermal reduction of graphene oxide was preformed via simple thermal annealing of the soot (**Figure 4b**), which resulted in the loss of oxygen in the form of carboxylic groups, verified by the XRD, FTIR and Raman characterisation.

The reduced graphene oxide was then used as an active material in a composite electrode also containing polyvinylidene difluoride (PVDF) and N-methyl-2-pyrrolidone (NMP). The composite slurry was spread over a nickel plate substrate and dried for 12 h at 100 °C. Thus, simple oven-based processes were used for all stages of the supercapacitor electrode preparation directly from biowastes. The electrochemical analysis demonstrated that the highest specific capacitance of 111.1 F/g was achieved. Importantly, the material showed excellent performance stability of 99% over 3,000 charge/ recharge cycles.



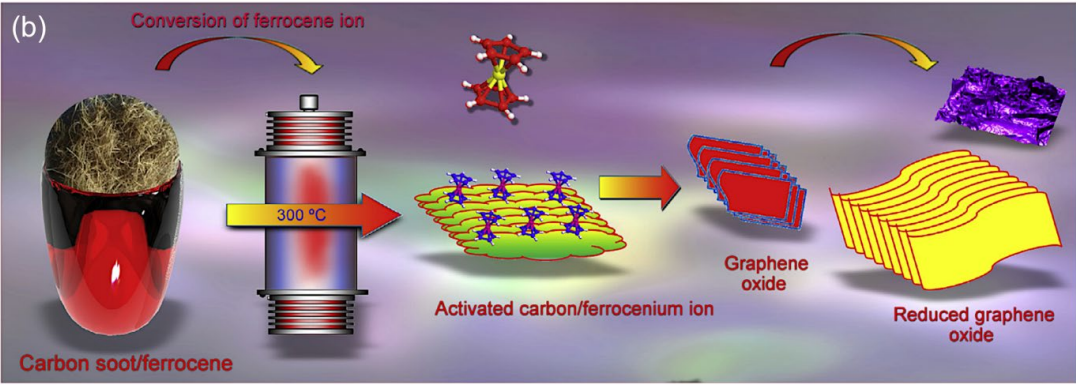


**Figure 4.** (a) Direct conversion of coconut waste fibre into reduced graphene oxide by means of catalytic oxidation, with an efficient and affordable ferrocene-based catalytic platform. The quality, structure and properties of thus-synthesised materials are highly dependent on the processing temperature and time. Due to process simplicity and abundance of input materials, this approach is amenable to scale up to facilitate manufacturing of graphene oxide electrodes in quantities needed for *e.g.* electrical transportation systems. (b) Mechanism of fibre decomposition and subsequent reduced graphene oxide formation. A brief annealing step is used for graphene oxide reduction in to thermally remove carboxylic groups. Extending the annealing step results in the loss of carboxylic and epoxy groups, loss of carbon and formation of defects in the carbon lattice, with CO<sub>2</sub> and CO released as by-products. Reprinted with permission from *Renew. Energy* **2020.** [96]

✓ These results confirm the method's potential in efficient rapid conversion of waste to high quality reduced graphene oxides with quality and performance that render these value-add materials suitable for use in high performance flexible supercapacitors.

While the thermochemical methods of waste valorization usually do not presume the use of potentially harmful chemicals, there is an ongoing drive to reduce the environmental footprint of nanocomposite synthesis by not only replacing the source material but also by reducing the energy cost of the method, and by employing thus-produced materials in energy generation and storage applications. This approach aims to reduce our reliance and consumption of crude oil and fossil fuels. Tamilselvi *at al.* presented one such example, where a facile hydrothermal method was employed to synthesise multifunctional nickel-based reduced graphene oxide composites directly from the *negative value coconut coir*. Decoration of thus-produced graphene oxide using functional NiO and NiFe<sub>2</sub>O<sub>4</sub> nanoparticles resulted in a material with complex hierarchical architecture and excellent energy storage and photocatalytic characteristics. [98,99] The synergistic combination of NiFe<sub>2</sub>O<sub>4</sub> nanoparticles and reactive edge-rich rGO nanoflakes allowed the material to produce excellent specific capacitance of about 600 F/g at current density of 1 Ag<sup>-1</sup>. The retention rate was also very good, at 86.5% after 2000 cycles. In addition to good energy storage performance, this material showed promising efficiency in visible light-driven photocatalytic degradation applications, at 96.5%. Hence, a simple hydrothermal technology (soft bubble assembly) was able to produce an essentially multifunctional material with excellent electrochemical and photocatalytic activities.

Schematics of the synthesis is illustrated in **Figure 5a**. Briefly, a finely ground powder of coconut coir was subjected to a simple oxidation/reduction reaction in a muffle furnace, with ferrocene used as a heterogeneous catalyst. The graphene oxide formed after the reaction was allowed to proceed for 15 mins at 300 °C. Standard characterisation confirmed high quality of thus-synthesised graphene. The structure and chemistry of the composite makes it a particularly good material for the indirect degradation of pollutants, *e.g.* dyes generated by the textile industry, through the oxidation and reduction mechanism outlined in **Figure 5b** (see more details in Ref. [98]).

#### GRAPHENE OXIDE COMPOSITES FROM COCONUT COIR

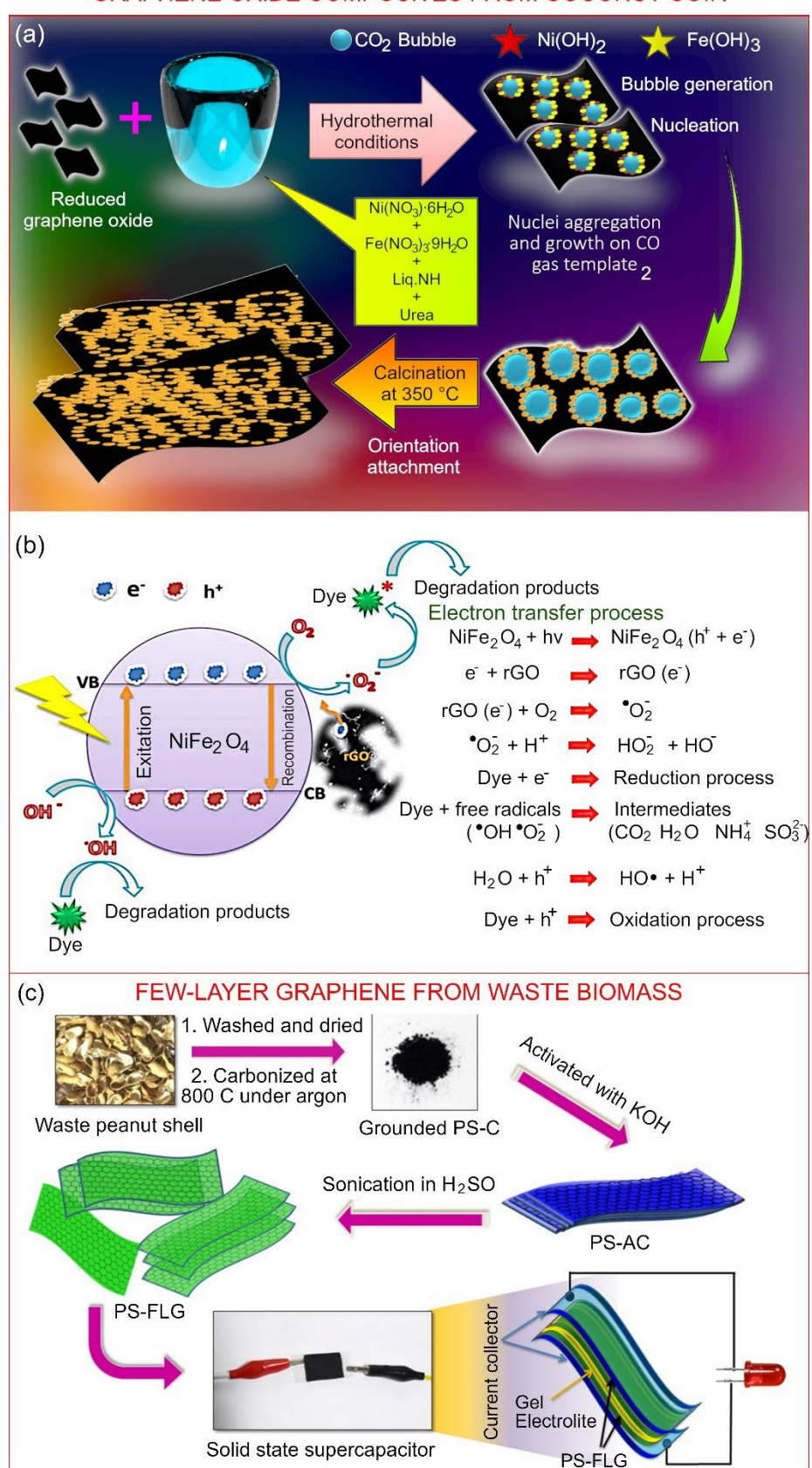


**Figure 5.** (a) Synthesis pathway for direct conversion of coconut coir into multifunctional composites. CO<sub>2</sub> bubbles produced within the hydrothermal reactor perform the function of a template on which metal oxide particles can grow. During the reaction under high temperature and pressure conditions, Fe<sup>3+</sup> is being converted into FeOOH. Graphene oxide acts as a site of nucleation for the subsequent growth of nanostructures. Anisotropic directional growth was facilitated by calcination at 350°C. (b) Photocatalytic activity of coir-derived nanocomposite. OH radicals generated by the holes in the valence band enable fast and efficient oxidation of the pollutant, in this study a dye. Reprinted with permission from *Renew. Energy* 2022.<sup>[98]</sup> (c) Schematic representation for the synthesis of peanut shell – few-layer graphene active material and its subsequent integration into a solid-state device. Reprinted from *Sci. Rep.* 2017 under terms and conditions of CC BY 4.0 license.<sup>[100]</sup>

One more example is the conversion of the *negative value peanut shell*, a very plentiful waste of agriculture industry. <sup>[100]</sup> In this work, Purkait *et al*. have demonstrated the synthesis of few-layer graphene-like nanosheets which feature high density of micro- and meso-pores, using the mechanical exfoliation of the peanut shell biomass. The produced material was used to fabricate the binder-free supercapacitor, which has demonstrated the specific capacity of 186 F×g<sup>-1</sup> at the highest energy density of 58.125 W×h×Kg<sup>-1</sup> and the highest power density of 37.5 W×Kg<sup>-1</sup> without the binder. The graphene production method was based on activation using KOH, and the following exfoliation. After washing the peanut shell wastes in water and drying for several days in air, they were then dried in vacuum, crushed to fine powder, pyrolyzed at 800 °C in argon gas for 2 hours, and finally washed in isopropanol. Next, the product was activated by mixing it with KOH and heating again for two hours in argon. Finally, exfoliation was performed using simple sonification in H<sub>2</sub>SO<sub>4</sub> solution for one hour, washing in isopropanol, centrifuging and drying at 80 °C (see more technical details in the relevant publication Ref. [100]).

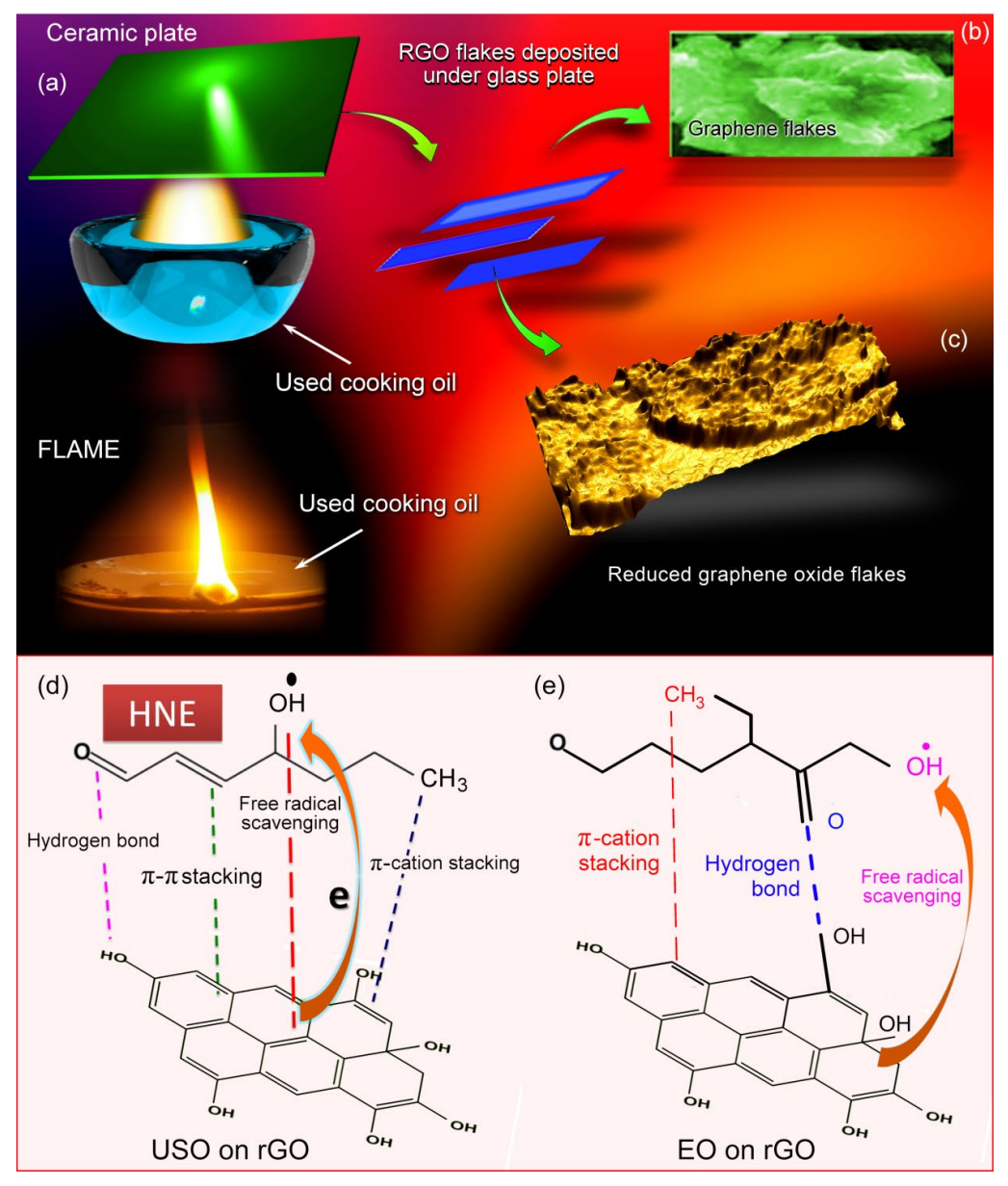
**Figure 5c** illustrates the general scheme of the conversion of negative value peanut shell into graphene. Importantly, walnut and almond shells also could be conversed into graphene-like material following the above described scheme. This method does not presume the use of graphitizing agents. The produced graphene products feature very high specific surface area and porosity, with both micropores and mesopores present. The results demonstrate the great potential for using very abundant negative-value shall waste of various types of nuts for the supercapacitor technology. [101,102,103]

#### 3.2. Graphene oxide nanostructures by facile synthesis from used oils

Another characteristic example is the synthesis of graphene oxide nanostructures using facile wick and oil flame technology (**Figure 6a**). In this case, the simplest technology based on combustion of *used sunflower cooking oil* was utilized to produce graphene-like structures that were proven as an effective means for absorbing used commercial sunflower and engine oils, thus providing an efficient and low-cost approach for environment remediation [48]. Used oils are generated in large quantities globally, both in food preparation and machine industries, and their disposal presents a significant challenge. When done unethically, these oils can enter waterways and landfill, becoming a source of significant pollution and threatening the wellbeing of local flora and fauna. People becoming a source of significant pollution and threatening the wellbeing of local flora and fauna. People become a source of significant pollution and threatening the wellbeing of local flora and fauna. People become a source of significant pollution and threatening the wellbeing of local flora and fauna. Another than the cooking oil leads to the increased levels toxic substance which cause extensive damage of proteins and cell membranes, and finally cause alterations to the permeability and fluidity of the membranes. Morbidities associated with exposure to these substances include cardiovascular diseases, kidney and liver damage, and cancers. Repeated use of oils rich in linoleic acid, *e.g.* sunflower and soybean oils, is even more concerning, since their exposure to elevated temperatures result in the creation of acrylamide and polycyclic aromatic hydrocarbons (PAHs). These are highly soluble and as such are readily absorbed through gastrointestinal tract, causing mutations and the development of malignancies.

Lekshmi *et al.* demonstrated that it was possible to covert used oil into carbon nanomaterials that could then be effectively used to remove oil-based pollutants from the ecosystem. The detailed scheme of the process is shown in **Figure 6**, while the detailed protocols and conditions could be found in several previous publications. Burning of the oil under controlled conditions resulted in the formation of the soot that could be easily and efficiently collected by means of a porcelain plate placed immediately above the open flame (**Figure 6a**). Despite the simplicity of the process, thus-formed material was the particles of high quality 4-layered reduced graphene oxide (**Figure 6b,c**). The material contained about 95% of carbon and about 5% of oxygen, without any impurities, with atomic carbon-to-oxygen ratio of about 20, as it was previously reported for the reduced graphene oxides. [115]

The flame-produced reduced graphene oxide-based materials were then tested for the contact angle and absorption characteristics towards sunflower oil, engine oil and water, and it was found that the produced material is oleophilic and moderately hydrophilic. **Figure 6d,e** illustrates the mechanism of oil absorption on the surface of reduced graphene oxide flakes. The Langmuir isotherms with  $R^2 = 0.99$  for sunflower oil and  $R^2 = 0.98$  for engine oil provides the best fit for the data that describes the removal of oils from the oil-water emulsion using the flame synthesized graphene oxides. Moreover, a cost comparison between thus-fabricated material (lab scale) and its equivalent retailed by *e.g.* Sigma Aldrich (at USD500/gram) confirms the former is a lower cost



alternative.[36]

**Figure 6.** Synthesis pathway for the formation of reduced graphene oxide (rGO) particles directly from used cooking or engine oil (a). Thus-produced material is made of flakes and each flake comprises multiple layers of reduced graphene oxide, as confirmed by SEM (b), and three-dimensional topography visualisation (c). Inset depicts a photograph of the precursor oil during combustion. Mechanism of adsorption for used sunflower oil pollutant (d) and used engine oil pollutant (e) when rGO flakes are used to remove oils from water. Sunflower oil interacts with rGO flakes through  $\pi$ - $\pi$  interactions, hydrogen bonding,  $\pi$ -cation stacking and scavenging of radicals, whereas the interactions with engine oil are limited to hydrogen bonding,  $\pi$ -cation stacking and radical scavenging. Reprinted with permission from *Carbon Lett.* **2021.** [48]

#### 3.4. Gelatin-derived carbon aerogels for advanced supercapacitors

A combination of thermal technology and freeze drying method was recently demonstrated as another useful, simple and environmentally friendly technology for the waste valorization by synthesis of nanomaterials for the advanced supercapacitor applications. Moreover, this technology, despite its simplicity, was able to produce quite complex hierarchical nanomaterials. Kandasami *et al.* used nitrogen-rich gelatin as the input material for the synthesis of graphene-based aerogels inherently doped with nitrogen, where the hierarchical architecture of the material featured three levels of pores. [116] The larger pores (at meso- and macro-levels) were a result of the aerogel preparation, and consisted of a complex amorphous carbon/3D graphene framework that emerged as a result of carbonization (Figure 7). [117,118] Potassium hydroxide was used for chemical activation of the framework. Exposing the amorphous carbon/3D graphene framework to high temperature in a nitrogen atmosphere removed the amorphous phase, leaving behind a stable N-doped graphene structure. The material displayed promising

specific capacitance, at 232-170 F×g<sup>-1</sup>, and stability over numerous cycles, confirming their potential as an electrode material for solid asymmetric supercapacitors.

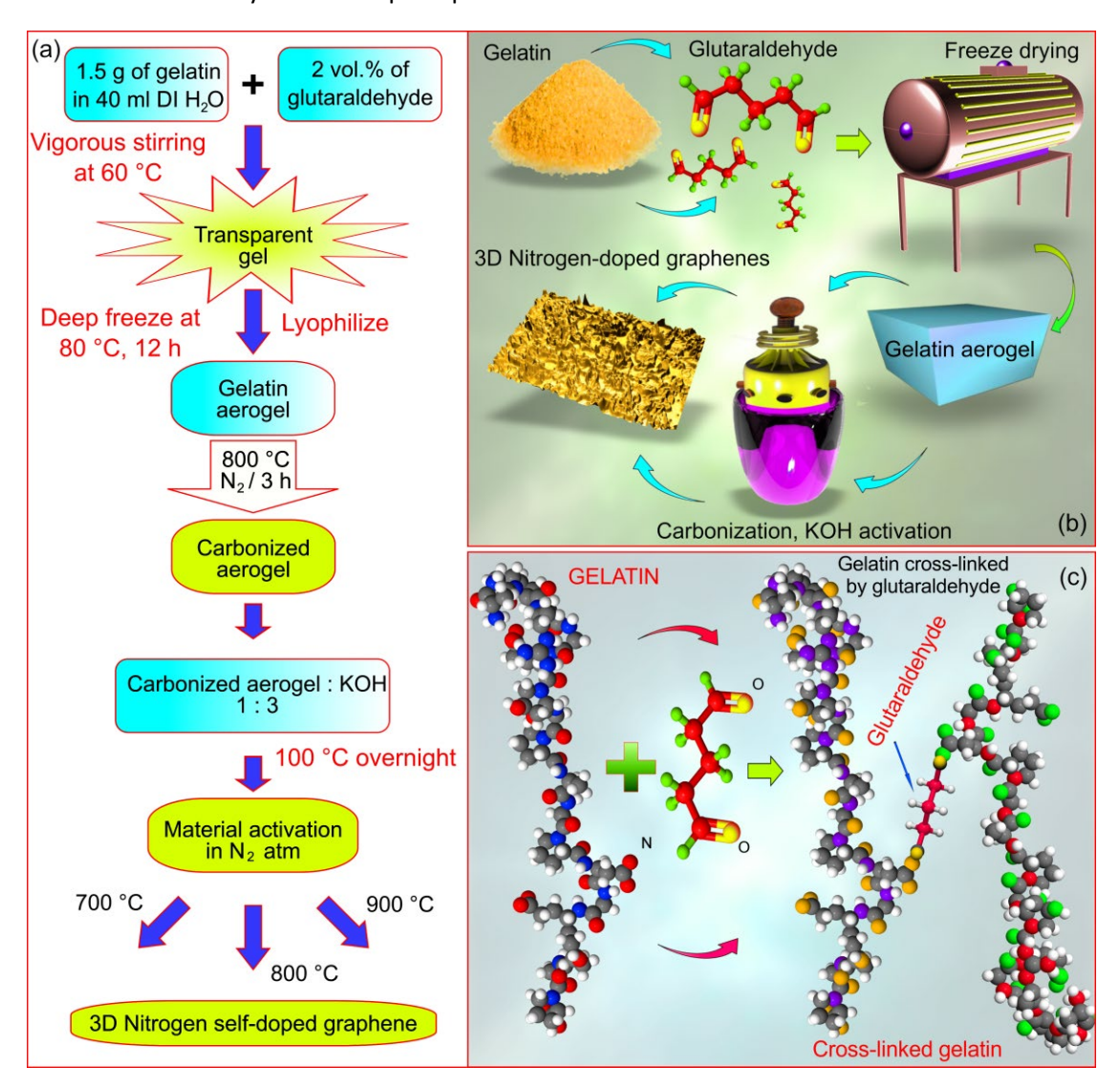


**Figure 7.** (a) Fabrication of 3D nitrogen self-doped graphene-based carbon aerogels from gelatin; (b) Multiple levels of porosity are realised via deep freezing of the gelatine gel, with glutaraldehyde used as a cross-linker (c). Reprinted with permission from *Nanomaterials* **2021.**<sup>[116]</sup>

In this study, freeze drying was demonstrated to be an effective strategy to develop the required multiple levels of porosity. The method itself is simple, and requires gelatin powder to be dissolved in deionized water, followed by the addition of glutaraldehyde solution used as a cross-linker. Vigorous stirring is used to ensure uniform mixing (Figure 7a). Thus-prepared transparent highly viscos solution is then allowed to stand for 120 min, and then is frozen to -80 °C for 12h. At this point, the frozen matter is lyophilized into an aerogel (Figure 7b). Carbonization of the aerogels via pyrolysis at 800 °C for 3h in flowing nitrogen transformed the gel into nitrogen-rich carbon networks without loss of its desired porous structure (Figure 7c).

✓ This simple hybrid technique involving cheap, environmentally benign processes including (i) preparation of gelatin aerogels via freezing, (ii) carbonization, and (iii) activation in nitrogen gas enabled the synthesis of 3D nitrogen self-doped activated graphene aerogels with very high porosity and excellent surface-to-volume ratio. The highest achieved capacitance was 236 F×g⁻¹ at 2 A×g⁻¹, confirming the potential of this material made of low-cost natural resource (gelatin) as an electrode material for high-performance energy storage devices.

#### 3.5. Biowaste valorization by conversion to nanokeratin-urea composites

Synthesis of advanced nanostructure-based nanokeratin-urea fertilizers from the biowaste (chicken feathers) is one more example of biowaste valorization via simple, cheap technology. [119]

Poultry feathers is another source of waste that tends to persist in the environment due to its slow break-down, and at the same time presents a valuable source of nutrients for plants. When used in their milled form, feather powders do not release the needed levels of nutrients quickly enough. However, Sree et al. have recently demonstrated the fabrication of bio-fertilizer nanocomposite platforms from feather-derived keratin, where urea coating was used to provide a pathway to supplement nitrogen release during early stages of fertiliser deployment, and where loading into a sustainable wood chip-based matrix provided a means to retain the fertiliser particles in the soil, preventing them from being washed away during watering. [119] The method used in the production of these fertiliser composites allowed for the retention of a large fraction of the valuable organic and inorganic nutrients. Plant germination rate, and subsequent plant growth, health and productivity were improved compared to solely applying urea. This was due to nutrients being released in a sustained fashion, without under- or over-fertilization. As such, the proposed method of feather utilisation is a potentially useful means of benefiting soil fertility that does not require a release of nitrous oxide, the latter being a green house emission gas of considerable concern. This simple, cheap process is illustrated in Figure 8. In this study, the feathers were obtained from a local poultry processing facility and were washed with distilled water to remove blood and tissue, and then rinsed in 70% ethanol, minced and air dried in an oven. Once dehydrated, feather pieces were placed into 5% NaOH solution and allowed to undergo hydrolysis. [120] Once completed, the hydrolysed solution was filtered, and the keratin filtrate was dried. Thus-produced keratin filtrate was then resuspended in deionised water and subjected to sonication to deagglomerate the particles and ensure uniformity of the dispersion. Adding ethanol to the suspension, and then a small amount of glutaraldehyde crosslinker resulted in the production of keratin nanoparticles after continuous overnight stirring. [121,122] Centrifugation was used to separate the particles, which were then dried and used as the base material for several types of nanostructurebased nanokeratin-urea composite fertilizers. Please find the detailed description, along with process specifications and reagent concentrations, in the relevant publication<sup>[119]</sup> and references therein.

The prepared nanostructure-based nanokeratin-urea fertilizers were tested directly on plants. Cowpea seeds were put into pots and allowed to undergo germination and seedling growth. In addition to providing a physical means of protection for the urea-coated keratin nanoparticles against being washed away, the wood chips enable controlled release by contracting or expanding its pores in response to varying humidity levels. Overall, the fertilizer based on urea-coated keratin nanoparticles provides a better source of nutrient supply to soil microbiota and plants when compared to pure chemical fertilizer, in this case urea, alone.

✓ This very simple and very cheap technology for the production of nanostructured fertilizers with highly controllable release of nutrients out of negative-value waste (feathers) demonstrates the strong potential of simple hybrid techniques for biowaste valorization.

Some of the thermochemical methods and techniques for the valorization of biowaste and cheap natural products, along with negative-value natural waste are relatively simple, cheap, but still quite efficient to significantly add value to a wide range of industries and sectors. Efficient production of various useful products and materials such as carbon aerogels for energy storage, graphene oxide-based supercapacitors, nanokeratin-urea composite fertilizers and graphene-based nanomaterials for the photocatalytic dye degradation and oil absorption were demonstrated. Very simple techniques such as facile wick and oil flame synthesis, soft bubble assembly, simple catalytic oxidation, freeze drying and others were found to be capable of producing quite complex hierarchical functional nanomaterials. Further development of thermochemical techniques through their scale up to industrial scales, as well as through the production of more valuable complex, hierarchical multifunctional nanomaterials would ensure further economic benefits

from biowaste valorization and waste management.

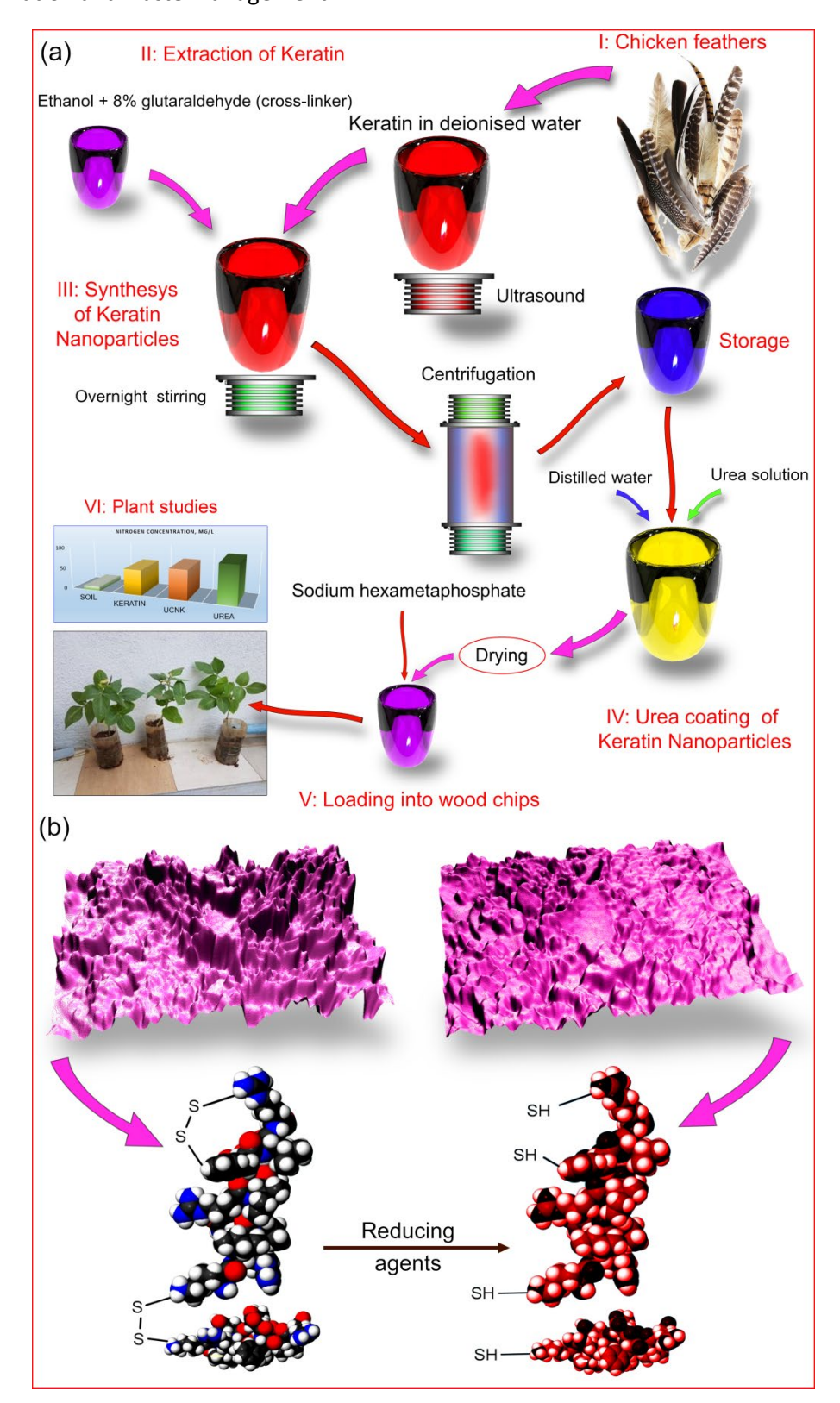


**Figure 8**. (a) Collected chicken feather waste is ground and hydrolysed to extract keratin, which is then used to synthesise keratin nanoparticles. These are coated with urea, and then loaded into a carrier, in this study the wood chips, to enable gradual release and facilitate fertiliser retention in the soil. The composite fertiliser is used to supplement the soil with nutrients and stimulate the growth of desirable soil microbiota. (b) Sodium hydroxide is used to hydrolyse the feather powder. These three simple environmentally friendly steps produce an efficient triplex fertilizer system for controlled release of nitrogen into soil. Reprinted with permission from *Carbon Trends* **2021.**<sup>[119]</sup>

#### 4. Plasma-based methods for biowaste-nanomaterial conversion

Among presently available techniques, plasma-based methods ensure very high flexibility and adaptivity of the biowaste conversion and valorization due to the high specific energy and controllability intrinsic to the plasma environments.[123-125] The demand for more sustainable solutions has driven the field of nanofabrication, and plasma nanofabrication in particular, to search to replace traditional input materials, i.e. high purity gases and solid targets, with minimally-processed raw and waste biomass that has variable chemical composition and physical form, while still producing high quality graphene and other types of nanoscale materials. [126-128] The goal was to use these mixed-origin materials directly, without additional processing steps, so as not to increase the complexity of plasma synthesis. [129-131] Thus far, graphene has been successfully produced from essential and cooking oils, food and waste from food industry, animal products and their waste, and many other alternative precursors. While in many of these cases, the conversion took place in the presence of a catalyst and high temperature (e.g. by means of catalytic thermal chemical vapour deposition (CVD)), lower temperature, catalystfree deposition has also been realised by introducing plasma as a catalytic environment. In thermal CVD, temperatures in the range of 800-1000 °C are needed to decompose the input material into usable building blocks, e.g. carbon atoms in the case of graphene synthesis, and then re-assemble these blocks into a nanostructure. Furthermore, nickel or copper catalyst is generally needed to enable the surface growth of nanosheets or nanotubes, [132] the latter often being slow, possibly taking hours to complete. [133] Importantly, this method often does not provide the means to control the directionality of the growth. In the case of graphene, this generally leads to the deposition of horizontally-oriented graphene sheets that need to be transferred from the growth substrate to their intended surface or device element by dissolving away the metal in an acid bath. [134] Many of these issues stand in the way of making nanofabrication a truly environmentally sustainable solution, yet they could potentially be circumvented or reduced through the use of plasma-based technologies. For example, when compared to traditional CVD, plasma-enhanced CVD (PECVD) has a wider range of possible control mechanisms that allows deposition of both horizontal as well as vertically aligned graphene, as well as nanostructured oriented at a prescribed angle to the surface, providing a greater range of opportunity for the development of functional structures with unusual geometry and characteristics. In addition to conventional mechanisms that PECVD shares with its thermal counterpart, namely gas chemistry, temperature of the substrate, and length of treatment, PECVD also benefits from the presence of highly chemically-reactive species, [135,136] including energetic electrons and ions the energy and make up of which can be controlled, and electric fields. [137] Most importantly, because many of the particles that make up the plasma are charged, it becomes possible to guide the direction and intensity of fluxes of energy and matter by means of externally applied electric and magnetic fields.[138]

#### 4.1. General consideration of growth processes in plasma

As mentioned above, the nanostructure nucleation and growth in plasma-based technological environments involves a complex set of physical and chemical processes and what is most important, these processes occur in both the bulk plasma and at the substrate/nanostructure surfaces, in contrast to the thermal technology that relies mainly on the surface processes (**Figure 2**).

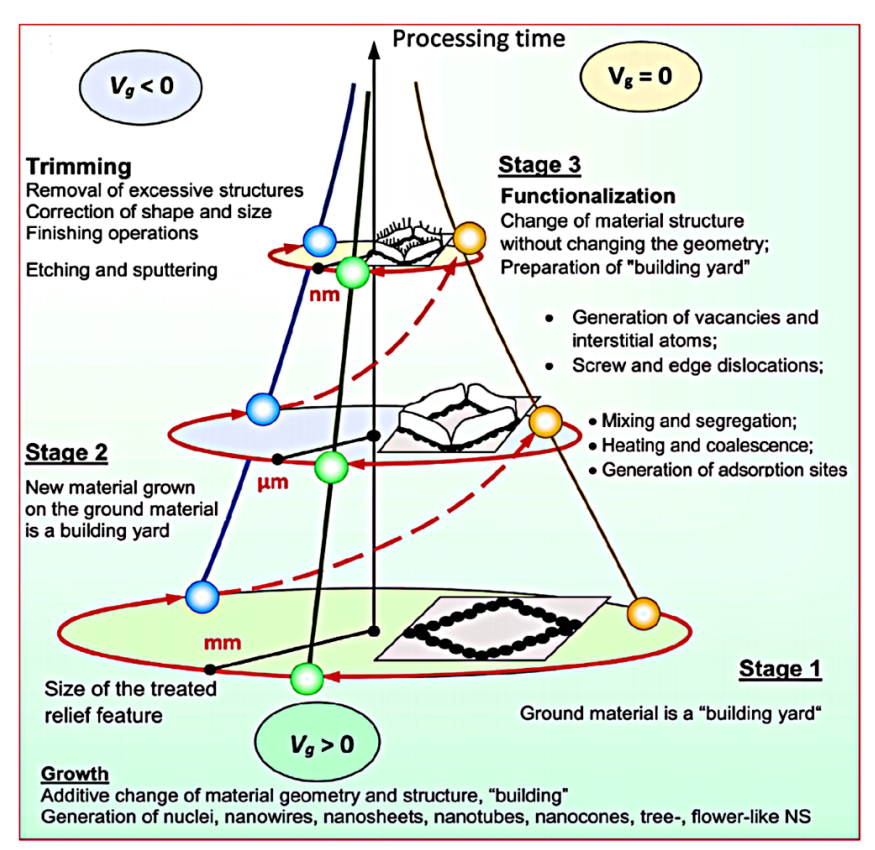
How do nanostructures grow on plasma-exposed surfaces? **Figure 9** summarises the key principles of growth for architecturally complex nanostructures in plasma environments, where larger (*e.g.* millimetre) scale surface features that form at earlier stages of the treatment become the foundation on which smaller features (*e.g.* at micro- or nano-meter) are built.

The formation of these features follows the same pathway, beginning with the transformation of the target surface into one amenable for subsequent growth of material. It is possible for this step to produce chemical modification (e.g. activation or functionalisation) of the surface without changing its geometry. This is because this step serves to alter atomic bonding characteristics of the surface so as to improve the probability of subsequent adhesion interactions with building blocks arriving from the plasma bulk. This change in atomic bonding can result from the introduction of vacancies and interstitial atoms within material lattice; screw and edge dislocations that arise from forming precipitates; ion bombardment induced mixing and thermal segregation of phases of material within the surface layer; grain coalescence resulting from ion bombardment induced heating of the surface, etc. These defects and active sites is where adsorption is likely to happen, enabling additive surface

growth of structures from the building blocks delivered from the plasma bulk. The rate with which the new nanostructure will form and the dominant direction of the growth depends on the control mechanisms being used. For example, graphene flakes may grow perpendicular to the surface of the substrate to produce connected networks of vertically-oriented walls with sharp edges. "Trimming" processes, where material is removed from the surface of the newly formed structure, also take place. Continuing with graphene as an example, this stage is associated with the removal of amorphous carbon (a-C) phase from the graphene network. More details could be found in the relevant publications. [138,139]

This set of processes often requires the application of more complex equipment, as compared to the thermochemical methods. [140,141] To date, many types of plasma systems have been designed such as e.g. DC discharge-based platforms, [142-144] microwave systems, [145-148] inductively-coupled plasma (ICP) [149-151] and capacitively coupled plasma (CCP) [152,153] systems, radio-frequency (RF) and magnetrons, [154-157] and many others. [158-161]

Figure 9. Growth of architecturally complex 3D structures involves successive cycles of surface activation, feature growth and excess material removal at millimetre, micrometre nanometre scales. Activation functionalisation changes surface chemistry to make it amenable to material growth while leaving surface geometry virtually unchanged. The additive growth and trimming alter both surface chemistry and geometry. Once this cycle is completed, the next cycle of these processes commences, allowing for the deposition of smaller structures over the freshly grown larger surface features. Reprinted with permission from Carbon 2020.[138]



Several examples of plasma-based technological platforms that use various principles for plasma ignition, sustaining, and control are shown in Figure 10. Efforts have also been made to combine the benefits and address the shortcoming of individual systems through the design of modular multifunctional systems that would be able to facilitate the production of even more complex functional materials [136]. The flexible modular multifunctional platform could sustain a much wider variety of processes that would typically require dedicated plasma-based systems, including deposition of metallic layers and nanostructures as well as the synthesis of complex nanomaterials from low- and negative-value sources. This is achieved by combining multiple plasma generation sub-modules, each capable of creating a unique set of plasma conditions optimised for a given purpose, thus reducing the economic, labour and environmental cost of fabrication of complex multi-component material architectures. These sub-modules may employ different physical mechanisms of plasma generation, and jointly, cover a very broad range of plasma parameters. Amongst the parameters that have most impact on the processes that take place in plasma and at the plasma-surface interface, plasma density  $n_{\rm p}$ , ion temperature  $T_{\rm i}$ , electron temperature  $T_{\rm e}$ , and energy density are considered critical as they define the outcome of the treatment step. Thus, these modules should collectively be able to produce plasmas over the plasma density range  $n_0 \approx 10^{12} \cdot 10^{20}$ m<sup>-3</sup>, electron temperature range  $T_e \approx 0.1\text{-}100$  eV, incident ion energy 0-10<sup>4</sup> V, and gas pressures 10<sup>-3</sup>-10<sup>5</sup> Pa. In addition to plasma generating units (a) that produce environments with different plasma density, ion chemistry, and electron temperatures, the synthesis and assembly in such a platform could be controlled by means of plasma-conditioning sub-modules (b-h) that could be used to fine-tune each nanofabrication step. [136] Active plasma-generation system, where a hollow cathode base system<sup>[162]</sup> is augmented by a series of control submodules for the management and fine tuning of plasma processes may provide the needed range of coverage of parameters.<sup>[163]</sup>

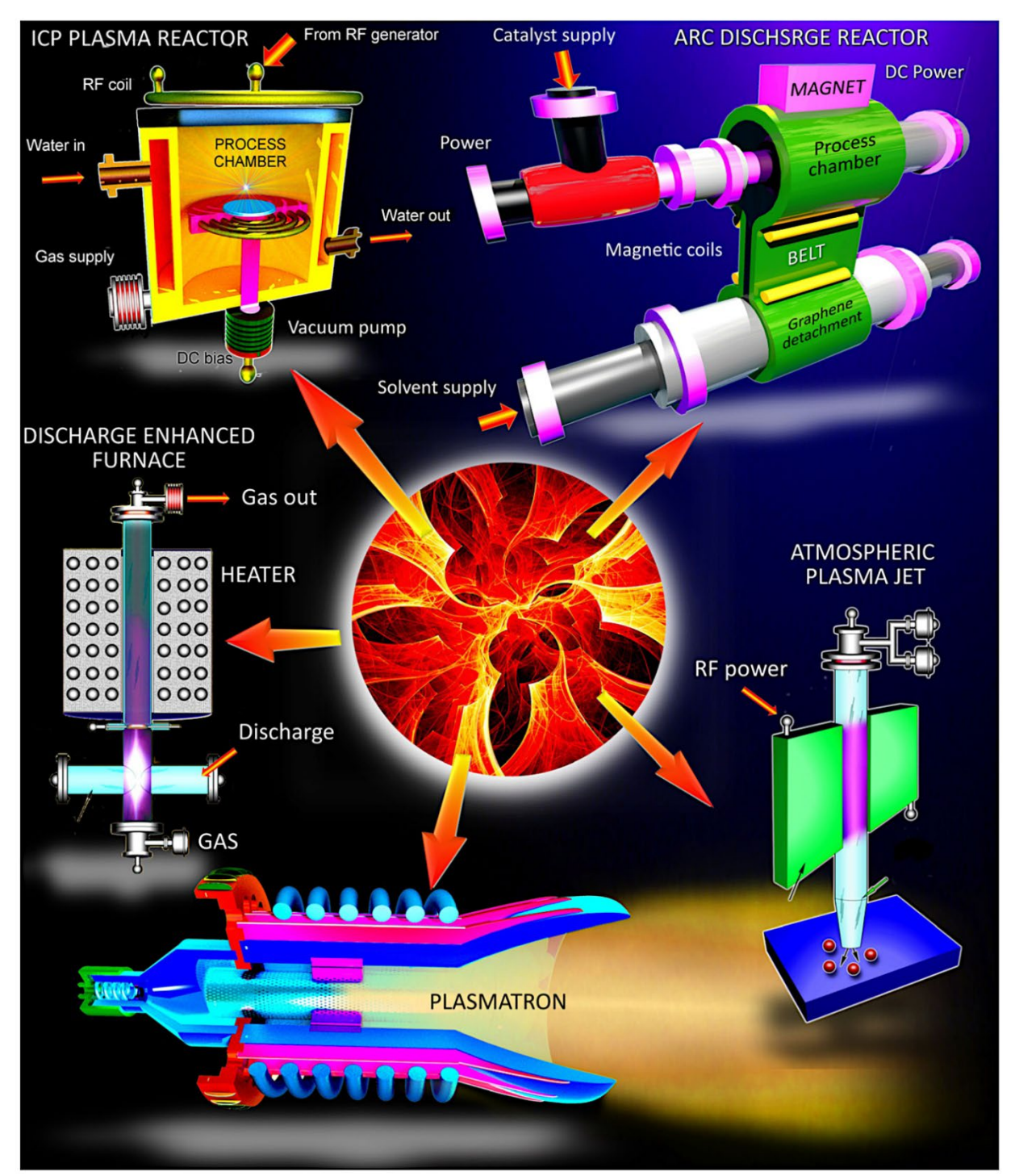


**Figure 10.** Several examples of plasma-based technological platforms with various principles of plasma ignition, sustaining, and control. In the inductively coupled plasma (ICP), electromagnetic induction is used to sustain the plasma within the reactor. In contrast, in vacuum arc and magnetron plasmas, strong direct currents are primarily responsible for sustaining the plasma. The performance and flexibility of the conventional thermochemical furnaces can be further enhanced by means of plasma, by combining the reactivity stemming from the use of high temperatures and plasma-generated effects. Jets of plasma generated at atmospheric pressure using radio frequency electromagnetic energy are highly versatile, and can be relatively easily integrated into existing industrial processes. Very dense plasmas with a high degree of ionisation can be generated in a DC plasmatron due to an interaction of DC current and an externally applied magnetic field. Reprinted with permission from *Appl. Phys. Rev.* **2017.**<sup>[137]</sup>

Modular flexible plasma treatment platforms may be quite promising for the valorization of biowastes and low-value produce by synthesis of the higher-value functional nanomaterials that are more complex and multi-component in nature, e.g. for energy storage and conversion applications, at industrial scale. The high value of the

final product (e.g., electrodes for supercapacitors) could compensate for the higher price of equipment, provided that the raw materials and precursors are extremely cheap, and the fabrication system support single-environment processing.

#### 4.2. Natural resource-derived graphenes in plasma

In plasma-based technology, usually the two different routes of nanosynthesis are considered, namely the bottom-up or top-down approaches (**Figure 11**). In the bottom-up approach, feedstock or precursor materials are injected into the plasma region, broken down into building blocks and delivered to the surface (in the case of surface-based synthesis), then nucleate after supersaturation and grow further via surface reactions, with the building material continuing being supplied from the plasma bulk. In the top-down route, the cleavage and subsequent removal of layered materials using plasma-generated species is used to form the nanoparticles on the surface. [164,165] In this case, the removal of the material is a result of both physical (bombardment, desorption) and chemical (reactions with highly active plasma-generated species) processes.

As a characteristic example of plasma-based synthesis of nanomaterials out of a natural product, we describe here the growth of vertical graphene in radio frequency plasma from *cold-pressed Citrus sinensis oil*, a low-value by-product of orange juice production. Alancherry *et al.* have presented the experimental insights into the conversion of the *Citrus sinensis* oil into graphene, using simulation to explain the mechanism of precursor break down and reassembly into vertically-oriented graphene walls of high quality, providing novel insights into the dynamics of graphene network formation with a focus on network morphology. Fabrication of affordable high quality graphene remains a challenge, with vertically-oriented graphene being of particular interest due to its potential in energy, green catalysis and environmental remediation.

The experimental methodology used in this study is briefly outlined in **Figure 12**, also showing the three-dimensional graphene structure that could be realised under these conditions. In contrast to thermochemical methods of graphene synthesis, metal catalysts are not required to facilitate surface synthesis of graphene in plasmas, opening up opportunities to synthesise graphene directly on suitable substrates, and avoiding the need to lift and transfer graphene from metal. In this particular example, graphene was grown directly on the thermally oxidized SiO<sub>2</sub> layer present on the surface of Si wafer. The latter is the most widespread semiconducting material presently used electronics, from integrated circuits to mobile phones and tablets, wearable sensors and devices [64], photovoltaics, sensors and others. Following standard cleaning to remove impurities from the surface, and immediately prior to the synthesis stage, substrates were exposed to hydrogen plasma to remove any possible contaminants that may have remained from the cleaning. The vapours of *Citrus sinensis* oil were then released into the chamber. Because essential oils are inherently volatile, and have sufficiently high vapour pressure under ambient conditions, it was not necessary to use heating to generate oil vapours. Previous studies have also shown similar graphene quality when using essential oils (a mixture of >100 plant secondary metabolites) and their individual components, allowing for the use of oils directly, without purification or modification.

#### TIMELINE FOR DEVELOPMENT OF HIGH TEMPERATURE GRAPHENE SYNTHESIS

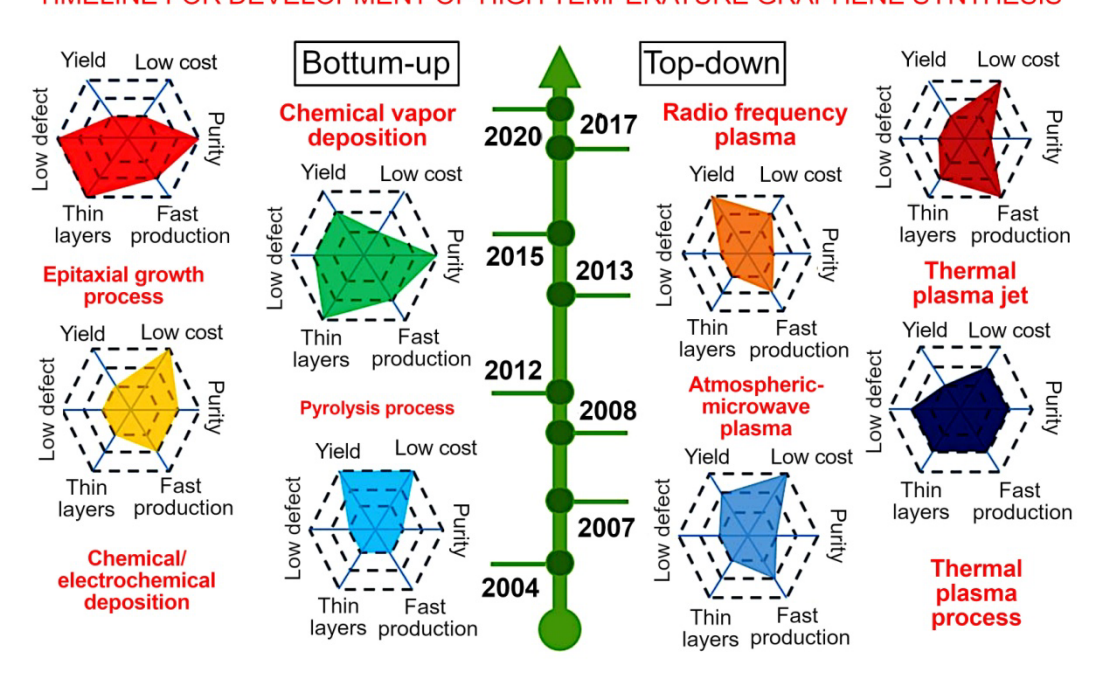


**Figure 11**. Bottom-up or top-down routes of nanosynthesis in plasma environments, and the timeline for the development of high temperature graphene synthesis. Each product has been evaluated in terms of 6 critical elements: (1) presence of defects, (2) yield, (3) cost, (4) purity, (5) production rate and (6) the number of layers. The inner, middle and outer hexagons correspond to low, medium and high levels, respectively. Reproduced with permission from *ACS Nano* **2021.**<sup>[166]</sup>

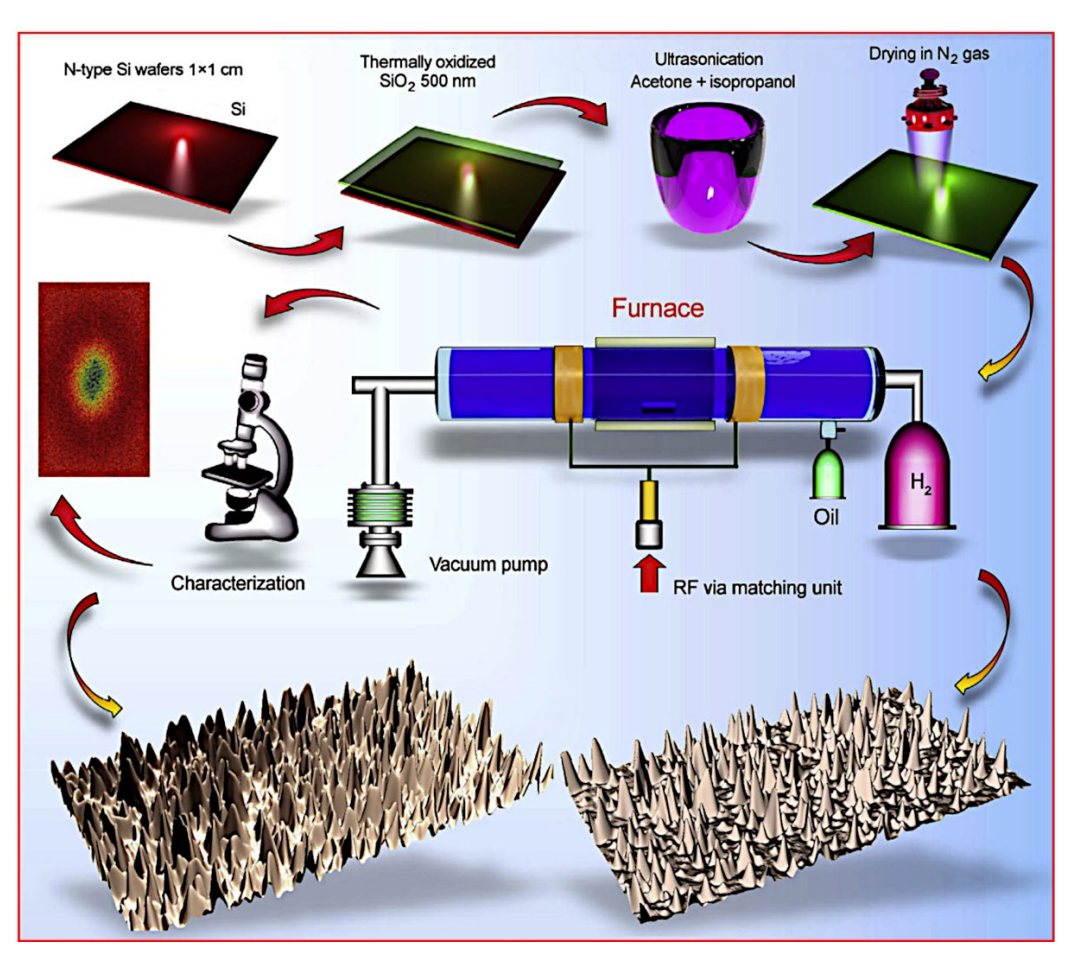
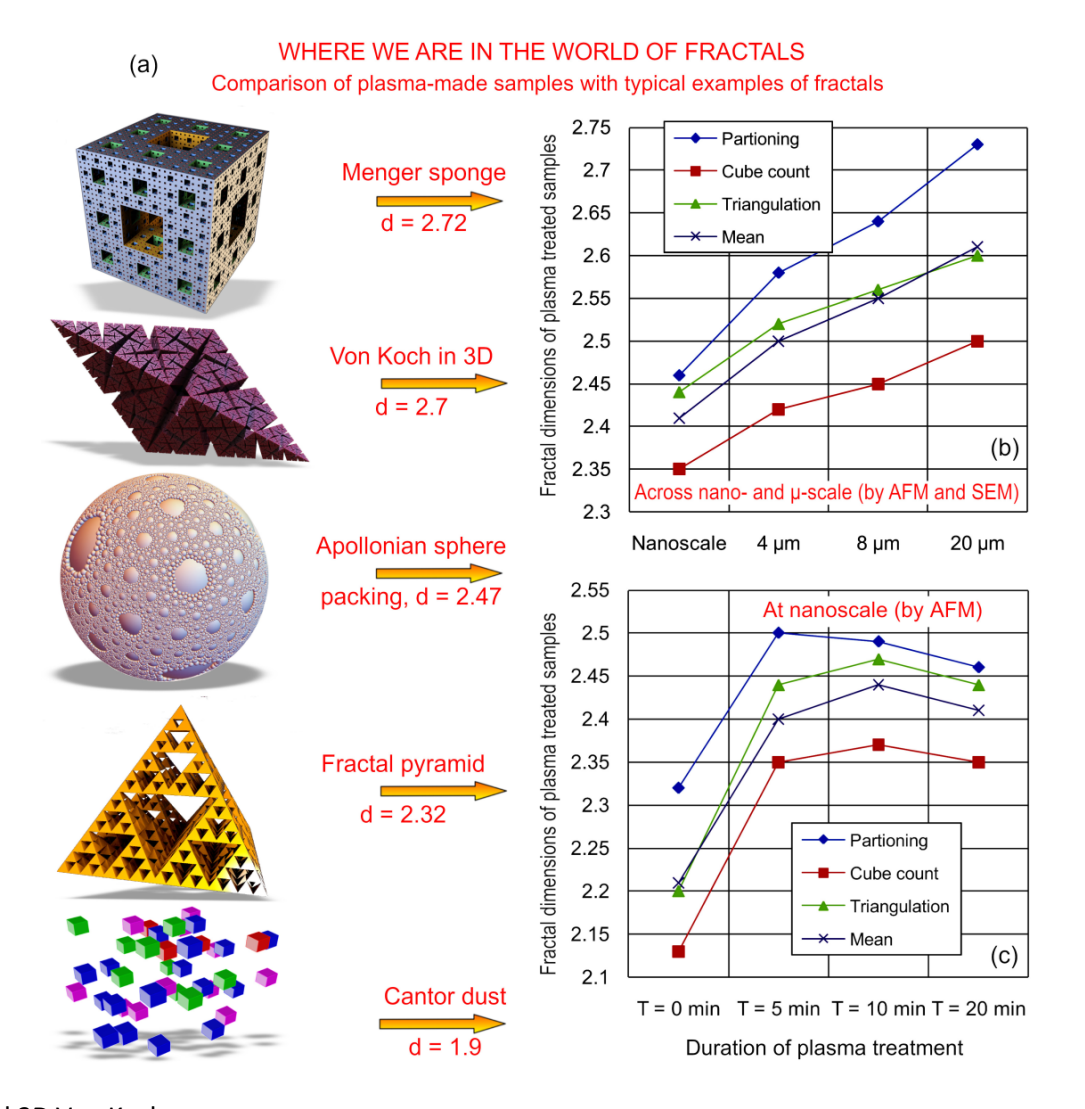


Figure 12. Top panel: Brief overview of the key stages of direct conversion of essential oil into surface-bound graphene networks that are oriented orthogonally to the substrate in low-temperature plasmas, in the absence of catalyst. While most substrate heating is due to ion bombardment that transfer energy from plasma to surface, a furnace is also used to provide an additional increase in substrate temperature for optimal building block diffusion across the surface, and hence optimal growth of desired graphene structures over a wider range of plasma input powers. Bottom panel: Representative three-dimensional morphology of surface patterns that could be realised using this system. Dense networks are seen on the left and more rarefied arrays of vertical graphene are seen on the right. Reprinted with permission from Carbon 2020.<sup>[138]</sup>

While in this particular example, some external heating was used to supplement plasma-induced heating to optimise the movement of building blocks and control the rate of graphene growth on the surface, it may be possible to lower the temperature budget through a careful selection of environmentally sustainable catalysts. Furthermore, many natural materials, e.g. plant biomass and honey, carry in their composition a small quantity of minerals. These mineral particles may act as catalytic sites where the growth may be initiated, circumventing the need for an additional catalyst material. Furthermore, many natural materials have inherent patterns and multiple levels of organisation. It may be possible to use the se inherent patterns as a template to realise even more complex material architectures while maintain the single step, green, and environmentally friendly nature of this PECVD process.

The technology used in this example also illustrates much higher controllability of the plasma-based process over the thermochemical counterpart. Indeed, even a relatively limited set of parameters that was examined by this study has shown great potential in controlling the array morphology, with additional control mechanisms also available. Moreover, plasma-based technology allows sophisticated control over higher-order morphological characteristics of the produced nanomaterials, such as the distributions of Minkowski boundaries and fractal dimensions. [167-169] Interestingly, the fractal dimensions of the plasma-made functional nanomaterials can be directly related to the fractal properties of the surface morphology. [170-173] Recently, Piferi *et al.* has demonstrated that very strong hydrophilic behaviour could be realised by oxygen plasma treatment of the surface. This is because wetting of the surface is inherently linked to the nature of surface patterns, particularly their ordering, connectedness and fractal dimensions. The latter could potentially be the most important descriptor to predict and hence control the surface

properties. [3] Such a deep level of controllability of the nanomaterial properties has been achieved by application of highly reactive plasma environments. **Figure 13** illustrates the fractal dimensions estimated for the set of samples resulting from this experiment, as well as 3D objects that display similar fractal properties, including an Apollonian



sphere and 3D Von Koch.

**Figure 13**. Illustration of fractal objects that share similar features with samples processed in the plasma environment (a). Fractal dimensions estimated for the set of samples resulting from these experiments, and their distribution across nano- (b) and micro-scales (c). Reprinted with permission from *Adv. Mater. Interfaces* **2021.**<sup>[3]</sup> The images of Menger sponge and Von Koch objects are reprinted under conditions of Creative Commons licenses. The image of Apollonoan sphere are reprinted from *Class. Quantum Grav.* **2020**<sup>[174]</sup> under the conditions of Creative Commons 3.0 license.

Another example of graphene synthesis directly from the low-value organic products is the production of high-quality graphene nanoflakes through the decomposition of the organic bio-precursor<sup>[175]</sup> in the *atmospheric pressure plasma* environment. In this work, the authors used a very simple technology for the single-step break down and reforming of biofuels, *e.g.* ethanol, in the absence of any metal catalyst or specific substrates. This technology offers a number of advantages over similar low-pressure plasma approaches that necessitate the use of vacuum chambers, pumps and other expensive and complex equipment.<sup>[176,177]</sup> These factors make this technology easier to incorporated into existing industrial workflows, at a significantly lower production cost. Importantly, materials produced using this technology show excellent reproducibility, due to superior stability of this technology across a wide range of experimental conditions. **Figure 14a** illustrates the basic design and operating principles of the set-up. The waveguide element of the torch enables wave-mode conversion, and the coaxial elements enable impedance matching. The plasma discharge was produced at the terminal (tip) point of the cylindrical hollow metallic rod. The discharge had a flame-like morphology, and protruded from the discharge area into the atmosphere, where the plasma-generated species come into contact and interact with the ambient species (*e.g.* atoms of nitrogen), thereby changing both the chemistry of the ambient air and the kinetics of the

plasma jet. **Figure 14b** shows the complex relationship between the mechanism of ethanol decomposition and such operating parameters as the flow of argon (used for plasma generation due to its low ionisation potential and stability of thus-generated plasmas) and ethanol. The rate of graphene production increased with an increased ethanol flow, reaching a maximum at 3.40 g  $h^{-1}$  (at 300W), with higher flow rates resulting in the reduction in the graphene production in favour of methane and ethylene. **Figures 14c,d** illustrate the physical appearance of the plasma torch for different rates of Ar flow.

#### **GRAPHENES IN PLASMA**

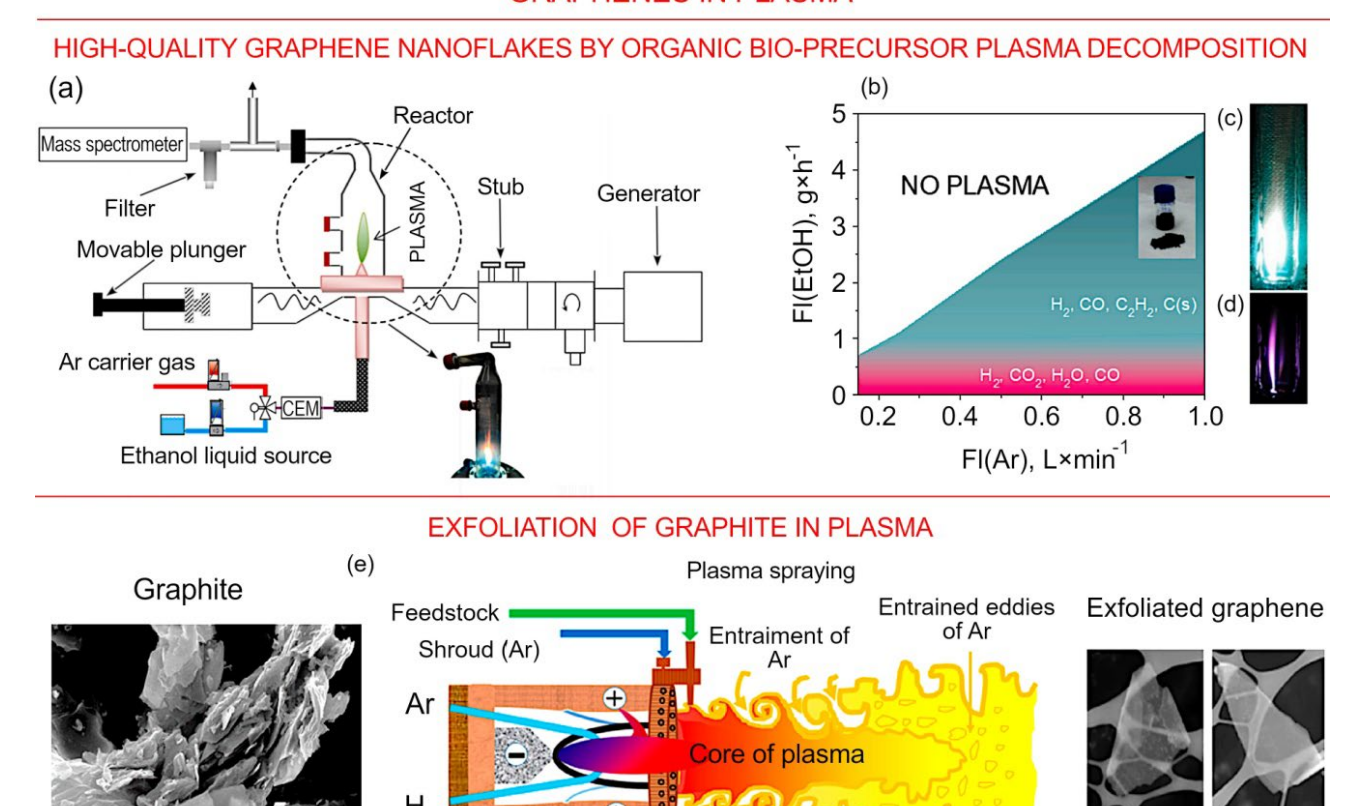


**Figure 14**. (a-d) Schematics of the experiment on the production of high-quality graphene nanoflakes by *organic bio-precursor* plasma decomposition. Schematics of products obtained from ethanol decomposition in a microwave argon plasma torch sustained by Ar and ethanol. Reproduced from *Fuel Proc. Technol.* **2021**<sup>[175]</sup> under the CC BY license. (e) Schematic representation of the exfoliation mechanism of graphite. Reproduced with permission from *ACS Nano* **2021**. [166]

12000 - 9000 K 9000 - 6000 K 6000 - 4000 K 4000 - 3000 K

2000 - 1000 K

Vorticity-contained fluid

Ar 1

Laminar region

Turbulent region

In addition to graphene flakes, high quality photoluminescent carbon dots for medical applications can be produced from ethanol during its plasma-assisted conversion into hydrogen gas<sup>[178]</sup> at very mild conditions of  $40^{\circ}$ C and in the absence of catalyst. The dots are formed from the carbon atoms that would otherwise form a CO and CO<sub>2</sub> gaseous by-products. In addition to offering a hydrogen yield exceeding 90% at ~0.95 kWh/m³ of H<sub>2</sub> produced, this plasma system is highly flexible, supporting several modes of spark plasma discharges, specifically, the single spark, multiple spark, and gliding spark modes, each having its unique combination of energy transfer and distribution.

It should be noted that plasma can also contribute to the generation of biofuels and precursors for subsequent synthesis of materials via a number of pathways. For one, plasma can substantially reduce the cost and energy of depolymerisation of lignin and other recalcitrant biomolecules into value-add aromatics and dicarboxylic acid derivatives. Zhou *et al.* used plasma discharges created over ethanol containing lignin to create highly energetic and chemically-reactive environments for lignin conversion, reaching a base yield of 42.6% and up to 66.0% when Fe<sub>2</sub>O<sub>3</sub> and H<sub>2</sub>O<sub>2</sub> were used. The increased yield was attributed to the more oxidative environment under these conditions.<sup>[179]</sup> When this set-up was used to directly convert wet microalgae into platform chemicals, a liquid yield of 73.95 wt % was obtained after 3 min of processing in the presence of the acid catalyst, and of 69.80 wt %

generated after 7 min in the presence of the basic catalyst.<sup>[180]</sup> The ability to reform wet algae is a highly attractive feature of this technology, since the cost of drying that is necessary for most thermochemical routs carries a significant cost. The solid product that forms during liquefication is a 3D carbon network that can be easily upgraded for energy storage and water purification applications. Secondly, plasma can be used to enhance the efficacy of fermentation of ethanol using industrial microorganisms. Recek *et al.* has shown that plasma treatment of microorganisms prior to their placement into the fermentation reactor enhances the speed with which they gain biomass and convert sugar into ethanol.<sup>[181]</sup>

In addition to using various types of biomass and biomass-derived precursors, plasma-enabled technologies can be used for bulk (sub-kilogram) production of quality graphene from graphite. Islam *et al.* has recently reported a novel method for ultrafast exfoliation of graphite using a plasma spray in the absence of intercalants or solvents. with the process shows high single-layer selectivity (~85%) at a considerable rate of production of ~48 g/h. The mechanism is believed to involve the sequence of a sudden thermal shock and two-stage shear, a phenomenon intrinsic to plasma. Schematics of the structure is illustrated in **Figure 14e**. Injection of graphite particles into the laminar region of hot plasma results in an immediate high temperature (>3400 °C) shock, with the damage to the graphene lattice being prevented with the help of a gas shroud made of inert argon. [166]

#### 4.3. Plasma-synthesised bioactive polymers and coatings from natural products

Bioactive nanomaterials promise to significantly advance several fields in nanomedicine, [182,183] bioapplications<sup>[184,185]</sup> and bioactive nanomaterials.<sup>[186-188]</sup> In addition to reactions where natural materials are broken down to atoms or small fragments and then rebuild into carbonaceous materials with a completely different structure, e.g. graphene, plasma environment can be sufficiently gentle to sustain the fabrication of polymers and polymer-like structures where the chemical structure and hence inherent biochemical activity of the precursor is preserved. [189] One such example is the use of RF plasma to produce antibacterial coatings from Melaleuca alternifolia essential oil, a traditional oil often used as an over-the-counter antimicrobial and in the production of cleaning and animal grooming products due to its very broad-spectrum activity against bacteria, fungi and viruses. Importantly, due to gentle nature of this process, the coating can be applied over virtually any material, including thermally sensitive and thin film devices without damaging their structure. This opens up their use for optoelectronic and biomedical applications, e.g. as optically transparent defect-free coatings capable of preventing microorganism settlement and biofilm formation. [190] Depending on the parameters used during plasma synthesis, it is possible to fabricate highly stable biocompatible coatings that have electron-blocking hole transporting properties that can be used to control charge transport in organic electronics. [126,191] By reducing the intensity of plasma, it is also possible to fabricate coatings with strong antimicrobial activity and biodegradable profile. Figure 15 illustrates the general flowchart of the experiments for controlling bioactivity of polymers deposited from oil, in this case the Melaleuca alternifolia essential oil (tea tree oil). As mentioned previously, the use of essential oils for RF-PECVD synthesis of polymer and carbonaceous coatings is attractive due to their inherent volatility under the ambient temperature and pressure, which alleviates the need for precursor heating or the use of solvents and carrier gases. By using very low input energy of 10-30 W, it was possible to preserve much of the chemical structure of the precursor while at the same time producing a solid coating that is well attached to the surface of the substrate. Due to the low degree of ionisation, the temperature of the substrate did not exceed 30 °C (**Figure 15**).<sup>[192]</sup>

These coatings are highly effective against attachment and proliferation by *Staphylococcus aureus* and *Pseudomonas aeruginosa*, common pathogens responsible for a large proportion of infections associated with orthopaedic and urinary tract implants, respectively. Moreover, due to their controlled degradation profile, these coatings may be used over bioresorbable implants, *e.g.* magnesium sutures, to slow down the degradation of the latter, so that the mechanical properties of the implant are maintained to support tissue healing. Interestingly, the bioactivity of some of these polymers may receive a further boost from an *in situ* treatment with atmospheric pressure plasma jet used in dental treatment and wound decontamination. This brief plasma treatment of surfaces and surrounding liquids may lead to the formation of loosely attached bioactive fragments on the surface

of the polymer, that could rapidly release active agents into the peri-implant milieu and thus contribute to the baseline concentration of active agents available. Thus, the bioactive polymers were produced at a very low plasma power and without energy-consuming external heating, and thus this process could be quite suitable for the production of high-value medical devices.

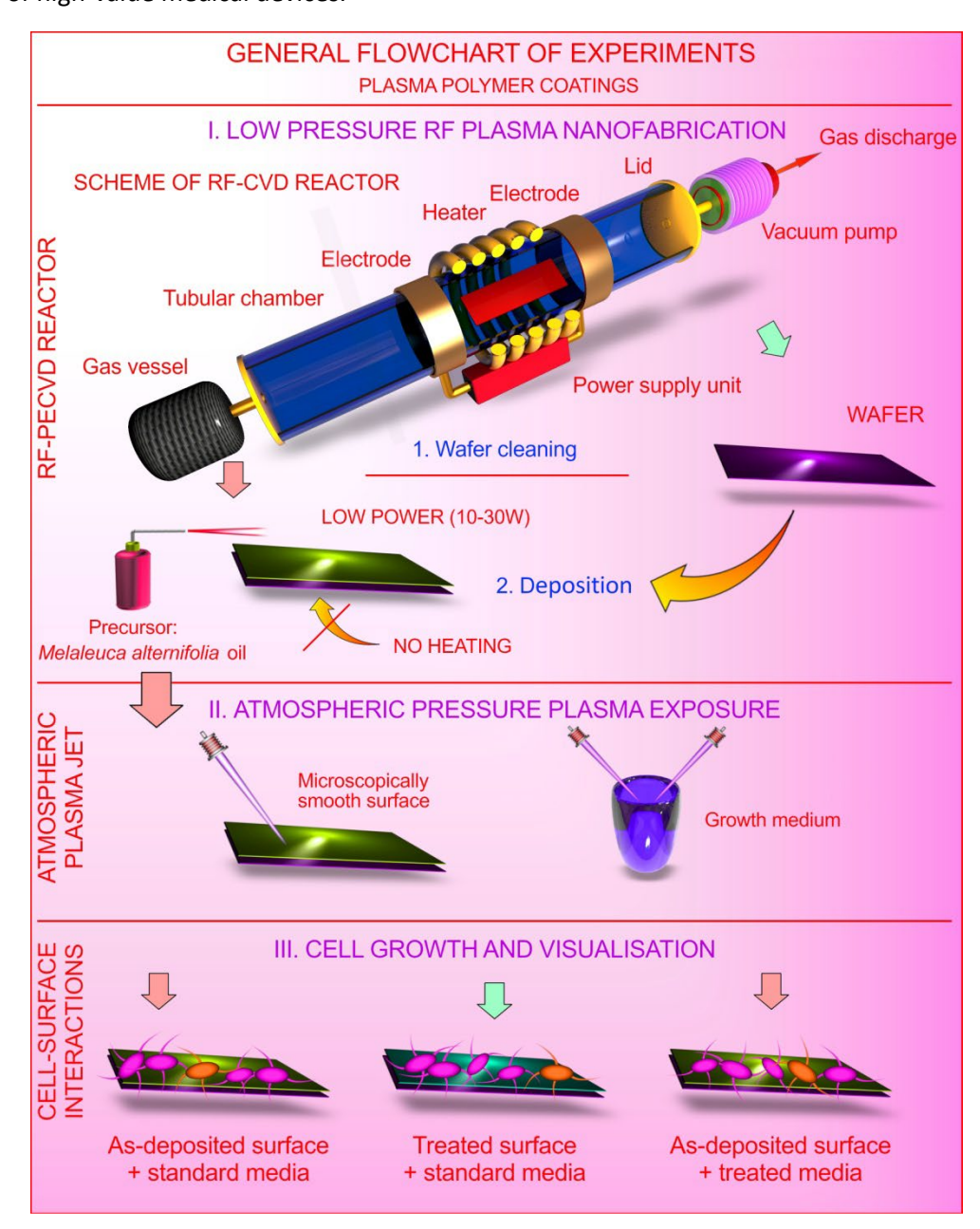


**Figure 15**. Schematics of the experiment where antimicrobial polymers were first fabricated from the vapours of *Melaleuca alternifolia* (tea tree) oil, and then exposed to atmospheric pressure plasma treatment that has been designed for *in situ* decontamination of implants and wound treatment. The bioactivity of some of the polymers was improved as a result of this exposure, suggesting a possible pathway to take advantage of synergies that may result from some polymer-surface treatment combinations. Reprinted from *Molecules* **2021**<sup>[192]</sup> under the terms of CC BY license.

#### 4.4. Carbonous core-shall and nanoporous nanomaterial from natural by-products

One more successful technology for the valorization of *Citrus sinensis* essential oil, an abundant and affordable by-product of orange juice production, has been recently demonstrated by Alancherry *et al.*<sup>[82]</sup> Using radio-frequency (RF) plasma, the *vertically oriented multilayer graphene nanosheets interspersed with carbon nano-onions* were fabricated in a single step using a relatively simple set of control mechanisms (**Figure 16(I)**). The nano-onions were hollow and quasi-spherical in structure, and were integrated into high-quality graphene layers during graphene growth. Similar to the previously discussed example, a simple tubular reactor was connected to the RF generator by means of two capacitively coupled copper electrodes, using an impedance matching network to ensure

efficient energy transfer from the generator to the deposition chamber. Pre-etching in hydrogen plasma was once again used to remove remaining contaminants from the surface. The synthesis was initiated immediately upon vapour release into the chamber and lasted several minutes (find more details in the relevant publication.<sup>[82]</sup>

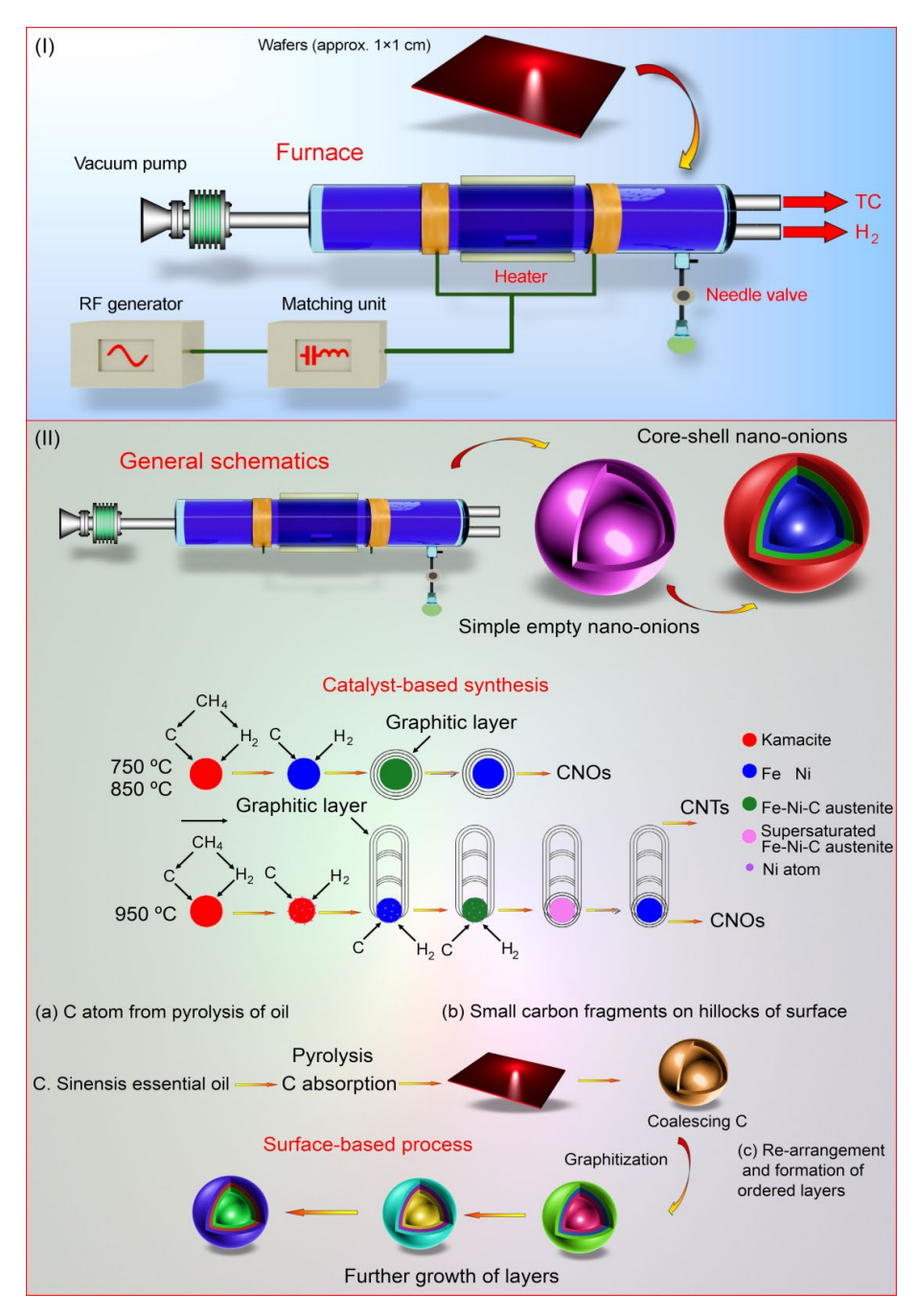


**Figure 16**. Schematics of the experimental set and growth mechanism for the formation of complex graphene nanostructures with embedded nano-onions directly from the vapours of *C. sinensis* essential oil in plasma. The growth follows the initial stage of formation of sub-microscopic graphene nuclei on copper and surface that do not have high solubility of carbon, the subsequent stage of edge growth, formation of a carbon ring or, alternatively, a multilayered structure, and continued growth that produced layered two- or three-dimensional microscale structures. Reprinted with permission from *ACS Appl. Mater. Interfaces* **2020.** [82]

The material platforms produced in this study displayed excellent hydrophobicity, as well as favourable electrical properties and unique morphology, confirming its potential across multiple fields. For example, when used in a *chemiresistor sensor*, this material displayed good p-type semiconductor response to acetone vapours at ambient temperature. The mechanism behind the synthesis and incorporation of nano-onion into the surface of growing graphene flakes is presented in **Figure 16(II)**. It should be noted that the where typical thermochemical synthesis of such onion structures would demand externally generated temperatures in excess of 1000 °C, plasma-based technology can support the production of these structures at significantly lower temperatures, thanks to high reactivity and energy of ion fluxes to the surface. [194,195] In addition to the immediate cost and time savings

stemming from this phenomenon, such an environment may facilitate a greater level of control, [196] and less damage to the crystalline lattices of the substrates and carbon lattice of the growing nanostructure. [197,198] Biowaste-derived carbon nano-onions are very promising for various application of high importance including energy storage devices. [199,200]

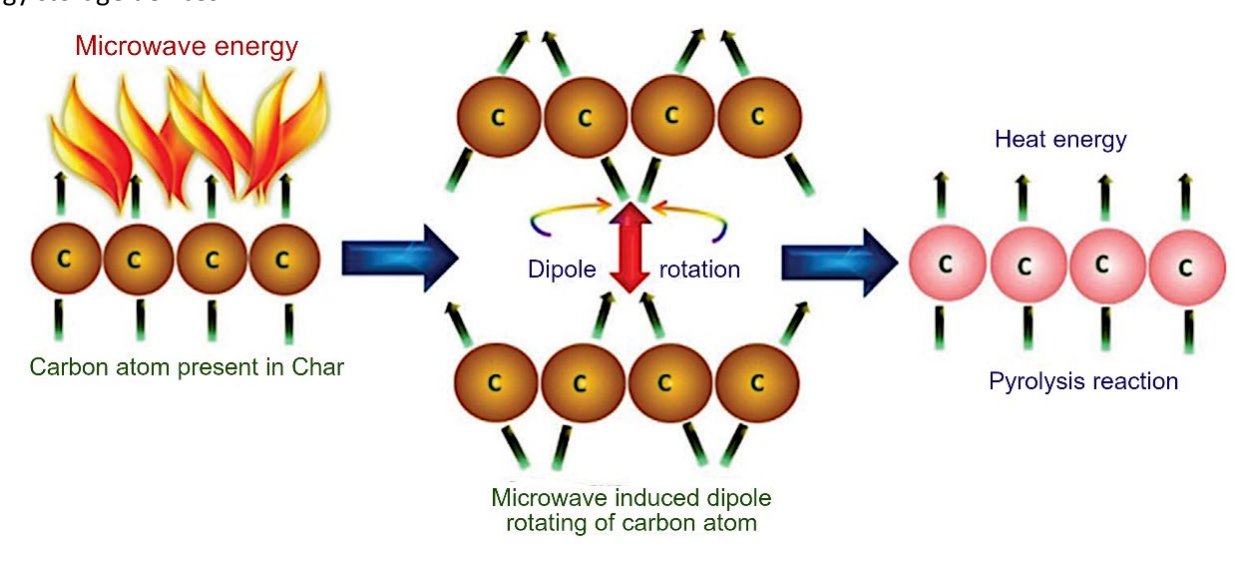


**Figure 17.** Microwave pyrolysis technology to synthesize nanoporous carbon materials from banana peels. Scheme of microwave-enabled pyrolysis cracking via heat generated through the dipole rotation of carbon molecules. Reproduced with permission from *Bioresour. Technol.* **2018**. [201]

Banana peel waste is one more example of widely abundant biowaste. The total production of banana reached 22.2 million tonnes in 2020,<sup>[202]</sup> this makes the banana peel a very attractive biowaste for the production of nanostructures.<sup>[203]</sup> Commonly, banana peel is disposed using the landfill technology that implies high energy and labour resources and causes the release of methane and carbon dioxide which are produced during the microbial decomposition of organics. Liew *et al.*<sup>[201]</sup> used the microwave pyrolysis technology to synthesize nanoporous carbon materials from the banana peels (**Figure 17**). The peels were first rinsed, then cut to smaller pieces and dried at 110 °C for 24 hours. Then, carbonization and chemical activation was made using the microwave energy with a frequency of 2.45 GHz in nitrogen for 20 minutes, 700 W of microwave power. Importantly, banana peels efficiently absorb the microwave energy, this makes the process quite efficient. Several cycles of chemical activation and microwaving were used (please find more details in the original publication<sup>[201]</sup>). This material possesses the micro-mesoporous structure with a high BET (Brunauer, Emmett and Teller) surface area reaching 1038 m<sup>2</sup>g<sup>-1</sup>, efficient for the textile dye absorption. The authors demonstrated that the novel material is capable of removing about 90% of the Malachite green dye.

#### 4.5. Nanocarbons and vertically oriented graphenes from oil and plant wastes

Groundnut shells, an abundant natural biowaste, was used to produce nano-carbons (NCs) via a cost-effective, green technology. To do this, Yallappa *et al.*<sup>[204]</sup> (**Figure 18a,b**) used a simple, single step pyrolysis technique, with the nitrogen as a plasma-carrying gas. Importantly, the synthesised nano-carbons feature remarkable biocompatibility. Along with this, the produced nanocarbons have demonstrated also the biocidal activity towards several types of bacteria, including *Chromobacterium violaceum* and *Bacillus cereus*. The authors stress that the nano-carbons could find application as a mean for inhibition of microbial growth, as well as in drug delivery systems. In a different study, Wu and colleagues demonstrated the conversion of waste lard oil, another abundant waste material, into vertical graphenes using the inductively coupled plasma technology<sup>[205]</sup> generated in a very simple, cheap reactor consisting of a furnace, a quarts tube and an induction coil used to ignite plasma in the

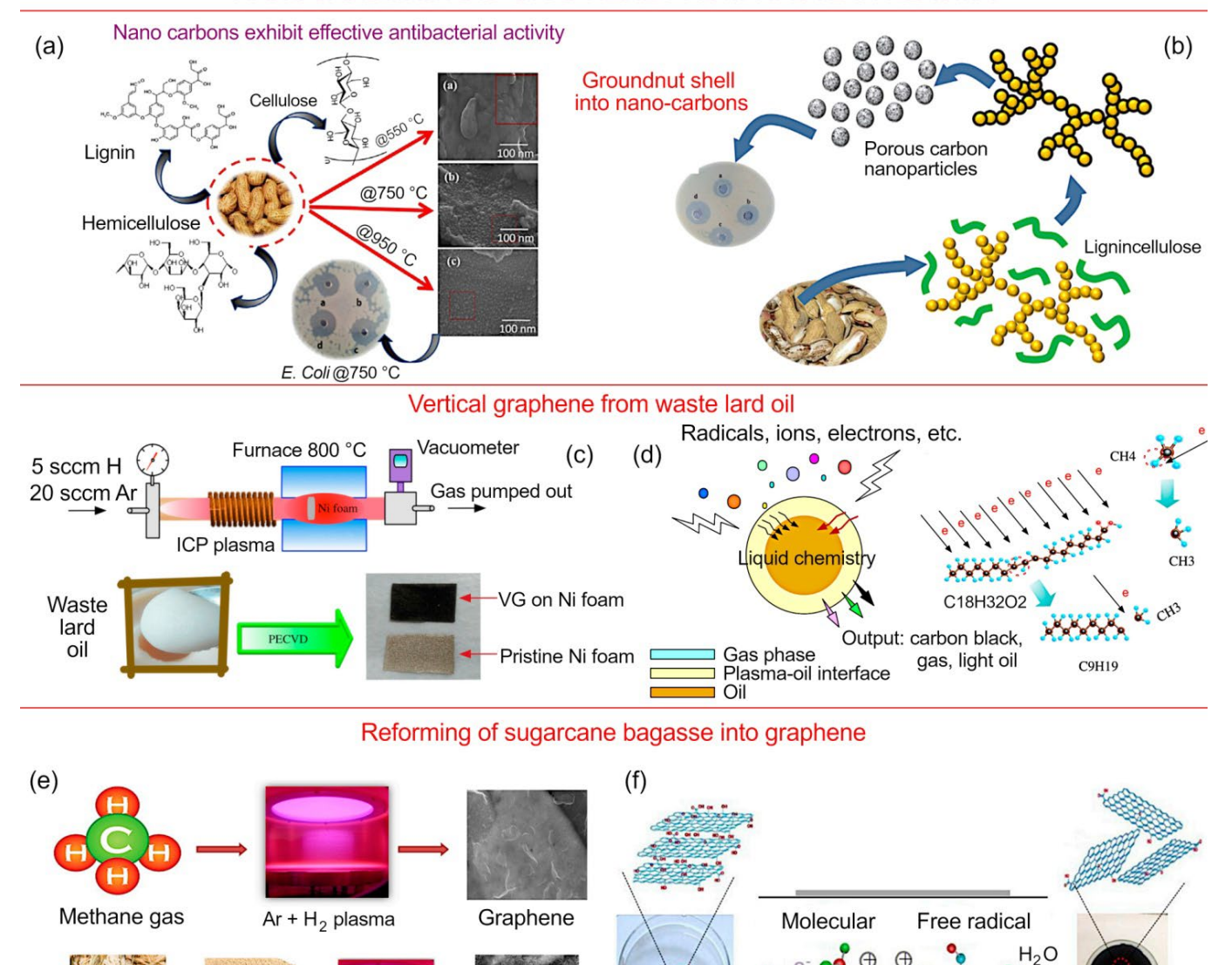
tube. To control the conversion process, temperature and concentration of hydrogen in the process environment were used (**Figure 18c**). In this process, the fatty acid chains were primary broken by the electron flux from the plasma (**Figure 18d**). Moreover, the produced graphenes exhibit super-hydrophobic properties with the contact angle for water exceeding 140°.

Prasad et al. demonstrated the conversion of methane and sugarcane bagasse, another abundant and difficult to utilise source of waste, into graphenes nanowalls<sup>[206]</sup> and confirmed its antifouling properties, important for e.g. marine antifouling technology. [207] Attachment of both Gram-positive Staphylococcus aureus and Gram-negative Escherichia coli bacteria were tested and compared with their attachment onto copper, which is a good antibacterial agent. The total process time for the material synthesis was only 10 minutes, and the processing temperature was about 400 °C. In all antimicrobial studies, as-produced graphenes were used, and additional functionalisation was not involved thus keeping the simplicity and cost at the minimum (Figure 18e). In the similar technology, plasma exfoliation of graphenes from natural graphite flakes and possible application of this material for application in lithium batteries were demonstrated by Luo et al. [89] (Figure 18f). In these experiments, a simple setup with a dielectric barrier discharge was used and the process was conducted in a hydrogen environment. Thus-synthesized graphenes have few layers. When tested as a promising material for cathodes in Li-Ion batteries, they demonstrated quite remarkable properties including high capacity, as compared with carbon black. The synthesis is environmentally friendly, since no harmful substances were used at any stage of the process. Kuang at al. demonstrated the fabrication of vertical graphenes from waste oil. The characteristics promising for the supercapacitor applications were also demonstrated. [208] A simple inductively coupled plasma reactor operating with Ar gas was used to enable the formation of vertical graphenes on substrates with a large area (Figure 18g,h). Nanocomposites of MnO<sub>2</sub> and vertical graphenes were also prepared and tested, and provided the power density of 10.2 kW/kg. The authors analyzed the cost of the graphenes and concluding that it could be reduced by more than 30%.

To better understand the formation of vertical graphene in plasmas generated using affordable and abundant qaseous precursors such as CH<sub>4</sub> (widely available as a waste gas in e.g. an agricultural industry), Baranov et al. have developed a multi-scale, multi-factor model. [209] This model was developed and tested against experimental results reported in a substantial body of literature, and provided insights into critical chemical and physical processes that govern the outcome of key stages in the plasma growth, including nucleation of the graphene lattice, vertical and horizontal growth of the flake, and eventual formation of interconnected graphene walls in plasma. The model also allowed for the investigation of processes that at present may be difficult to capture and analysed experimentally, including diffusion of adatoms and radicals across the substrate surface. [210,211] Surface diffusion fluxes and not direct fluxes from the gaseous bulk were shown to play a critical role in the growth. Ion bombardment was identified as an important 'switch' between different growth modes. This is because ion bombardment is knows to introduce defects into the surface, thereby increasing its energy of surface adsorption. This model shows that the ion bombardment-induced production of hydrocarbon radicals on the surface of the substrate, and their subsequent diffusion towards the nanoflake is what drives and sustains the growth of the latter. Importantly, this study has confirmed the leading role of the intrinsic plasma processes that are not present in the thermochemical routes of nanosynthesis - ion bombardment from plasma and radical generation in the bulk plasma and on the surface.

- ✓ The above discussed examples of plasma-based technologies for the production of complex functional nanomaterials from the biowaste and cheap natural products show the great potential of plasma methods for the cases when very complex material systems should be produced. This may be impossible with the simple thermochemical routes, but application of more expensive plasma-based techniques would be justified to produce the nanomaterials with exceptional properties and hence, with very high value.
- ✓ The theoretical analysis of the processes in plasma during the nanostructure growth from a simple gaseous precursors such as methane, which is a by-product of many agricultural and food industries, evidenced very

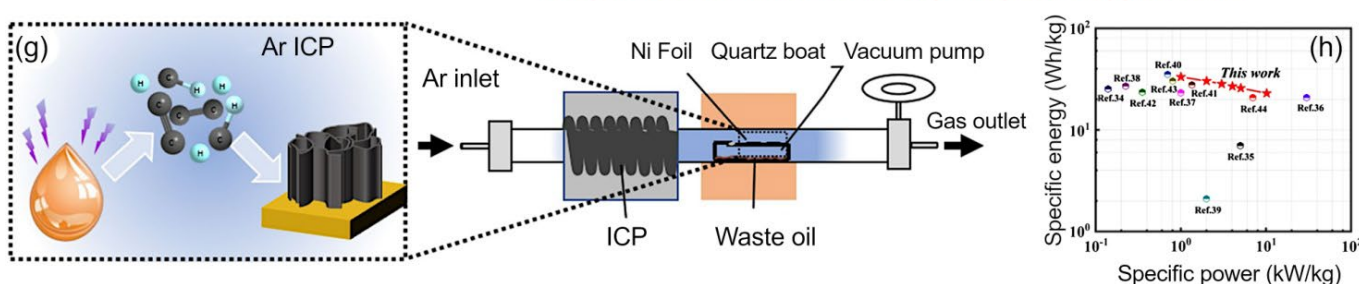
#### NANOCARBONS AND GRAPHENE FROM WASTE IN PLASMA



#### Graphenes from waste oil for supercapacitor applications

DBD plasma treatment

**PEGN** 



GO

Graphene

 $Ar + H_2$ 

plasma

Sugarcane

bagasse powder

Sugarcane

bagasse

**Figure 18**. Nanocarbons and graphenes produced from natural waste via plasma-based technology. (a,b) nanocarbons derived from natural biowaste of groundnut shell demonstrate remarkable antibacterial activity. Reprinted with permission from *Nano-Struct. Nano-Objects* **2017**. [204] (c,d) Reforming waste lard oil into vertical graphenes using ICP CVD process. Scheme of the setup (c); mechanism of decomposition of waste lard oil, and breakdown of fatty acid chains induced by electron collisions. Reprinted from *Nanomaterials* **2017** under the conditions of CC BY license. [205] (e) Conversion of methane and reforming of sugarcane bagasse into graphene using plasma technology. Reprinted from *Nanomaterials* **2017** under the conditions of CC BY license. [206]. (f) Plasma exfoliation of graphenes from natural graphite flakes for application in lithium batteries. Reprinted from *Materials* **2019** under the conditions of CC BY license. [89] (g) Synthesis of vertically oriented

### 5. Plasma and thermal methods – thus, what to prefer?

Plasma-based methods and techniques for the valorization of biowaste and cheap natural produce, along with negative-value natural wastes are relatively simple and cheap yet more expensive than thermochemical technologies that utilize furnaces and simple burning methods. On the other hand, plasma-based methods are capable of significantly enhancing the quality and complexity of thus-produced functional nanomaterials. Efficient production of various useful products and materials such as *e.g.* carbon nano-onions from orange oil for sensing applications, and vertical graphene for energy applications and flexible electronics, and others were demonstrated. Relatively simple techniques such as capacitively coupled radio-frequency and plasma-enhanced chemical vapour deposition (PECVD) are capable of the production of very complex nanostructures with the great potential for various applications.

Productivity is one of the main parameters of any process (Figure 19), and it can be boosted by increasing the reaction area and the reactivity of the components involved in the process. Growth of nanostructures to create a surface with high surface-to-volume characteristics, such as growing nanorods, nanosheets, nanotrees etc., as well as introduction of solid seeds into gas phase are the routes applied in thermochemical technologies. These control mechanisms can be further exploited in plasma to get the additional benefits, such as a directional and ordered growth of nanostructures on a surface by use of self-masking or self-patterning in plasma to realise the synthesis of more complex structures. Plasma also expands the application possibilities by implementing the processes of ejection of solid clusters and liquid droplets into the gas environment, such as those taking place in an arc discharge. In addition, the rate of the introduction of the neutrals into a gas can be accelerated greatly through the use of physical sputtering of the material from the surface caused by the bombardment with ions; the latter are created in glow discharge or in the capacitively coupled plasma (CCP) enhanced by a magnetic field. Here, implementation of the traditional means of thermal chemistry coupled with the ion bombardment allows increasing the rate of the sputtering by an order of magnitude, and shifts it from the conventional sputtering to plasma etching. In turn, the rate of evaporation of neutrals is also increased greatly when adsorbing the arc discharge power on the surface, and transforming the physical sputtering or chemical etching into thermionic emission of atoms from the surface.

The control over the concentration of reagents and the creation of the reagent mixtures directed to a specified area of a reactor define the reaction area. Pressure gradients created by the difference in the concentrations of neutrals, and heat fluxes, are traditional tools that are successfully used in thermal chemistry for this purpose, while plasma ensures the control of the fluxes of neutrals by converting them into charged particles guided by the magnetic field and the electric field generated in plasma. In addition, the application of the electromagnetic focusing of plasma fluxes allows controlling the ion-to-neutral ratio in the fluxes that is beneficial in controlling the growth of the surface nanostructures. To increase the reactivity of the components, activation of chemical bonds in gas or on the surface is necessary, which is performed by use of the rich diversity of traditional chemistry; however, the transition of the matter into the plasma state opens up new opportunities such as formation of metastable materials that cannot be done under conditions of thermal equilibrium. Here, various methods of plasma generation in electrodeless reactors like the inductively coupled, microwave, and their magnetically enhanced versions (helicon, electron-cyclotron resonance sources) allows increasing the rate of the process drastically. [212,213]

Moreover, the surface can be activated (or functionalized) by the ballistic processes of generation of vacancies and dislocations caused by the ion bombardment, exposure to the electron beams, or by subjecting to the thermal-elastic processes of ejection of the clusters or droplets followed by the generation of craters on the treated surface. As for the gas phase, generation of plasma makes it possible to grow various nanostructures directly in gas phase, like the growth of graphene flakes in arc discharge. At the same time, the thermal chemistry processes allow conducting the growth of nanostructures with much more perfect crystallinity, since the irradiation by the ion and electron fluxes results in the formation of the morphology enriched with the defects. However, the perfect

crystalline structure comes at the cost of the processing time, when a typical time of growth is measured by hours in the thermal chemistry processes, while the time lap for the plasma enhanced technologies usually do not exceed dozens of minutes.

On the other hand, plasma-based technologies are usually more expensive and more complex, requiring more educated personnel and expensive equipment, as compared with the thermochemical techniques. [214,215] Indeed, the structure of both plasma-based and thermal types of materials synthesis systems includes (i) the reaction vacuum/gas supply systems which are commonly similar for plasma and thermal systems; (ii) reaction chamber which is simple for the thermal system but could be quite complex for the plasma system as it includes additional coils, multiple power supply leads and other specific units and instruments to ignite, sustain and control the plasma, and (iii) power supply system which is also very simple for the thermal reactors needing heating only, and quite complex for the plasma systems which are often powered by radio-frequency current, require matching units and other specific electronic equipment. Apparently, this results in the significant differences in the costs of the equipment. [52,136,137] While the cost of typical small-size experimental equipment for thermal methods (furnace) is about 3000 to 5000 euros, the costs for plasma systems (e.g. microwave plasma) well above 15000 euros and could be very high for special systems incorporating several types of plasma sources e.g. ICP plasma, DC arc discharges and magnetrons.

#### PLASMA versus THERMOCHEMICAL ROUTE: ADDITIONAL BENEFITS PLASMA GAS **MEANS MEANS PURPOSE** Directed solid structures Neutrals Vapours with high surface-to-**EFFECTS EFFECTS** Creation of volume developed REACTION net of **AREA** surface Sputtering structures Eiection of seeds from Clusters Clusters **Etching** solid into & droplets gas phase Thermal CONTROLS CONTROLS Etching Pressure Segregation Control of gradients Control of oncentration discharge of reagents power Segregation Heat flow PLASMA GAS Thermal-Reagent Thermal Flectro-Electric elastic Heat flow mixing & magnetic field guiding to control of **PRODUCTIVITY** selected plasma **FLEXIBILITY** Magnetic area fluxes Modification field **METHODS METHODS** Deposition Deposition Electron Excited impact molecules Ballistic Activation ionization of chemical in gas Growth bonds & Reactivity of Radicals Radicals change Growth of surface interaction **PROCESSES** energy Craters **PROCESSES** Ion ombardmen on surface Vacancies &

**Figure 19.** A large number of surface and in-bulk processes intrinsic to the thermochemical and plasma techniques for material treatment allows selecting plasma or thermal technology for each specific case, taking into account various criteria – cost, energy efficiency, complexity of the target nanomaterial, and many others. This would ensure further economic benefits from the biowaste valorization and environmental remediation.

Thus, the choice between these two types of technology should be made on the basis of a complex optimization that takes into account a whole set of factors, including (i) cost and availability of precursors which is typically very low for the cases we have discussed but these precursors should be available *en masse* for the upscaled production; (ii) initial outlay and operating cost of equipment which is typically higher for plasma systems; cost of energy which may be significantly lower for plasma systems, owing to absence of large hot furnaces; (iii) cost of labour which is typically higher for the plasma-based systems; (iv) cost of production engineering including the R&D efforts for designing the industrial technology, which is typically higher for the plasma-based systems.

✓ A complex approach is needed to select the route between thermochemical and plasma-based technological platforms to implement the production of complex multifunctional nanomaterials that would ensure further economical benefits from the biowaste valorization and environmental remediation. [216]

Also, the importance of environmental remediation should be taken into account when selecting the specific technological route – thermochemical or plasma-based.

Water content in precursors is also a very important factor affecting the waste-to-material conversion techniques. It is well known that water could be a useful catalytic additive for some nanomaterial synthesis routes<sup>[217]</sup> and could also be used in the direct plasma-water processes, <sup>[198]</sup> yet other technologies could be affected by high water content. Indeed, some raw biowaste and food wastes commonly contain significant content of water, and importantly, water content is very different for various biowastes. As several examples, the water content could vary from about 80% for raw banana peel, to about 15% of water in rice husk after milling and to about 10% of water content in coir and pineapple fibre. <sup>[218]</sup> The raw peanut shell contain only about 6% of water, thus it can be used energy purposes without drying. <sup>[219]</sup> On the other hand, the water content in used oils which are quite abundant and very attractive for nanomaterial conversion, ranges from 0.05 to 0.3%. <sup>[220,221]</sup>

Thus, we could consider here the two main cases: (i) when the contents of water in the waste is low and thus, the participation of water molecules in the nanomaterial synthesis could be disregarded; and (ii) when the raw waste with a significant content of water is being treated without any previous drying. The first case (low water content) is the most common since oils does not content a significant amount of water and could be supplied directly into the process atmosphere. Several relevant examples were described in this review, e.g. nanofabrication using used commercial sunflower, soybean and engine oils, [48] reassembly of *cold-pressed Citrus sinensis oil* into vertically-oriented graphene walls of high quality, [138] *Melaleuca alternifolia* essential oil to produce antibacterial coatings, [192] conversion of waste lard oil, another abundant waste material, into vertical graphenes, [222] and others. These processes did not involve special pre-treatment to remove water from oils, and the oil vapours were supplied directly into the reactor using heating. The wastes with relatively high (e.g. peanut shell) and very high (banana peels) water contents are usually dried before the conversion.

The peanut shell wastes are typically washed in water, then dried for several days in air, and finally dried in vacuum before synthesis of few-layer graphene-like nanosheets. [223] In this case, water is fully removed from the waste and did not affect the conversion process. Similar technology is applied to the banana peels which contain a large portion of water: The peels are rinsed, cut to smaller pieces and dried at 110 °C for 24 hours; [201] hence, water is fully removed before the conversion. In the case of a "direct" thermal treatment of water-containing wastes without prior drying, the first stage (heating of the precursor) usually results in complete drying and thus, dry waste is then converted to the nanomaterial. Given that the process usually requires the temperature much exceeding the water evaporation temperature (e.g., 300 to 800 °C [98]), the precursors could be considered completely dry during the reaction.

In the case of plasma-based nano-synthesis, presence of water could be beneficial in some reactions. Apparently, the presence of water vapour can facilitate the oxidation of biowaste into oxides, e.g. graphene oxide. Similar processes could be released directly in water. [224,225] The presence of water molecules in the reaction environment modifies the plasma-chemical processes, it important to examine the specific reactions involved in each specific process of material synthesis. Water can be also useful for the degradation of refractory organic compounds. For example, Han *et al.* studied the degradation of *Dimethyl phthalate* (DMP), an environmental hormone, by the dielectric barrier discharge plasma and graphene in water via advanced oxidation processes. The degradation of the organic compound was mainly attributed to the chemical effect produced in the water reaction system, such as  $\bullet$ OH, O<sub>3</sub> and H<sub>2</sub>O<sub>2</sub> species. [226] Another successful example of direct water-plasma nanomaterial synthesis is the

recent work by Stein *at al.* Fungal mycelium was directly carbonized by microwave plasmas pyrolysis *without any prior drying*. The microwave plasma pyrolysis in argon converted the mycelium into a myco-diamond matrix containing nanostructures formed by ultra-nanocrystalline diamond.<sup>[227]</sup>

Due to plethora of physical and chemical processes that could be realized in plasma in the presence of water vapours, and also directly in the water affected by plasma (**Figure 20**), the conversion of water-containing biowastes into advanced nanomaterials could be also efficient.

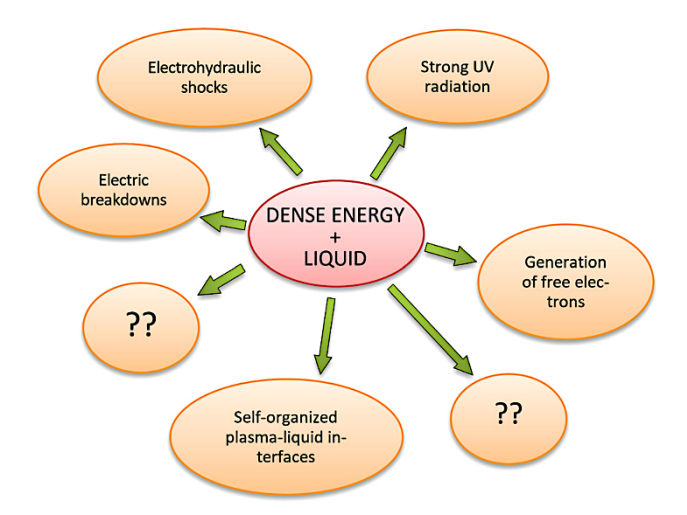


**Figure 20**. Examples of strong non-equilibrium processes in liquids under action of high-dense power. The list is open: many processes are still not fully understood and not identified. Further achievements and deeper levels of understanding are anticipated. Reprinted with permission from *Appl. Phys. Rev.* **2018**. [198]

#### 6. Outlook and Perspectives

Thermochemical methods and techniques for the valorization of biowaste and cheap natural products, along with negative-value natural wastes are simple, cheap, but still quite efficient to significantly enhance the biotechnological and agricultural sectors. Efficient production of various useful products and materials such as carbon aerogels for energy storage, graphene oxide-based supercapacitors, nanokeratin-urea composite fertilizers and graphene-based nanomaterials for the photocatalytic dye degradation and oil absorption were demonstrated. Very simple techniques such as facile wick and oil flame synthesis, soft bubble assembly, simple catalytic oxidation, freeze drying and others were found to be capable of producing quite complex hierarchical functional nanomaterials.

✓ Further development of thermochemical techniques by upscaling them to the industrial scales, as well as production of more complex, hierarchical multifunctional nanomaterials would ensure further economical benefits from the biowaste valorization and environmental remediation

The nanostructure nucleation and growth in plasma-based technological environments involves a complex set of physical and chemical processes and what is most important, these processes occur in both bulk plasma and substrate/nanostructure surfaces, in contrast to the thermal technology that relies mainly on the surface processes. Apparently, this set of processes requires the application of more complex equipment, as compared to the thermochemical methods.

✓ Modular flexible plasma treatment platforms may be quite promising for the valorization of biowastes and low-value produce by synthesis of the high-value functional nanomaterials, e.g. for energy storage and conversion applications, in the industrial scale. The high cost of the final production (e.g., electrodes for supercapacitors) could compensate the high price of the equipment, provided that the raw materials and precursors are extremely cheap.

The choice between these two types of technology should be that of a cost-benefit analysis, understanding that while the cost of plasma-enhanced may appear higher due to the higher cost of infrastructure, these costs may be recouped by the higher value quality product produced in these systems, and economic and labour savings that stem from the much shorter processing time associated with the use of plasma. Appropriate selection of a valorisation technological platform, be it thermochemical or plasma-based, or a combination of the two, will

provide a pathway for the fabrication of complex multifunctional nanomaterials that would deliver further economic benefit to the society and at the same time assist biowaste management and environmental remediation (Figure 21).

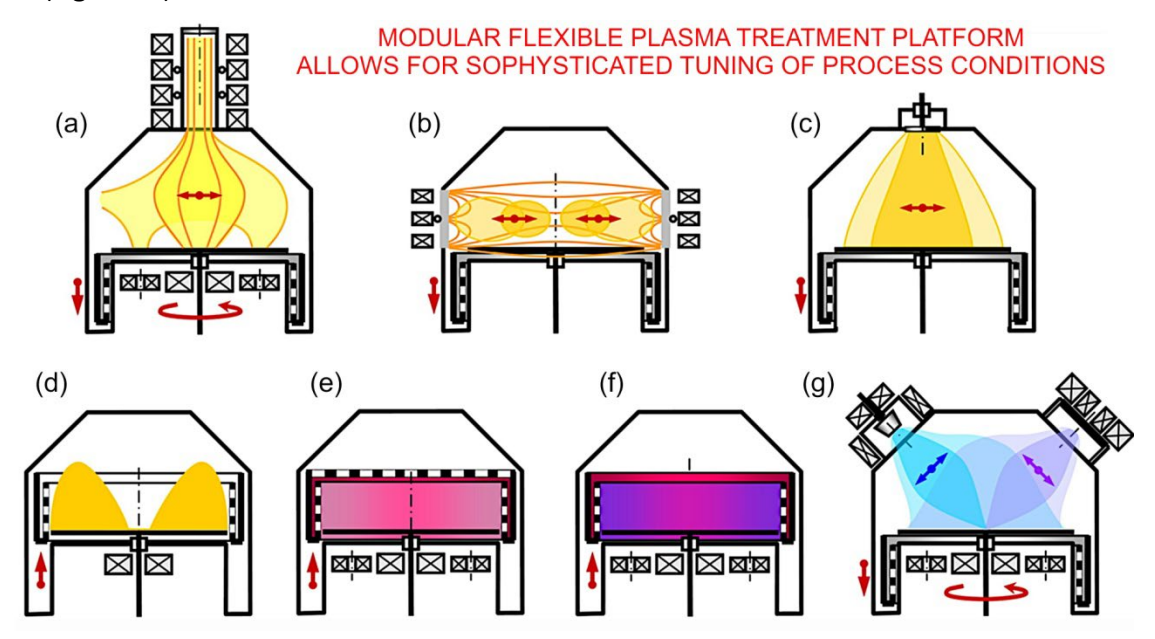


**Figure 21.** Modular flexible plasma treatment platforms may be promising for the valorization of biowastes and low-value biomass via the synthesis of high-value functional nanomaterials, *e.g.* for energy storage and conversion applications, at the industrial scale. Various configurations of magnetic and electric fields, as well as discharge localizations, plasma parameters and possibility of localised targeted heating could allow for the synthesis of very complex nanomaterials and metamaterials. Reproduced with permission from *Rev. Mod. Plasma Phys.* **2018.**<sup>[136]</sup>

Impact on carbon footprint. Decrease of carbon footprint and emission of carbonous material into atmosphere from food and other biowastes is one more important factor that is intrinsic to the direct biowaste-to-nanomaterial conversion technologies. Indeed, with the total mass of wasted food exceeding one billion tons per year, [39] the grindhouse gas generated by the wastes significantly exacerbates the climate change. [228,229] Indeed, the emission of CO<sub>2</sub> from the food waste end-of-life phase accounts for 20.2% of the total emission from the whole life cycle of food production and utilization. To compare, the cycle of agricultural goods production accounts for 63.1%. [230] The development of advanced techniques for direct conversion of wastes to useful materials via carbonization, i.e. without release of carbon and greenhouse gas into atmosphere, will essentially contribute to mitigating the global warming (Figure 22). The most advanced waste-to-nanomaterial techniques demonstrate near negligible rates of carbon emission. [231,232]

✓ Development of advanced techniques for direct conversion of biowastes to the nanostructured materials could significantly help to mitigate the global warming and thus ensure additional benefits

Bio-wastes routinely contain a large amount of mineral matter and moreover, this content could be different for similar types of bio-wastes and in particular for food wastes, depending on various parameters such as e.g. type soil, used fertilizers, harvesting time and others. The inorganic materials could affect the conversion process and cause poisoning of catalysts such as e.g. ferrocenes that are used to obtain graphene oxide in the techniques that do not use plasma. [233,234] Importantly, the plasma-based synthesis in most cases does not require catalysts. [235,236]

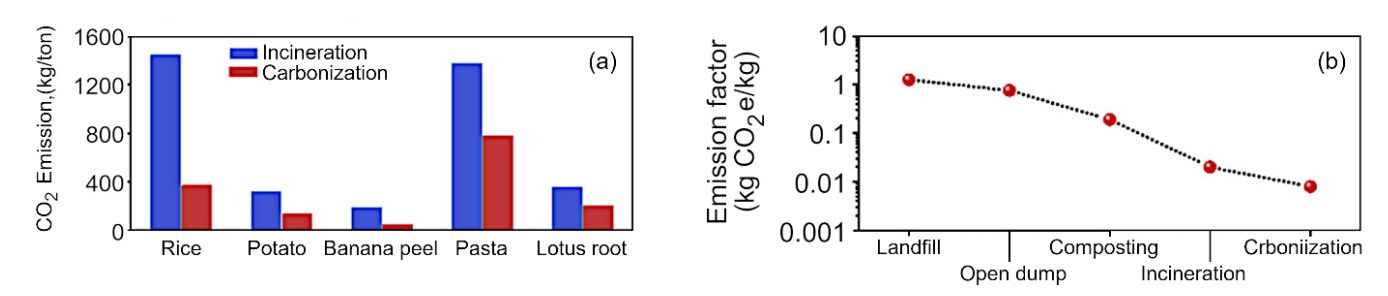


Figure 22. CO<sub>2</sub> emission for conventional incineration and the carbonization treatment (a). Estimated emission factor (in CO<sub>2</sub>)

of carbonization in comparison to predominant waste treatments (b). Reprinted with permission from *Nano Energy* **2019**. [39] conventional incineration and conventional incineration and the proposed carbonization treatment

On the other hand, the presence of inorganic minerals could in general make the synthesized material impure. In literature there are few studies in which impurities superimposed from precursors of complex chemical composition are reported and quantified. In most cases, the approach is to validate the goodness of the synthesized material by employing it for the specific application. [192,82] Specifically designed studies have shown that the conversion techniques could significantly reduce the content of unwanted impurities in the final product, as compare with raw materials and precursors. In one of such studies, a quantification of impurities in the carbonaceous products has been made by Pak et al. [237] The plasma arc process at atmospheric pressure was used to produce an ultrafine carbon product and a mixture of gases such as methane, hydrogen and carbon monoxide out of waste tires. Starting from a 2% sulphur content in the untreated material, the produced material had a 0.2% sulphur content after the treatment. The ash residues (Zn, Ti, Si and others) contained in the tire in percentage of 7% and after treatment, depending on the power used, were reduced up to 0.4% of the total weight.

Selective chemical processes could be employed for the rice husk bio-waste, which is an abundant source of carbon having silica as the impurity that must be removed before its conversion into carbon materials. [238] Alternatively, silica and carbon could be obtained simultaneously. For example, Wang et al. synthesized nano particles of mesoporous silica with quantum dots of biocompatible graphene using a thermal method and physical-chemical process to extract silica. [239] Kuang *et al.* produced vertically oriented graphenes from waste oil without any purification techniques, demonstrating its application for supercapacitors. [208]

**Table 3**. A summary table of produced materials, type of wastes, used technology, and type of used catalysts outlined described in the Review, with the relevant references.

Material produced	Waste	Technology	Catalyst	Ref.
Reduced graphene oxide	Conut coir, coconut shell	Catalytic oxidation	Ferrocene	96
Reduced graphene oxide	Conut coir	Soft bubble assembly	Ferrocene/Nickel	98
Few-layer graphene	Peanut shell	Sonication	No catalyst	100
Reduced graphene oxide	Used cooking (sunflower) oil	Controlled combustion	No catalyst	48
Graphene-based carbon aerogel	Gelatin powder from bovine skin	Thermal technology and freeze drying	No catalyst (KOH for activation)	116
Nanokeratin-urea nanocomposite (bio- fertilizer)	Chicken feathers	Ultrasonication	No catalyst	119
Vertically-oriented graphene walls	Citrus sinensis essential oil	RF plasma	No catalyst (directly on thermally oxidized SiO <sub>2</sub> )	138
Graphene nanoflakes	Ethanol	Microwave plasma decomposition	No catalyst	175
Antimicrobial polymers	Melaleuca alternifolia (tea tree) oil	Radio-frequency plasma	No catalyst	192
Carbon nano-onions	Citrus sinensis essential oil	Radio-frequency plasma	No catalyst	82
Nanoporous carbon materials	Banana peels	Microwave-enabled pyrolysis	No catalyst (chemical activation using NaOH/KOH)	201
Biocompatible nano-carbons	Groundnut shells	Pyrolysis	No catalyst	204
Vertical graphenes	Waste lard oil	ICP CVD process	No catalyst	205
Graphenes nanowalls	Sugarcane bagasse	Plasma-enabled technology	No catalyst	206

Graphene	Natural graphite flakes	DBD plasma exfoliation	No catalyst	89
Vertically oriented graphenes	Waste oil from the waste oil processing plant	Inductively coupled plasma reactor	No catalyst	208

Here we can conclude that the problem of converting bio- and food wastes containing considerable amount of mineral impurities into a high-quality functional nanomaterial requires further studies, yet many conversion processes are capable of reducing the percentage of unwanted impurities in the final product, and the high-quality nanomaterials still could be produced from biowastes. Importantly, the mineral elements contained in the biowastes could be use directly as catalysts since some plants are capable of hyperaccumulating transition metals. [240,241] The adverse effect of mineral impurities on the formation and behaviour of catalysts also requires further studies, but in the general case the mineral impurities do not poison catalysts in the catalytic reactions, and moreover, many plasma-based technologies are catalyst free and thus could not be affected by mineral impurities at the synthesis stage.

Catalysts and other parameters used in the waste conversion process are important for selecting the proper technology. To form a wide view in this aspect, we have present here a table where the produced materials, type of wastes, used technology, type of used catalysts and the relevant references are summarized (**Table 3**).

#### **ACKNOWLEGEMENTS**

I.L. acknowledges the support from the Nanyang Technological University, Plasma Sources and Applications Centre; K.B. acknowledges the support from the National Australian University and Australian Research Council (DP180101254, DE130101550); O.B. acknowledges the support through an Australian Government Research Training Program Scholarship.

#### **REFERENCES**

<sup>&</sup>lt;sup>1</sup> I. Levchenko, K. Bazaka, M. Keidar, S. Xu, J. Fang. Hierarchical multicomponent inorganic metamaterials: Intrinsically driven self-assembly at the nanoscale. *Adv. Mater.* **2018**, 30, 1702226. <a href="https://doi.org/10.1002/adma.201702226">https://doi.org/10.1002/adma.201702226</a>

P. Wang, H. Zhang, H. Wang, D. Li, J. Xuan, L. Zhang. Hybrid manufacturing of 3d hierarchical porous carbons for electrochemical storage. Adv. Mater. Technol. 2020, 5, 1901030. <a href="https://doi.org/10.1002/admt.201901030">https://doi.org/10.1002/admt.201901030</a>

<sup>&</sup>lt;sup>3</sup> C. Piferi, K. Bazaka, D. L. D'Aversa, R. Di Girolamo, C. De Rosa, H. E. Roman, C. Riccardi, I. Levchenko. Hydrophilicity and hydrophobicity control of plasma-treated surfaces via fractal parameters. *Adv. Mater. Interfaces* **2021**, 8, 2100724. https://doi.org/10.1002/admi.202100724

<sup>&</sup>lt;sup>4</sup> F. J. Martin-Martinez, K. Jin, D. López Barreiro, M. J. Buehler, The rise of hierarchical nanostructured materials from renewable sources: Learning from Nature. *ACS Nano* **2018**, 12, 7425–7433. https://doi.org/10.1021/acsnano.8b04379

R. Granberry, J. Barry, B. Holschuh, J. Abel. Kinetically tunable, active auxetic, and variable recruitment active textiles from hierarchical assemblies. *Adv. Mater. Technol.* **2021**, 6, 2000825. <a href="https://doi.org/10.1002/admt.202000825">https://doi.org/10.1002/admt.202000825</a>

I. Levchenko, I. I. Beilis, M. Keidar. Nanoscaled metamaterial as an advanced heat pump and cooling media. *Adv. Mater. Technol.* **2016**, 1, 1600008,. <a href="https://doi.org/10.1002/admt.201600008">https://doi.org/10.1002/admt.201600008</a>

H. Röhm, T. Leonhard, A. D. Schulz, S. Wagner, M. J. Hoffmann, A. Colsmann. Ferroelectric properties of perovskite thin films and their implications for solar energy conversion. *Adv. Mater.* **2019**, 31, 1806661. <a href="https://doi.org/10.1002/adma.201806661">https://doi.org/10.1002/adma.201806661</a>

C. Xu, A. R. Puente-Santiago, D. Rodríguez-Padrón, M. J. Muñoz-Batista, M. A. Ahsan, J.C. Noveron, R. Luque, Nature-inspired hierarchical materials for sensing and energy storage applications, *Chem. Soc. Rev.* 2021, 50, 4856-4871. <a href="https://doi.org/10.1039/C8CS00652K">https://doi.org/10.1039/C8CS00652K</a>

B. Graves, S. Engelke, C. Jo, H. G. Baldovi, J. de la Verpilliere, M. De Volder, A. Boies, Plasma production of nanomaterials for energy storage: continuous gas-phase synthesis of metal oxide CNT materials via a microwave plasma, *Nanoscale* 2020, 12, 5196-5208. <a href="http://dx.doi.org/10.1039/C9NR08886E">http://dx.doi.org/10.1039/C9NR08886E</a>

H. P. Zhou, X. Ye, W. Huang, M. Q. Wu, L. N. Mao, B. Yu, S. Xu, I. Levchenko, K. Bazaka. Wearable, flexible, disposable plasma-reduced graphene oxide stress sensors for monitoring activities in austere environments. ACS Appl. Mater. Interfaces 2019, 11, 15122-15132. https://doi.org/10.1021/acsami.8b22673

- <sup>11</sup> J. D. Miller, D. Cabarkapa, M. J. Hermes, A. C. Fry, C. J. Berkland. Soft magnetic composites as quantitative 3d compression sensors for wearable technology. *Adv. Mater. Technol.* **2021**, 2100784, in press. <a href="https://doi.org/10.1002/admt.202100784">https://doi.org/10.1002/admt.202100784</a>
- R. Abdel-Karim, Y. Reda, A. Abdel-Fattah, Review-nanostructured materials-based nanosensors. *J. Electrochem. Soc.* **2020**, 167, 037554. <a href="https://iopscience.iop.org/article/10.1149/1945-7111/ab67aa">https://iopscience.iop.org/article/10.1149/1945-7111/ab67aa</a>
- <sup>13</sup> M. Kaur, T.-H. Kim, W. S. Kim. New Frontiers in 3D Structural Sensing Robots. *Adv. Mater.* **2021**, 33, 2002534. https://doi.org/10.1002/adma.202002534
- <sup>14</sup> E. C. Welch, J. M. Powell, T. B. Clevinger, A. E. Fairman, A. Shukla, Advances in Biosensors and diagnostic technologies using nanostructures and nanomaterials. *Adv. Funct. Mater.* **2021**, 2104126, in press. https://doi.org/10.1002/adfm.202104126
- Q. Xiang, X. Ma, D. Zhang, H. Zhou, Y. Liao, H. Zhang, S. Xu, I. Levchenko, K. Bazaka. Interfacial modification of titanium dioxide to enhance photocatalytic efficiency towards H<sub>2</sub> production. *J. Colloid Interface Sci.* 2019, 556, 376-385. <a href="https://doi.org/10.1016/j.jcis.2019.08.033">https://doi.org/10.1016/j.jcis.2019.08.033</a>
- N. Kosinov, E. M. Hensen. Reactivity, Selectivity, and stability of zeolite-based catalysts for methane dehydroaromatization. *Adv. Mater.* **2020**, 32, 2002565. <a href="https://doi.org/10.1002/adma.202002565">https://doi.org/10.1002/adma.202002565</a>
- V. Sadykov, S. Pavlova, J. Fedorova, A. Bobin, V. Fedorova, M. Simonov, A. Ishchenko, T. Krieger, M. Melgunov, T. Glazneva, T. Larina, V. Kaichev, A.-C. Roger, Structured catalysts with mesoporous nanocomposite active components for transformation of biogas/biofuels into syngas, *Catalysis Today* 2021, 379, 166-180. https://doi.org/10.1016/j.cattod.2020.10.017
- B. Han, Y.-Y. Gao, L. Zhu, Z.-C. Ma, X.-L. Zhang, H. Ding, Y.-L. Zhang. In situ integration of SERS Sensors for On-chip catalytic reactions. *Adv. Mater. Technol.* **2020**, 5, 1900963. <a href="https://doi.org/10.1002/admt.201900963">https://doi.org/10.1002/admt.201900963</a>
- K. Li, Y. de Rancourt de Mimérand, X. Jin, J. Yi, J. Guo, Metal Oxide (ZnO and TiO<sub>2</sub>) and Fe-Based metal—organic-framework nanoparticles on 3D-printed fractal polymer surfaces for photocatalytic degradation of organic pollutants, *ACS Appl. Nano* Mater. **2020**, 3, 2830-2845. <a href="https://doi.org/10.1021/acsanm.0c00096">https://doi.org/10.1021/acsanm.0c00096</a>
- W. Yang, S. Cai, Y. Chen, W. Liang, Y. Lai, H. Yu, Y. Wang, L. Liu. Modular and customized fabrication of 3D functional microgels for bottom-up tissue engineering and drug screening. Adv. Mater. Technol. 2020, 5, 1900847. <a href="https://doi.org/10.1002/admt.201900847">https://doi.org/10.1002/admt.201900847</a>
- L. Ma, L. Diao, Z. Peng, Y. Jia, H. Xie, B. Li, J. Ma, M. Zhang, L. Cheng, D. Ding, X. Zhang, H. Chen, F. Mo, H. Jiang, G. Xu, F. Meng, Z. Zhong, M. Liu. Immunotherapy and prevention of cancer by nanovaccines loaded with whole-cell components of tumor tissues or Cells. Adv. Mater. 2021, 2104849, in press. <a href="https://doi.org/10.1002/adma.202104849">https://doi.org/10.1002/adma.202104849</a>
- K. Fu, H. Wu, Z. Su, Self-assembling peptide-based hydrogels: Fabrication, properties, and applications, *Biotechnol. Adv.* **2021**, 49, 107752. <a href="https://doi.org/10.1016/j.biotechadv.2021.107752">https://doi.org/10.1016/j.biotechadv.2021.107752</a>
- R. Zeng, C. Lv, C. Wang, G. Zhao, Bionanomaterials based on protein self-assembly: Design and applications in biotechnology, *Biotechnol. Adv.* **2021**, 52, 107835. https://doi.org/10.1016/j.biotechadv.2021.107835
- N. Natter, N. Kostoglou, C. Koczwara, C. Tampaxis, T. Steriotis, R. Gupta, O. Paris, C. Rebholz, C. Mitterer. Plasma-derived graphene-based materials for water purification and energy storage. *J. Carbon Res.* 2019, 5, 16. https://doi.org/10.3390/c5020016
- <sup>25</sup> X. Zhang, Y. Liu, Nanomaterials for radioactive wastewater decontamination, *Environ. Sci.: Nano* **2020**, 7, 1008-1040. http://dx.doi.org/10.1039/C9EN01341E
- <sup>26</sup> I. Levchenko, M. Keidar, J. Cantrell, Y.-L. Wu, H. Kuninaka, K. Bazaka, S. Xu. Explore space using swarms of tiny satellites. *Nature* **2018**, 562, 185-187. <a href="https://doi.org/10.1038/d41586-018-06957-2">https://doi.org/10.1038/d41586-018-06957-2</a>
- <sup>27</sup> I. Levchenko, K. Bazaka, T. Belmonte, M. Keidar, S. Xu. Advanced materials for next generation spacecraft. *Adv. Mater.* **2018**, 30, 1802201. <a href="https://doi.org/10.1002/adma.201802201">https://doi.org/10.1002/adma.201802201</a>
- I. Levchenko, S. Xu, G. Teel, D. Mariotti, M. L. R. Walker, M. Keidar. Recent progress and perspectives of space electric propulsion systems based on smart nanomaterials. *Nat. Commun.* 2018, 9, 879. https://doi.org/10.1038/s41467-017-02269-7
- N. Singhal, I. Levchenko, S. Huang, L. Xu, G.-C. Potrivitu, O. Cherkun, J. Fang, K. Bazaka, S. Xu. 3D-Printed multilayered reinforced material system for gas supply in cubeSats and small satellites. *Adv. Eng. Mater.* **2019**, 21, 1900401. <a href="https://doi.org/10.1002/adem.201900401">https://doi.org/10.1002/adem.201900401</a>
- <sup>30</sup> Z. Chen, S. Zhang, I. Levchenko, I. I. Beilis, M. Keidar. In vitro demonstration of cancer inhibiting properties from stratified self-organized plasma-liquid interface. *Sci. Rep.* **2017**, 7, 12163. <a href="https://doi.org/10.1038/s41598-017-12454-9">https://doi.org/10.1038/s41598-017-12454-9</a>
- P. Liu, G. Wang, Q. Ruan, K. Tang, P. K. Chu, Plasma-activated interfaces for biomedical engineering, *Bioactiv. Mater.* **2021**, 6, 2134-2143. <a href="https://doi.org/10.1016/j.bioactmat.2021.01.001">https://doi.org/10.1016/j.bioactmat.2021.01.001</a>

- <sup>32</sup> G. Maduraiveeran, M. Sasidharan, V. Ganesan, Electrochemical sensor and biosensor platforms based on advanced nanomaterials for biological and biomedical applications, *Biosens. Bioelectron.* **2018**, 103, 113-129. https://doi.org/10.1016/j.bios.2017.12.031
- K. Ganguly, D. K. Patel, S. D. Dutta, W. C. Shin, K. T. Lim, Stimuli-responsive self-assembly of cellulose nanocrystals (CNCs): Structures, functions, and biomedical applications, *Int. J. Biol. Macromolec.* **2020**, 155, 456-469. https://doi.org/10.1016/j.ijbiomac.2020.03.171
- S. W. Leung, B. Williams, K. De Jesus, J. C. K. Lai. Critical review of removal of nano materials in waste streams. *IOP Conf. Ser.: Earth Environ*. Sci. **2017**, 68 012019. https://doi.org/10.1088/1755-1315/68/1/012019
- A. A. Keller, S. McFerran, A. Lazareva, S. Suh. Global life cycle releases of engineered nanomaterials. *J. Nanopart. Res.* **2013**, 15, 1692. https://doi.org/10.1007/s11051-013-1692-4
- <sup>36</sup> Sigma Aldrich: <a href="https://www.sigmaaldrich.com">https://www.sigmaaldrich.com</a>
- J. Chun, J. H. Lee. Recent progress on the development of engineered silica particles derived from rice husk. *Sustainability* **2020**, 12, 10683. <a href="https://doi.org/10.3390/su122410683">https://doi.org/10.3390/su122410683</a>
- <sup>38</sup> V. Zarei, M. Mirzaasadi, A. Davarpanah, A. Nasiri, M. Valizadeh, M.J. S. Hosseini. Environmental method for synthesizing amorphous silica oxide nanoparticles from a natural material. *Processes* **2021**, 9, 334. <a href="https://doi.org/10.3390/pr9020334">https://doi.org/10.3390/pr9020334</a>
- <sup>39</sup> Y. Zhang, S. Kishore. Ravi, S. C. Tan. Food-derived carbonaceous materials for solar desalination and thermo-electric power generation. *Nano Energy* **2019**, 65, 104006. <a href="https://doi.org/10.1016/j.nanoen.2019.104006">https://doi.org/10.1016/j.nanoen.2019.104006</a>
- M. R. Abukhadra, M. Shaban. Recycling of different solid wastes in synthesis of high-order mesoporous silica as adsorbent for safranin dye. *Int. J. Environ. Sci. Technol.* **2019**, 16, 7573–7582. https://doi.org/10.1007/s13762-019-02231-8
- 41 X. Liu, S. Zhang, X. Wen, et al. High yield conversion of biowaste coffee grounds into hierarchical porous carbon for superior capacitive energy storage. *Sci. Rep.* **2020**, 10, 3518. <a href="https://doi.org/10.1038/s41598-020-60625-y">https://doi.org/10.1038/s41598-020-60625-y</a>
- R. Ajdary, B. L. Tardy, B. D. Mattos, L. Bai, O. J. Rojas, Plant nanomaterials and inspiration from Nature: Water interactions and hierarchically structured hydrogels. *Adv. Mater.* **2021**, 33, 2001085. <a href="https://doi.org/10.1002/adma.202001085">https://doi.org/10.1002/adma.202001085</a>
- J. Y. Zhu, U. P. Agarwal, P. N. Ciesielski, et al. Towards sustainable production and utilization of plant-biomass-based nanomaterials: a review and analysis of recent developments. *Biotechnol. Biofuels* **2021**, 14, 114. <a href="https://doi.org/10.1186/s13068-021-01963-5">https://doi.org/10.1186/s13068-021-01963-5</a>
- 44 R. Abolghasemi, M. Haghighi, M. Solgi & A. Mobinikhaledi. Rapid synthesis of ZnO nanoparticles by waste thyme (Thymus vulgaris L.). *Int. J. Environ. Sci. Technol.* **2019**, 16, 6985–6990. <a href="https://doi.org/10.1007/s13762-018-2112-1">https://doi.org/10.1007/s13762-018-2112-1</a>
- F. Part, N. Berge, P. Baran, A. Stringfellow, W. Sun, S. Bartelt-Hunt, D. Mitrano, L. Li, P. Hennebert, P. Quicker, S. C. Bolyard, M. Huber-Humer. A review of the fate of engineered nanomaterials in municipal solid waste streams. *Waste Manag.* 2018, 75, 427-449. <a href="https://doi.org/10.1016/j.wasman.2018.02.012">https://doi.org/10.1016/j.wasman.2018.02.012</a>
- <sup>46</sup> Emergen Research (<a href="https://www.emergenresearch.com/industry-report/fullerene-market">https://www.emergenresearch.com/industry-report/fullerene-market</a>). Accessed March 2022.
- <sup>47</sup> Nanoshel LLC (https://www.nanoshel.com/global-demand-nanomaterials). Accessed March 2022.
- <sup>48</sup> G. S. Lekshmi, R.Tamilselvi, K. Prasad, O. Bazaka, I. Levchenko, K. Bazaka, M. Mohandas, M. Growth of rGO nanostructures via facile wick and oil flame synthesis for environmental remediation. *Carbon Lett.* **2021**, 31, 763–777. <a href="https://doi.org/10.1007/s42823-021-00244-3">https://doi.org/10.1007/s42823-021-00244-3</a>
- <sup>49</sup> J. Ramirez, B. McCabe, P. D. Jensen, R. Speight, M. Harrison, L. van den Berg, I. O'Hara. Wastes to profit: a circular economy approach to value-addition in livestock industries. *Animal Prod. Sci.* **2021**, 61, 541. <a href="https://doi.org/10.1071/AN20400">https://doi.org/10.1071/AN20400</a>
- G. Xu, H. Jiang, M. Stapelberg, J. Zhou, M. Liu, Q.-J. Li, Y. Cao, R. Gao, M. Cai, J. Qiao, M. S. Galanek, W. Fan, W. Xue, B. Marelli, M. Zhu, J. Li. Self-perpetuating carbon foam microwave plasma conversion of hydrocarbon wastes into useful fuels and chemicals. *Environ. Sci. Technol.* **2021**, 55, 9, 6239–6247. <a href="https://doi.org/10.1021/acs.est.0c06977">https://doi.org/10.1021/acs.est.0c06977</a>
- <sup>51</sup> S. M. Abdelbasir, K. M. McCourt, C. M. Lee, D. C. Vanegas. Waste-derived nanoparticles: Synthesis approaches, environmental applications, and sustainability considerations. *Front. Chem.* **2020**, 8, 782. https://doi.org/10.3389/fchem.2020.00782
- <sup>52</sup> I. Levchenko, K. Bazaka, O. Baranov, O. Cherkun, M. Keidar, S. Xu. Processes at Plasma-Matter Interfaces: An Overview and Future Trends. *AAPPS Bulletin* **2020**, 30, 37-48. <a href="https://doi.org/10.22661/AAPPSBL.2020.30.3.37">https://doi.org/10.22661/AAPPSBL.2020.30.3.37</a>
- E. Alvarez de Eulate, A. Gheorghiu, C. Amoura, A. Whiteley, C. Priest, M. N. MacGregor. Plasma deposited polyoxazoline thin films for the biofunctionalization of electrochemical sensors. *Adv. Mater. Technol.* **2021**, 6, 2001292. <a href="https://doi.org/10.1002/admt.202001292">https://doi.org/10.1002/admt.202001292</a>
- <sup>54</sup> B. Canto, M. Otto, M. J. Powell, V. Babenko, A. O'Mahony, H. C. M. Knoops, R. S. Sundaram, S. Hofmann, M. C. Lemme, D.

- Neumaier. Plasma-enhanced atomic layer deposition of  $Al_2O_3$  on graphene using monolayer hBN as interfacial layer. *Adv. Mater. Technol.* **2021**, in press. https://doi.org/10.1002/admt.202100489
- P. J. Bruggeman, F. Iza, R. Brandenburg, Foundations of atmospheric pressure non-equilibrium plasmas, *Plasma Sources Sci. Technol.* **2017**, 26, 123002. <a href="https://doi.org/10.1088/1361-6595/aa97af">https://doi.org/10.1088/1361-6595/aa97af</a>
- A. E. Rider, I. Levchenko, K. Ostrikov. Surface fluxes of and adatoms at initial growth stages of quantum dots. *J. Appl. Phys.* 2007, 101, 044306. https://doi.org/10.1063/1.2433752
- <sup>57</sup> I. Levchenko, M. Romanov, M. Keidar. Investigation of a steady-state cylindrical magnetron discharge for plasma immersion treatment. *J. Appl. Phys.* **2003**, 94, 1408-1413. https://doi.org/10.1063/1.1590054
- <sup>58</sup> I. Levchenko, K. Ostrikov, A. B. Murphy. Plasma-deposited Ge nanoisland films on Si: is Stranski–Krastanow fragmentation unavoidable? *J. Phys. D: Appl. Phys.* **2008**, 41, 092001. https://doi.org/10.1088/0022-3727/41/9/092001
- <sup>59</sup> G. D. Cha, W. H. Lee, C. Lim, M. K. Choi, D. H. Kim, Materials engineering, processing, and device application of hydrogel nanocomposites, *Nanoscale* **2020**,12, 10456-10473. <a href="https://doi.org/10.1039/D0NR01456G">https://doi.org/10.1039/D0NR01456G</a>
- B. O. Okesola, A. K. Mendoza-Martinez, G. Cidonio, B. Derkus, D. K. Boccorh, D. Osuna de la Peña, S. Elsharkawy, Y. Wu, J. I. Dawson, A. W. Wark, D. Knani, D. J. Adams, R. O. C. Oreffo, A. Mata, De Novo design of functional coassembling organic—inorganic hydrogels for hierarchical mineralization and neovascularization. ACS Nano 2021, 15, 11202-11217. <a href="https://doi.org/10.1021/acsnano.0c09814">https://doi.org/10.1021/acsnano.0c09814</a>
- <sup>61</sup> C. Chen, M. K. Singh, K. Wunderlich, S. Harvey, C. J. Whitfield, Z. Zhou, M. Wagner, K. Landfester, I. Lieberwirth, G. Fytas, K. Kremer, D. Mukherji, D. Y. W. Ng, T. Weil. Polymer cyclization for the emergence of hierarchical nanostructures. *Nat. Commun.* 2021, 12, 3959. <a href="https://doi.org/10.1038/s41467-021-24222-5">https://doi.org/10.1038/s41467-021-24222-5</a>
- N. K. Kaushik, N. Kaushik, N. N. Linh, B. Ghimire, A. Pengkit, J. Sornsakdanuphap, S.-J. Lee, E. H. Choi. Plasma and nanomaterials: Fabrication and biomedical applications. *Nanomaterials* **2019**, 9, 98. <a href="https://doi.org/10.3390/nano9010098">https://doi.org/10.3390/nano9010098</a>
- <sup>63</sup> Q. Zhang, J. Yu, A. Corma. Applications of Zeolites to C1 chemistry: Recent advances, challenges, and opportunities. *Adv. Mater.* 32, **2020**, <a href="https://doi.org/10.1002/adma.202002927">https://doi.org/10.1002/adma.202002927</a>
- <sup>64</sup> X. Yang, L. A. Berglund, Water-based approach to high-strength all-cellulose material with optical transparency. *ACS Sustainable Chem. Eng.* **2020**, *8*, 1146. <a href="https://doi.org/10.1021/acssuschemeng.7b02755">https://doi.org/10.1021/acssuschemeng.7b02755</a>
- <sup>65</sup> I. Levchenko, K. Ostrikov, J. D. Long, S. Xu. Plasma-assisted self-sharpening of platelet-structured single-crystalline carbon nanocones. *Appl. Phys. Lett.* **2007**, 91, 113115. <a href="https://doi.org/10.1063/1.2784932">https://doi.org/10.1063/1.2784932</a>
- O. Baranov, M. Košicek, G. Filipic, U. Cvelbar. A deterministic approach to the thermal synthesis and growth of 1D metal oxide nanostructures. *Appl. Surf. Sci.* **2021**, 566, 150619. <a href="https://doi.org/10.1016/j.apsusc.2021.150619">https://doi.org/10.1016/j.apsusc.2021.150619</a>
- <sup>67</sup> X. Zhu, W. Zhang, Q. Lin, M. Ye, L. Xue, J. Liu, Y. Wang, H. Cheng. Direct microdroplet synthesis of carboxylic acids from alcohols by preparative paper spray ionization without phase transfer catalysts. *ACS Sust. Chem. Eng.* **2019**, 7, 7, 6486-6491. https://doi.org/10.1021/acssuschemeng.9b00427
- <sup>68</sup> B. Borca, T. Michnowicz, R. Pétuya, M. Pristl, V. Schendel, I. Pentegov, U. Kraft, H. Klauk, P. Wahl, R. Gutzler, A. Arnau, U. Schlickum, K. Kern. Electric-field-driven direct desulfurization. *ACS Nano* **2017**, 11, 4703-4709. https://doi.org/10.1021/acsnano.7b00612
- <sup>69</sup> I. Levchenko, S. Xu, O. Cherkun, O. Baranov, K. Bazaka. Plasma meets metamatertials: Three ways to advance space micropropulsion systems. *Adv. Phys.: X* **2021**, 6, 1834452. https://doi.org/10.1080/23746149.2020.1834452
- A. Almansoori, R. Masters, K. Abrams, J. Schäfer, T. Gerling, C. Majewski, C. Rodenburg. Surface modification of the laser sintering standard powder polyamide 12 by plasma treatments. *Plasma Proc. Polym.* **2018**, 15, 1800032. https://doi.org/10.1002/ppap.201800032
- E. A. de Eulate, A. Gheorghiu, C. Amoura, A. Whiteley, C. Priest, M. N. MacGregor. Plasma deposited polyoxazoline thin films for the biofunctionalization of electrochemical sensors. *Adv. Mater. Technol.* **2021**, 6, 2001292. https://doi.org/10.1002/admt.202001292
- D. Z. Pai, Nanomaterials synthesis at atmospheric pressure using nanosecond discharges. J. Phys. D.: Appl. Phys. **2011**, 44, 174024. https://doi.org/10.1088/0022-3727/44/17/174024
- D. Z. Pai, K. Ostrikov, S. Kumar, D. A. Lacoste, I. Levchenko, C. O. Laux. Energy efficiency in nanoscale synthesis using nanosecond plasmas. *Sci. Rep.* **2013**, 3, 1221. <a href="https://doi.org/10.1038/srep01221">https://doi.org/10.1038/srep01221</a>
- D. Mariotti, R. M. Sankaran. Microplasmas for nanomaterials synthesis. J. Phys. D-Appl. Phys. 2010, 43, 323001. https://doi.org/10.1088/0022-3727/43/32/323001
- <sup>75</sup> T. Nozaki, K. Sasaki, T. Ogino, D. Asahi, K. Okazaki. Microplasma synthesis of tunable photoluminescent silicon

- nanocrystals. Nanotechnology 2007, 18, 235603. https://doi.org/10.1088/0957-4484/18/23/235603
- D. Mariotti, H. Lindstrom, A. C. Bose, K. Ostrikov. Monoclinic beta-MoO<sub>3</sub> nanosheets produced by atmospheric microplasma: application to lithium-ion batteries. *Nanotechnology* 2008, 19, 495302. <a href="https://doi.org/10.1088/0957-4484/19/495302">https://doi.org/10.1088/0957-4484/19/49/495302</a>
- Y. Shimizu, A. C. Bose, D. Mariotti, T. Sasaki, K. Kirihara, T. Suzuki, K. Terashima, N. Koshizaki. et al. Reactive evaporation of metal wire and microdeposition of metal oxide using atmospheric pressure reactive microplasma jet. *Jpn. J. Appl. Phys.* Part 1-Regul. *Pap. Brief Commun. Rev. Pap.* 2006, 45, 8228–8234. <a href="https://doi.org/10.1143/JJAP.45.8228">https://doi.org/10.1143/JJAP.45.8228</a>
- N. S. Tabrizi, M. Ullmann, V. A. Vons, U. Lafont, A. Schmidt-Ott. Generation of nanoparticles by spark discharge. *J. Nanopart. Res.* **2009**, 11, 315–332. https://doi.org/10.1007/s11051-008-9407-y
- A. Dato, V. Radmilovic, Z. H. Lee, J. Phillips, M. Frenklach. Substrate-free gas-phase synthesis of graphene sheets. *Nano Lett.* **2008**, 8, 2012–2016. <a href="https://doi.org/10.1021/nl8011566">https://doi.org/10.1021/nl8011566</a>
- 80 C. K. Chen, W. L. Perry, H. F. Xu, Y. B. Jiang, J. Phillips, Plasma torch production of macroscopic carbon nanotube structures. *Carbon* **2003**, 41, 2555–2560. <a href="https://doi.org/10.1016/S0008-6223(03)00361-0">https://doi.org/10.1016/S0008-6223(03)00361-0</a>
- J. H. Chen, G. H. Lu, L. Y. Zhu, R. C. Flagan. A simple and versatile mini-arc plasma source for nanocrystal synthesis. *J. Nanopart. Res.* **2007**, 9, 203–213. <a href="https://doi.org/10.1007/s11051-006-9168-4">https://doi.org/10.1007/s11051-006-9168-4</a>
- S. Alancherry, K. Bazaka, I. Levchenko, A. Al-Jumaili, B. Kandel, A. Alex, F. C. R. Hernandez, O. K. Varghese, M. V. Jacob. Fabrication of nano-onion-structured graphene films from Citrus sinensis extract and their wetting and sensing characteristics. ACS Appl. Mater. Interfaces 2020, 12, 29594–29604. https://doi.org/10.1021/acsami.0c04353
- J. Fang, I. Levchenko, Z. J. Han, S. Yick, K. Ostrikov. Carbon nanotubes on nanoporous alumina: from surface mats to conformal pore filling. *Nanoscale Res. Lett.* **2014**, 9, 1-8. <a href="https://doi.org/10.1186/1556-276X-9-390">https://doi.org/10.1186/1556-276X-9-390</a>
- 84 G. Primc, I. Levchenko, S. Kumar, U. Cvelbar, M. Mozetic, K. Ostrikov. Imaging of the asymmetric DC discharge: visualization to adjust plasma in the novel PECVD reactor. *IEEE Trans. Plasma Sci.* 2014, 42, 2564-2565. https://doi.org/10.1109/TPS.2014.2315789
- 85 Protech Technology Co., <a href="http://www.lab-heatingfurnace.com">http://www.lab-heatingfurnace.com</a> (Accessed March 2022)
- P.-A. Deyris, C. Grison. Nature, ecology and chemistry: An unusual combination for a new green catalysis, ecocatalysis. *Curr. Opin. Green Sustain. Chem.* **2018**, 10, 6-10. <a href="https://doi.org/10.1016/j.cogsc.2018.02.002">https://doi.org/10.1016/j.cogsc.2018.02.002</a>
- V. Escande, C. H. Lam, C. Grison, P. T. Anastas. EcoMnOx, a biosourced catalyst for selective aerobic oxidative cleavage of activated 1,2-Diols. ACS Sustainable Chem. Eng. 2017, 5, 4, 3214–3222. https://doi.org/10.1021/acssuschemeng.6b02979
- <sup>88</sup> V. Escande, C. H. Lam, P. Coish, P. T. Anastas. Heterogeneous sodium-manganese oxide catalyzed aerobic oxidative cleavage of 1,2-Diols. *Ang. Chemie Int. Ed.* **2017**, 56, 9561-9565. <a href="https://doi.org/10.1002/anie.201705934">https://doi.org/10.1002/anie.201705934</a>
- <sup>89</sup> Z. Luo, Y. Li, F. Wang, R. Hong. Plasma exfoliated graphene: Preparation via rapid, mild thermal reduction of graphene oxide and application in lithium batteries. *Materials* **2019**, 12, 707. <a href="https://doi.org/10.3390/ma12050707">https://doi.org/10.3390/ma12050707</a>
- <sup>90</sup> K. E. Kitko, Q. Zhang. Graphene-Based Nanomaterials: From Production to Integration With Modern Tools in Neuroscience. *Front. Syst. Neurosci.* **2019**, 13, 26. https://doi.org/10.3389/fnsys.2019.00026
- <sup>91</sup> R. Rajakumari, S. Thomas, N. Kalarikkal. Synthesis of eco-friendly graphene from agricultural wastes. in: "Agri-Waste and Microbes for Production of Sustainable Nanomaterials", Nanobiotechnology for Plant Protection **2022**, Chapter 9, 215-230. https://doi.org/10.1016/B978-0-12-823575-1.00010-X
- <sup>92</sup> J. Munuera, L. Britnell, C. Santoro, R. Cuéllar-Franca, C. Casiraghi. A review on sustainable production of graphene and related life cycle assessment. 2D Materials **2022**, 9, 012002. <a href="https://doi.org/10.1088/2053-1583/ac3f23">https://doi.org/10.1088/2053-1583/ac3f23</a>
- 93 M. T. Safian, U. S. Haron, M. N. Mohamad Ibrahim. A review on bio-based graphene derived from biomass wastes, *BioRes.* **2020**, 15, 9756-9785. https://doi.org/10.15376/biores.15.4.Safian
- <sup>94</sup> K. Qian, A. Kumar, H. Zhang, D. Bellmer, R. Huhnke, Recent advances in utilization of biochar. *Renew. Sustain. Energy Rev.* **2015**, 42, 1055–1064. <a href="https://doi.org/10.1016/j.rser.2014.10.074">https://doi.org/10.1016/j.rser.2014.10.074</a>
- J. K. Saha, A. Dutta. A review of graphene: Material synthesis from biomass sources. Waste Biomass Valor. 2022, 13, 1385–1429. https://doi.org/10.1007/s12649-021-01577-w
- <sup>96</sup> R. Tamilselvi, M. Ramesh, G. S. Lekshmi, O. Bazaka, I. Levchenko, K. Bazaka, M. Mandhakini. Graphene oxide-based supercapacitors from agricultural wastes: A step to mass production of highly efficient electrodes for electrical transportation systems. *Renew. Energ.* **2020**, 151, 731-739. <a href="https://doi.org/10.1016/j.renene.2019.11.072">https://doi.org/10.1016/j.renene.2019.11.072</a>
- <sup>97</sup> T. Somanathan, K. Prasad, K. Ostrikov, A. Saravanan, M. Vemula, Graphene oxide synthesis from agro waste, *Nanomaterials* 5, **2015**, 826-834. <a href="https://doi.org/10.3390/nano5020826">https://doi.org/10.3390/nano5020826</a>

- R. Tamilselvi, G. S. Lekshmi, N. Padmanathan, V. Selvaraj, O.Bazaka, I. Levchenko, K. Bazaka, M. Mandhakini. NiFe<sub>2</sub>O<sub>4</sub> / rGO nanocomposites produced by soft bubble assembly for energy storage and environmental remediation. *Renew. Energy* **2022**, 181, 1386-1401. https://doi.org/10.1016/j.renene.2021.07.088
- <sup>99</sup> C. Geng, Z. Li, J. Cui, Y. Kang, C. Zhang, P. Li, C. Yang. Low-temperature NO reduction performance of peanut shell-derived few-layer graphene loaded CeCo<sub>x</sub>Mn<sub>1-x</sub>O<sub>3</sub> catalyst. *J. Dispers. Sci. Technol.* **2021**, 42, 900-909. https://doi.org/10.1080/01932691.2020.1721008
- T. Purkait, G. Singh, M. Singh, D. Kumar, R. S. Dey. Large area few-layer graphene with scalable preparation from waste biomass for high-performance supercapacitor. *Sci. Rep.* **2017**, 7, 15239. <a href="https://doi.org/10.1038/s41598-017-15463-w">https://doi.org/10.1038/s41598-017-15463-w</a>
- M.-F. Wu, C.-H. Hsiao, C.-Y. Lee, N.-H. Tai. Flexible Supercapacitors Prepared Using the Peanut-Shell-Based Carbon. ACS Omega 2020, 5, 14417–14426. https://dx.doi.org/10.1021/acsomega.0c00966
- J. Ding, H. Wang, Z. Li, K. Cui, D. Karpuzov, X. Tan, A. Kohandehghan, D. Mitlin. Peanut shell hybrid sodium ion capacitor with extreme energy—power rivals lithium ion capacitors. *Energy Environ.* 2015, 8, 941–955. https://doi.org/10.1039/C4EE02986K
- D. J. Tarimo, K. O. Oyedotun, A. A. Mirghni, N. F. Sylla, N. Manyala. High energy and excellent stability asymmetric supercapacitor derived from sulphur-reduced graphene oxide/manganese dioxide composite and activated carbon from peanut shell. *Electrochim. Acta* 2020, 353, 136498. https://doi.org/10.1016/j.electacta.2020.136498
- P. Kumari, M. Alam, W. A. Siddiqi. Usage of nanoparticles as adsorbents for waste water treatment: An emerging trend. Sustain. Mater. Technol. **2019**, 22, e00128. <a href="https://doi.org/10.1016/j.susmat.2019.e00128">https://doi.org/10.1016/j.susmat.2019.e00128</a>
- S.-X. Liang, W. Zhang, L. Zhang, W. Wang, L.-C. Zhanga. Remediation of industrial contaminated water with arsenic and nitrate by mass-produced Fe-based metallic glass: Toward potential industrial applications. *Sustain. Mater. Technol.* 2019, 22, e00126. <a href="https://doi.org/10.1016/j.susmat.2019.e00126">https://doi.org/10.1016/j.susmat.2019.e00126</a>
- M. Litvina, T. R. Todoruk, C. H. Langford. Composition and structure of agentsresponsible for development of water repellency in soils following oil contamination. *Environ. Sci. Technol.* **2003**, 37, 2883. https://doi.org/10.1021/es026296l
- Y. Wan, B. Wang, J. S. Khim, S. Hong, W. J. Shim, J. Hu. Naphthenic acids in coastal sediments after the hebei spirit oil spill: A potential indicator for oil contamination. *Environ. Sci. Technol.* **2014**, 48, 4153–4162. https://doi.org/10.1021/es405034y
- G. Barrera, S. Pizzimenti, E. S. Ciamporcero, M. Daga, C. Ullio, A. Arcaro, G. P. Cetrangolo, C. Ferretti, C. Dianzani, A. Lepore, F. Gentile. Role of 4-hydroxynonenal-protein adducts in human diseases. ARS Antioxid. Redox. Sign. 2015, 22, 1681-1702. https://doi.org/10.1089/ars.2014.6166
- D. Domenico, F. Tramutola, A. Butterfield. Role of 4-hydroxy-2-nonenal HNE in the pathogenesis of alzheimer disease and other selected age-related neurodegenerative disorders. *Free Radical Biol. Med.* **2017**, 111, 253-261. https://doi.org/10.1016/j.freeradbiomed.2016.10.490
- LoPachin, T. Gavin. Molecular mechanisms of aldehyde toxicity: A chemical perspective. *Chem. Res. Toxicol.* **2014**, 27, 1081–1091. <a href="https://doi.org/10.1021/tx5001046">https://doi.org/10.1021/tx5001046</a>
- G. Barrera, S. Pizzimenti, M. U. Dianzani. Lipid peroxidation: control of cell proliferation, cell differentiation and cell death. *Mol. Aspects Med.* **2008**, 29, 1-8. https://doi.org/10.1016/j.mam.2007.09.012
- L. Ma, G. Liu, W. Cheng, X. Liu, H. Liu, Q. Wang, G. Mao, X. Cai, C. Brennan, M. A. Brennan. Formation of malondialdehyde, 4-hydroxy-hexenal and 4-hydroxynonenal during deep-frying of potato sticks and chicken breast meat in vegetable oil. Int. *J. Food Sci. Technol.* 2020, 55, 1833–1842. https://doi.org/10.1111/ijfs.14462
- H. I. Abdel-Shafy, M. S. M. Mansour. A review on polycyclic aromatic hydrocarbons: Source, environmental impact, effect on human health and remediation. *Egypt. J. Petrol.* **2016**, 25, 107–123. <a href="https://doi.org/10.1016/j.ejpe.2015.03.011">https://doi.org/10.1016/j.ejpe.2015.03.011</a>
- S. P. Suresh, G. S. Lekshmi, S. D. Kirupha, M. Ariraman, O. Bazaka, I. Levchenko, K. Bazaka, M. Mandhakini. Superhydrophobic fluorine-modified cerium-doped mesoporous carbon as an efficient catalytic platform for photo-degradation of organic pollutants. *Carbon* 2019, 147, 323-333. <a href="https://doi.org/10.1016/j.carbon.2019.02.074">https://doi.org/10.1016/j.carbon.2019.02.074</a>
- <sup>115</sup> K.-H. Hung, C.-H. Chan, H.-W. Wang. Aqueous only route toward graphene from graphite oxide. *Renew. Energ.* **2014**, 66, 150-158. https://doi.org/10.1021/nn1028967
- A. Kandasamy, T. Ramasamy, A. Samrin, P. Narayanasamy, R. Mohan, O. Bazaka, I. Levchenko, K. Bazaka, M. Mohandas. Hierarchical doped gelatin-derived carbon aerogels: Three levels of porosity for advanced supercapacitors. *Nanomaterials* 2020, 10, 1178. <a href="https://doi.org/10.3390/nano10061178">https://doi.org/10.3390/nano10061178</a>
- P. Hao, Z. Zhao, Y. Leng, J. Tian, Y. Sang, R.I. Boughton, C.P. Wong, H. Liu, B. Yang. Graphene-based nitrogen self-doped hierarchical porous carbon aerogels derived from chitosan for high performance supercapacitors. *Nano Energy* 2015, 15, 9. <a href="https://doi.org/10.1016/j.nanoen.2015.02.035">https://doi.org/10.1016/j.nanoen.2015.02.035</a>

- A. Jain, S. K. Tripathi. Nano-porous activated carbon from sugarcane waste for supercapacitor application. *J. Energy Storage* **2015**, 4, 121. https://doi.org/10.1016/j.est.2015.09.010
- <sup>119</sup> G. V. Sree, P. Rajasekaran, O. Bazaka, I. Levchenko, K. Bazaka, M. Mandhakini. Biowaste valorization by conversion to nanokeratin-urea composite fertilizers for sustainable and controllable release of carbon and nitrogen. *Carbon Trends* **2021**, 5, 100083. https://doi.org/10.1016/j.cartre.2021.100083
- <sup>120</sup> S. Meignanalakshmi, R. Legadevi, N. Afrin Banu, V. Gayathri, A. Palanisammy, A study on antibacterial activity of keratin nanoparticles from chicken feather waste against staphylococcus aureus [bovine mastitis bacteria] and its antioxidant activity, *Europ. J. Biotechnol. Biosci.* **2015**, 3, 1-5.
- G. Vanthana Sree, M. Mandhakini, Wood encapsulated nano-keratin based slow-release fertilizer. *Adv. Sci. Lett.* **2018**, 24, 828-832. <a href="https://doi.org/10.1166/asl.2018.10853">https://doi.org/10.1166/asl.2018.10853</a>
- S. Saravanan, D. K. Sameera, A. Moorthi, N. Selva Murugan, Chitosan scaffolds containing chicken feathers keratin nanoparticles for bone tissue engineering. *Int. J. of Biolog. Macromol.* **2013**, 62, 481-486. <a href="https://doi.org/10.1016/j.ijbiomac.2013.09.034">https://doi.org/10.1016/j.ijbiomac.2013.09.034</a>
- W. Zhang, Y. Tian, H. He, L. Xu, W. Li, D. Zhao, Recent advances in the synthesis of hierarchically mesoporous TiO<sub>2</sub> materials for energy and environmental applications, *Nat. Sci. Rev.* **2020**, 7, 1702–1725. https://doi.org/10.1093/nsr/nwaa021
- G. H. Jeong, S. P. Sasikala, T. Yun, G. Y. Lee, W. J. Lee, S. O. Kim, Nanoscale assembly of 2D Materials for energy and environmental applications. *Adv. Mater.* **2020**, 32, 1907006. <a href="https://doi.org/10.1002/adma.201907006">https://doi.org/10.1002/adma.201907006</a>
- M. Carrola, A. Asadi, H. Zhang, D. G. Papageorgiou, E. Bilotti, H. Koerner, Best of both worlds: Synergistically derived material properties via additive manufacturing of nanocomposites. *Adv. Funct. Mater.* 2021, 2103334, in press. <a href="https://doi.org/10.1002/adfm.202103334">https://doi.org/10.1002/adfm.202103334</a>
- K. Bazaka, M.V. Jacob, D. Taguchi, T. Manaka, M. Iwamoto, Investigation of interfacial charging and discharging in double-layer pentacene-based metal-insulator-metal device with polyterpenol blocking layer using electric field induced second harmonic generation, Chem. Phys. Lett. 2011, 503, 105-111. <a href="http://dx.doi.org/10.1016%2Fj.cplett.2010.12.072">http://dx.doi.org/10.1016%2Fj.cplett.2010.12.072</a>
- F. Torricelli, I. Alessandri, E. Macchia, I. Vassalini, M. Maddaloni, L. Torsi. Green materials and technologies for sustainable organic transistors. *Adv. Mater. Technol.* **2021**, 2100445, in press. <a href="https://doi.org/10.1002/admt.202100445">https://doi.org/10.1002/admt.202100445</a>
- M. P. Cenci, T. Scarazzato, D. D. Munchen, P. C. Dartora, H. M. Veit, A. M. Bernardes, P. R. Dias. Eco-friendly electronics—a comprehensive review. Adv. Mater. Technol. **2021**, 2001263, in press. <a href="https://doi.org/10.1002/admt.202001263">https://doi.org/10.1002/admt.202001263</a>
- S. Yang, W. Li, S. Bai, Q. Wang, High-performance thermal and electrical conductive composites from multilayer plastic packaging waste and expanded graphite, *J. Mater. Chem. C* **2018**, 6, 11209-11218. <a href="https://doi.org/10.1039/C8TC02840K">https://doi.org/10.1039/C8TC02840K</a>
- <sup>130</sup> Xiong Y., Wang B., Yan J., Hong J., Wang L., Zhang Y, et al. Plasma assisted preparation of nickel-based catalysts supported on CeO<sub>2</sub> with different morphologies for hydrogen production by glycerol steam reforming. *Powder Technol.* **2019**, 354, 324–32. <a href="https://doi.org/10.1016/j.powtec.2019.06.003">https://doi.org/10.1016/j.powtec.2019.06.003</a>
- B. Ates, S. Koytepe, A. Ulu, C. Gurses, V. K. Thakur. Chemistry, structures, and advanced applications of nanocomposites from biorenewable resources. *Chem. Rev.* **2020**, 120, 9304-9362. <a href="https://doi.org/10.1021/acs.chemrev.9b00553">https://doi.org/10.1021/acs.chemrev.9b00553</a>
- <sup>132</sup> A.K. Ray, R.K. Sahu, V. Rajinikanth, H. Bapari, M. Ghosh, P. Paul, Preparation and characterization of graphene and Nidecorated graphene using flower petals as the precursor material, *Carbon* **2012**, 50, 4123-4129. <a href="https://doi.org/10.1016/j.carbon.2012.04.060">https://doi.org/10.1016/j.carbon.2012.04.060</a>
- N. Lisi, T. Dikonimos, F. Buonocore, M. Pittori, R. Mazzaro, R. Rizzoli, S. Marras, A. Capasso, Contamination-free graphene by chemical vapor deposition in quartz furnaces, *Sci. Rep.* **2017**, 7, 9927. https://doi.org/10.1038/s41598-017-09811-z
- Y. Ding, R. Wu, I.H. Abidi, H. Wong, Z. Liu, M. Zhuang, L.-Y. Gan, Z. Luo, Stacking modes-induced chemical reactivity differences on chemical vapor deposition-grown trilayer graphene, *ACS Appl. Mater. Interfaces* **2018**, 10, 23424-23431. https://doi.org/10.1021/acsami.8b05635
- <sup>135</sup> J. Fang, I. Levchenko, Z. J. Han, S. Yick, K. K. Ostrikov. Carbon nanotubes on nanoporous alumina: from surface mats to conformal pore filling. *Nanoscale Res Lett* **2014**, 9, 390. <a href="https://doi.org/10.1186/1556-276X-9-390">https://doi.org/10.1186/1556-276X-9-390</a>
- O. Baranov, S. Xu, K. Ostrikov, B.B. Wang, K. Bazaka, I. Levchenko, Towards universal plasma-enabled platform for the advanced nanofabrication: plasma physics level approach, *Rev. Mod. Plasma Phys.* **2018**, 2, 4. https://doi.org/10.1007/s41614-018-0016-7
- O. Baranov, K. Bazaka, H. Kersten, M. Keidar, U. Cvelbar, S. Xu, I. Levchenko, I. Plasma under control: advanced solutions and perspectives for plasma flux management in material treatment and nanosynthesis, *Appl. Phys. Rev.* **2017**, 4, 041302. <a href="https://doi.org/10.1063/1.5007869">https://doi.org/10.1063/1.5007869</a>
- <sup>138</sup> S. Alancherry, M. V. Jacob, K. Prasad, J. Joseph, O. Bazaka, R. Neupane, O. K. Varghese, O. Baranov, S. Xu, I. Levchenko, K. Bazaka. *Carbon* **2020**, 159, 668-685. <a href="https://doi.org/10.1016/j.carbon.2019.10.060">https://doi.org/10.1016/j.carbon.2019.10.060</a>

- <sup>139</sup> T. He, Z. Wang, F. Zhong, H. Fang, P. Wang, W. Hu. Etching Techniques in 2D Materials. *Adv. Mater. Technol.* 4, **2019**, 1900064. https://doi.org/10.1002/admt.201900064
- <sup>140</sup> B. Graves, S. Engelke, C. Jo, H. G. Baldovi, J. De la Verpilliere, M. De Volder, A. Boies. Plasma production of nanomaterials for energy storage: continuous gas-phase synthesis of metal oxide CNT materials via a microwave plasma. *Nanoscale* 2020, 12, 5196-5208. https://doi.org/10.1039/C9NR08886E
- <sup>141</sup> K. Singh, S. Sharma, S. Shriwastava, P. Singla, M. Gupta, C.C. Tripathi, Significance of nano-materials, designs consideration and fabrication techniques on performances of strain sensors A review, *Mater. Sci. Semiconduct. Process.* **2021**, 123, 105581. <a href="https://doi.org/10.1016/j.mssp.2020.105581">https://doi.org/10.1016/j.mssp.2020.105581</a>
- Wahyudiono, H. Kondo, M. Yamada, N. Takada, S. Machmudah, H. Kanda, M. Goto. DC-Plasma over aqueous solution for the synthesis of titanium dioxide nanoparticles under pressurized argon. ACS Omega 2020, 5, 5443–5451. https://doi.org/10.1021/acsomega.0c00059
- <sup>143</sup> L. Čechová, F. Krčma, M. Kalina, O. Man, Z. Kozáková. Preparation of silver and gold nanoparticles by the pinhole DC plasma system. *J. Appl. Phys.* **2021**, 129, 233304. https://doi.org/10.1063/5.0044054
- <sup>144</sup> M. A. A. Mamun, H. Furuta and A. Hatta, Pulsed-DC discharge for plasma CVD of carbon thin films, *IEEE Trans. Plasma Sci.* **2019**, 47, 22-31. <a href="https://doi.org/10.1109/TPS.2018.2853717">https://doi.org/10.1109/TPS.2018.2853717</a>
- <sup>145</sup> M. Sahoo, S. Vishwakarma, C. Panigrahi, J. Kumar. Nanotechnology: Current applications and future scope in food. *Food Front*. **2020**, 2, 3-22. https://doi.org/10.1002/fft2.58
- D. Zhang, C. Han, H. Zhang, B. Zeng, Y. Zheng, J. Shen, Q. Wu, G. Zeng. The simulation design of microwave absorption performance for the multi-layered carbon-based nanocomposites using intelligent optimization algorithm. *Nanomaterials* 2021, 11, 1951. https://doi.org/10.3390/nano11081951
- <sup>147</sup> G. Xu, H. Jiang, M. Stapelberg, J. Zhou, M. Liu, Q. J. Li, Y. Cao, R. Gao, M. Cai, J. Qiao, M. S. Galanek, W. Fan, W. Xue, B. Marelli, M. Zhu, J. Li, Self-Perpetuating carbon foam microwave plasma conversion of hydrocarbon wastes into useful fuels and chemicals, *Environ. Sci. Technol.* **2021**, 55, 6239–6247. https://doi.org/10.1021/acs.est.0c06977
- <sup>148</sup> A. A. Zamri, M. Y. Ong, S. Nomanbhay, P. L. Show, Microwave plasma technology for sustainable energy production and the electromagnetic interaction within the plasma system: A review. *Environ. Res.* **2021**, 197, 111204. https://doi.org/10.1016/j.envres.2021.111204
- <sup>149</sup> C. A Beaudette, H. P. Andaraarachchi, C.-C. Wu, U. R. Kortshagen. Inductively coupled nonthermal plasma synthesis of aluminum nanoparticles. *Nanotechnology* **2021**, 32, 395601. <a href="https://doi.org/10.1088/1361-6528/ac0cb3">https://doi.org/10.1088/1361-6528/ac0cb3</a>
- D. Metarapi, J. T. van Elteren, M. Šala, K. Vogel-Mikuš, I. Arčon, V. S. Šelih, M. Kolar, S. B. Hočevar. Laser ablation-single-particle-inductively coupled plasma mass spectrometry as a multimodality bioimaging tool in nano-based omics. *Environ. Sci.: Nano*, **2021**, 8, 647-656. <a href="https://doi.org/10.1039/D0EN011346">https://doi.org/10.1039/D0EN011346</a>
- E. C. Dell'Orto, S. Caldirola, A. Sassella, V. Morandi, C. Riccardi, Growth and properties of nanostructured titanium dioxide deposited by supersonic plasma jet deposition. *Appl. Surf. Sci.* 2017, 425, 407–415. <a href="https://doi.org/10.1016/j.apsusc.2017.07.059">https://doi.org/10.1016/j.apsusc.2017.07.059</a>
- <sup>152</sup> C. Cho, K. You, S. Kim, Y. Lee, J. Lee, S. You. Characterization of SiO<sub>2</sub> Etching profiles in pulse-modulated capacitively coupled plasmas. *Materials* **2021**, 14, 5036. <a href="https://doi.org/10.3390/ma14175036">https://doi.org/10.3390/ma14175036</a>
- <sup>153</sup> H. Wu, Y. Zhou, J. Gao, Y. Peng, Z. Wang, W. Jiang. Electrical breakdown in dual-frequency capacitively coupled plasma: a collective simulation. *Plasma Sources Sci. Technol.* **2021**, 30, 065029. <a href="https://doi.org/10.1088/1361-6595/abff74">https://doi.org/10.1088/1361-6595/abff74</a>
- A. Bogaerts, X. Tu, J. C. Whitehead, G. Centi, L. Lefferts, O. Guaitella, F. Azzolina-Jury, H.-H. Kim, A. B. Murphy, W. F. Schneider, T. Nozaki, J. C. Hicks, A. Rousseau, F. Thevenet, A. Khacef, M. Carreon. The 2020 plasma catalysis roadmap. *J. Phys. D: Appl. Phys.* 2020, 53, 443001. <a href="https://doi.org/10.1088/1361-6463/ab9048">https://doi.org/10.1088/1361-6463/ab9048</a>
- <sup>155</sup> S. Zanini, R. Ziano, C. Riccardi, Stable poly(Acrylic Acid) films from acrylic acid/argon plasmas: Influence of the mixture composition and the reactor geometry on the thin films chemical structures, *Plasma Chem. Plasma Proc.* **2009**, 29, 535–547. https://doi.org/10.1007/s11090-009-9193-z
- <sup>156</sup> X. Pang, Q. Zhang, Y. Shao, M. Liu, D. Zhang, Y. Zhao. A flexible pressure sensor based on magnetron sputtered MoS<sub>2</sub>. *Sensors* **2021**, 21, 1130. https://doi.org/10.3390/s21041130
- <sup>157</sup> J. T. Gudmundsson, Physics and technology of magnetron sputtering discharges, *Plasma Sources Sci. Technol.* **2020**, 29, 113001. https://iopscience.iop.org/article/10.1088/1361-6595/abb7bd/meta
- <sup>158</sup> C. E. Knapp, J.-B. Chemin, S. P. Douglas, D. A. Ondo, J. Guillot, P. Choquet, N. D. Boscher. Room-Temperature Plasma-Assisted Inkjet Printing of Highly Conductive Silver on Paper. *Adv. Mater. Technol.* **2018**, 3, 1700326. <a href="https://doi.org/10.1002/admt.201700326">https://doi.org/10.1002/admt.201700326</a>

- K. Sun, W. Xiao, S. Ye, N. Kalfagiannis, K. S. Kiang, C. H. de Groot, O. L. Muskens. Embedded Metal Oxide Plasmonics Using Local Plasma Oxidation of AZO for Planar Metasurfaces. *Adv. Mater.* 2020, 32, 2001534. https://doi.org/10.1002/adma.202001534
- S. Dou, L. Tao, R. Wang, S. E. Hankari, R. Chen, S. Wang. Plasma-Assisted Synthesis and Surface Modification of Electrode Materials for Renewable Energy. *Adv. Mater.* **2018**, 30, 1705850. https://doi.org/10.1002/adma.201705850
- M. Okubo, Recent development of technology in scale-up of plasma reactors for environmental and energy applications. *Plasma Chem. Plasma Process* **2021**, In press. <a href="https://doi.org/10.1007/s11090-021-10201-7">https://doi.org/10.1007/s11090-021-10201-7</a>
- Y. D. Korolev, N. N. Koval. Low-pressure discharges with hollow cathode and hollow anode and their applications. *J. Phys. D: Appl. Phys.* **2018**, 51, 323001. https://doi.org/10.1088/1361-6463/aacf10
- <sup>163</sup> C. P. Fontoura, M. M. Rodrigues, C. S. C. Garcia, K. S. Souza, J. A. P. Henriques, J. E. Zorzi, M. Roesch-Ely, C. Aguzzoli. Hollow cathode plasma nitriding of medical grade Ti6Al4V: A comprehensive study. *J. Biomater. App.* **2020**, 35, 353-370. https://doi.org/10.1177/0885328220935378
- <sup>164</sup> K. S. Kim, T. H. Kim. Nanofabrication by thermal plasma jets: From nanoparticles to low-dimensional nanomaterials featured. *J. Appl. Phys.* **2019**, 125, 070901. https://doi.org/10.1063/1.5060977
- <sup>165</sup> F. Wang, F. Wang, R. Hong, X. Lv, Y. Zheng, H. Chen. High-purity few-layer graphene from plasma pyrolysis of methane as conductive additive for LiFePO<sub>4</sub> lithium ion battery. *J. M ater. Res. Technol.* **2020**, 9, 10004–10015. <a href="https://doi.org/10.1016/j.jmrt.2020.06.072">https://doi.org/10.1016/j.jmrt.2020.06.072</a>
- <sup>166</sup> A. Islam, B. Mukherjee, K. K. Pandey, A. K. Keshri. Ultra-fast, chemical-free, mass production of high quality exfoliated graphene. *ACS Nano* **2021**, 15, 1775–1784. https://dx.doi.org/10.1021/acsnano.0c09451
- <sup>167</sup> H. Reinhardt, M. Kroll, S. L. Karstens, S. Schlabach, N. A. Hampp, U. Tallarek, Nanoscaled fractal superstructures via laser patterning a versatile route to metallic hierarchical porous materials. *Adv. Mater. Interfaces* **2021**, 8, 2000253. <a href="https://doi.org/10.1002/admi.202000253">https://doi.org/10.1002/admi.202000253</a>
- Z. Fusco, M. Rahmani, T. Tran-Phu, C. Ricci, A. Kiy, P. Kluth, E. D. Gaspera, N. Motta, D. Neshev, A. Tricoli. Photonic fractal metamaterials: A metal-semiconductor platform with enhanced volatile-compound sensing performance. *Adv. Mater.* 32, 2020, 2002471. https://doi.org/10.1002/adma.202002471
- <sup>169</sup> E. K. Lee, R. K. Baruah, J. W. Leem, W. Park, B. H. Kim, A. Urbas, Z. Ku, Y. L. Kim, M. A. Alam, C. H. Lee. Fractal web design of a hemispherical photodetector array with organic-dye-sensitized graphene hybrid composites. *Adv. Mater.* **2020**, 32, 2004456. https://doi.org/10.1002/adma.202004456
- P. Zeng, B. Tian, Q. Tian, W. Yao, M. Li, H. Wang, Y. Feng, L. Liu, W. Wu. Screen-Printed, low-cost, and patterned flexible heater based on ag fractal dendrites for human wearable application. *Adv. Mater. Technol.* 2019, 4, 1800453. <a href="https://doi.org/10.1002/admt.201800453">https://doi.org/10.1002/admt.201800453</a>
- <sup>171</sup> J. Li, M. Chen, C. Zhang, H. Dong, W. Lin, P. Zhuang, Y. Wen, B. Tian, W. Cai, X. Zhang. Fractal-theory-based control of the shape and quality of CVD-grown 2D materials. *Adv. Mater.* **2019**, 31, 1902431. <a href="https://doi.org/10.1002/adma.201902431">https://doi.org/10.1002/adma.201902431</a>
- <sup>172</sup> I. Dierking. Relationship Between the Electro-Optic Performance of polymer-stabilized liquid-crystal devices and the fractal dimension of their network morphology. *Adv. Mater.* **2003**, 15, 152-156. https://doi.org/10.1002/adma.200390032
- <sup>173</sup> Z. Fusco, M. Rahmani, R. Bo, R. Verre, N. Motta, M. Käll, D. Neshev, A. Tricoli. Nanostructured dielectric fractals on resonant plasmonic metasurfaces for selective and sensitive optical sensing of volatile compounds. *Adv. Mater.* **2018**, 30, 1800931. https://doi.org/10.1002/adma.201800931
- <sup>174</sup> M. Fennen, D. Giulin. Lie sphere geometry in lattice cosmology. *Class. Quantum Grav.* **2020**, 37, 065007. https://doi.org/10.1088/1361-6382/ab6a20
- A. Casanova, R. Rincón, J. Muñoz, C. Ania, M. Calzada. Optimizing high-quality graphene nanoflakes production through organic (bio)-precursor plasma decomposition. *Fuel Proc. Technol.* **2021**, 212, 106630. https://doi.org/10.1016/j.fuproc.2020.106630
- <sup>176</sup> A. Dato. Graphene synthesized in atmospheric plasmas. J. Mater. Res. **2019**, 34, 1–17. <a href="https://doi.org/10.1557/jmr.2018.470">https://doi.org/10.1557/jmr.2018.470</a>
- <sup>177</sup> C. Melero, R. Rincón, J. Muñoz, G. Zhang, S. Sun, A. Perez, O. Royuela, C. González-Gago, M.D. Calzada, Scalable graphene production from ethanol decomposition by microwave argon plasma torch, *Plasma Phys. Control. Fusion* **2018**, 60, 014009, https://doi.org/10.1088/1361-6587/aa8480
- <sup>178</sup> R. Zhou, R. Zhou, Y. Xian, Z. Fang, X. Lu, K. Bazaka, A. Bogaerts, K. Ostrikov. Plasma-enabled catalyst-free conversion of ethanol to hydrogen gas and carbon dots near room temperature. *Chem. Eng. J.* **2020**, 382, 122745. https://www.sciencedirect.com/science/article/pii/S1385894719321552
- <sup>179</sup> R. Zhou, R. Zhou, S. Wang, U. G. M. Ekanayake, Z. Fang, P. J. Cullen, K. Bazaka, K. Ostrikov. Power-to-chemicals: Low-temperature plasma for lignin depolymerisation in ethanol. *Biores. Technol.* **2020**, 318, 123917.

#### https://www.sciencedirect.com/science/article/pii/S0960852420311895

- <sup>180</sup> R. Zhou, R. Zhou, X. Zhang, Z. Fang, X. Wang, R. Speight, H. Wang, W. Doherty, P. J. Cullen, K. Ostrikov, K. Bazaka. High-Performance Plasma-Enabled Biorefining of Microalgae to Value-Added Products. *ChemSusChem* **2019**, 12, 4976-4985. https://doi.org/10.1002/cssc.201901772
- <sup>181</sup> N. Recek, R. Zhou, R. Zhou, V. S. J. Te'o, R. E. Speight, M. Mozetič, A. Vesel, U. Cvelbar, K. Bazaka, K. Ostrikov. Improved fermentation efficiency of S. cerevisiae by changing glycolytic metabolic pathways with plasma agitation. *Sci. Rep.* 2018, 8, 8252. <a href="https://doi.org/10.1038/s41598-018-26227-5">https://doi.org/10.1038/s41598-018-26227-5</a>
- <sup>182</sup> Y. Esmaeili, A. Zarrabi, S. Z. Mirahmadi-Zare, et al. Hierarchical multifunctional graphene oxide cancer nanotheranostics agent for synchronous switchable fluorescence imaging and chemical therapy. *Microchem. Acta* **2020**, 187, 553. <a href="https://doi.org/10.1007/s00604-020-04490-6">https://doi.org/10.1007/s00604-020-04490-6</a>
- <sup>183</sup> N. A. Fatthallah, M. S. Selim, S. A. El Safty, M. M. Selim, M. A. Shenashen, Engineering nanoscale hierarchical morphologies and geometrical shapes for microbial inactivation in aqueous solution, *Mater. Sci. Eng. C* **2021**, 122, 111844. <a href="https://doi.org/10.1016/j.msec.2020.111844">https://doi.org/10.1016/j.msec.2020.111844</a>
- H. Cui, W. Wang, L. Shi, W. Song, S. Wang, Superwettable Surface engineering in controlling cell adhesion for emerging bioapplications. *Small Meth.* **2020**, 4, 2000573. <a href="https://doi.org/10.1002/smtd.202000573">https://doi.org/10.1002/smtd.202000573</a>
- E. Gkantzou, A. V. Chatzikonstantinou, R. Fotiadou, A. Giannakopoulou, M. Patila, H. Stamatis, Trends in the development of innovative nanobiocatalysts and their application in biocatalytic transformations, *Biotechnol. Adv.* **2021**, 51, 107738. <a href="https://doi.org/10.1016/j.biotechadv.2021.107738">https://doi.org/10.1016/j.biotechadv.2021.107738</a>
- A. Kanioura, P. Petrou, D. Kletsas, A. Tserepi, M. Chatzichristidi, E. Gogolides, S. Kakabakos, Three-dimensional (3D) hierarchical oxygen plasma micro/nanostructured polymeric substrates for selective enrichment of cancer cells from mixtures with normal ones, *Colloids Surf. B: Biointerfaces* 2020, 187, 110675. https://doi.org/10.1016/j.colsurfb.2019.110675
- <sup>187</sup> A.S. Rajashekharaiah, G.P. Darshan, H.B. Premkumar, P. Lalitha, S.C. Sharma, H. Nagabhushana, Hierarchical Bi<sub>2</sub>Zr<sub>2</sub>O<sub>7</sub>:Dy<sup>3+</sup> architectures fabricated by bio-surfactant assisted hydrothermal route for anti-oxidant, anti-bacterial and anti-cancer activities, *Mater. Chem. Phys.* **2020**, 242, 122468. <a href="https://doi.org/10.1016/j.matchemphys.2019.122468">https://doi.org/10.1016/j.matchemphys.2019.122468</a>
- <sup>188</sup> Z. Wang, G. Wang, W. Li, Z. Cui, J. Wu, I. Akpinar, L. Yu, G. He, J. Hu, Loofah activated carbon with hierarchical structures for high-efficiency adsorption of multi-level antibiotic pollutants, *Appl. Surf. Sci.* **2021**, 550, 149313. <a href="https://doi.org/10.1016/j.apsusc.2021.149313">https://doi.org/10.1016/j.apsusc.2021.149313</a>
- <sup>189</sup> G. A. Naikoo, M. Mustaqeem, I. U. Hassan, T. Awan, Fa. Arshad, H. Salim, A. Qurashi. Bioinspired and green synthesis of nanoparticles from plant extracts with antivira and antimicrobial properties: A critical review. *J. Saudi Chem. Soc.* **2021**, 25, 101304. https://doi.org/10.1016/j.jscs.2021.101304
- <sup>190</sup> K. Prasad, C. D. Bandara, S. Kumar, G. P. Singh, B. Brockhoff, K. Bazaka, K. Ostrikov. Effect of Precursor on Antifouling Efficacy of Vertically-Oriented Graphene Nanosheets. *Nanomaterials* **2017**, 7, 170. <a href="https://doi.org/10.3390/nano7070170">https://doi.org/10.3390/nano7070170</a>
- <sup>191</sup> M. V. Jacob, K. Bazaka, D. Taguchi, T. Manaka, M. Iwamoto. Electron-blocking hole-transport polyterpenol thin films. *Chem. Phys. Lett.* **2012**, 528, 26-28. <a href="https://doi.org/10.1016/j.cplett.2012.01.031">https://doi.org/10.1016/j.cplett.2012.01.031</a>
- O. Bazaka, K. Prasad, I. Levchenko, M. V. Jacob, K. Bazaka, P. Kingshott, R. J. Crawford, E. P. Ivanova. Decontamination-induced modification of bioactivity in essential oil-based plasma polymers. *Molecules* 2021, 26, 7133. <a href="https://doi.org/10.3390/molecules26237133">https://doi.org/10.3390/molecules26237133</a>
- <sup>193</sup> K. Bazaka, N. Ketheesan, M. V. Jacob. Polymer Encapsulation of magnesium to control biodegradability and biocompatibility. *J. Nanosci. Nanotechnol.* **2014**, 14, 8087-8093. <a href="https://doi.org/10.1166/jnn.2014.9409">https://doi.org/10.1166/jnn.2014.9409</a>
- J. Fang, I. Aharonovich, I. Levchenko, K. Ostrikov, P. G. Spizzirri, S. Rubanov, S. Prawer. Plasma-enabled growth of single-crystalline SiC/AlSiC core—shell nanowires on porous alumina templates. *Crystal Growth & Design* 2012, 12, 2917-2922. <a href="https://doi.org/10.1021/cg300103a">https://doi.org/10.1021/cg300103a</a>
- <sup>195</sup> I. Levchenko, S. Xu, O. Baranov, O. Bazaka, E. P. Ivanova, K. Bazaka. Plasma and Polymers: Recent Progress and Trends. *Molecules* **2021**, 26, 4091. https://doi.org/10.3390/molecules26134091
- <sup>196</sup> K. Bazaka, O. Baranov, U. Cvelbar, B. Podgornik, Y. Wang, S. Huang, L. Xu, J. W. M Lim, I. Levchenko, S. Xu. Oxygen plasmas: a sharp chisel and handy trowel for nanofabrication. *Nanoscale* **2018**, 10, 17494-17511. <a href="https://doi.org/10.1039/C8NR06502K">https://doi.org/10.1039/C8NR06502K</a>
- <sup>197</sup> A. E. Rider, I. Levchenko, K. Ostrikov. Surface fluxes of and adatoms at initial growth stages of quantum dots. *J. Appl. Phys.* **2007**, 101, 044306. https://doi.org/10.1063/1.2433752
- <sup>198</sup> I. Levchenko, K. Bazaka, O. Baranov, R. M. Sankaran, A. Nomine, T. Belmonte, S. Xu. Lightning under water: Diverse reactive environments and evidence of synergistic effects for material treatment and activation. *Appl. Phys. Rev.* 2018, 5, 021103. <a href="https://doi.org/10.1063/1.5024865">https://doi.org/10.1063/1.5024865</a>

- <sup>199</sup> S. Jung, Y. Myung, G. S. Das, A. Bhatnagar, J.-W. Park, K. M. Tripathi, T. Kim. Carbon nano-onions from waste oil for application in energy storage devices. *New J. Chem.* **2020**, 44, 7369-7375. <a href="https://doi.org/10.1039/D0NJ00699H">https://doi.org/10.1039/D0NJ00699H</a>
- <sup>200</sup> V. Dhand, M. Yadav, S. H. Kim, K. Y. Rhee. A comprehensive review on the prospects of multi-functional carbon nano onions as an effective, high-performance energy storage material. *Carbon* **2021**, 175, 534-575. https://doi.org/10.1016/j.carbon.2020.12.083
- <sup>201</sup> R. K. Liew, E. Azwar, P. N. Y. Yek, X. Y. Lim, C. K. Cheng, J. H. Ng, A. Jusoh, W. H. Lam, M. D. Ibrahim, N. L. Ma, S. S. Lam. Microwave pyrolysis with KOH/NaOH mixture activation: A new approach to produce micro-mesoporous activated carbon for textile dye adsorption. *Bioresour. Technol.* **2018**, 266, 1. <a href="https://doi.org/10.1016/j.biortech.2018.06.051">https://doi.org/10.1016/j.biortech.2018.06.051</a>
- <sup>202</sup> Banana market review Preliminary results 2020. Food and Agriculture Organization of the United Nations, Rome, 2021. https://www.fao.org/3/cb5150en/cb5150en.pdf
- <sup>203</sup> S. Joseph, G. Saianand, M. R. Benzigar, K. Ramadass, G. Singh, A.-I. Gopalan, J. H. Yang, T. Mori, A. H. Al-Muhtaseb, J. Yi, A. Vinu. Recent advances in functionalized nanoporous carbons derived from waste resources and their applications in energy and environment. *Adv. Sustainable Syst.* **2020**, 5, 2000169. https://doi.org/10.1002/adsu.202000169
- S. Yallappa, D. R. Deepthi, S. Yashaswini, R. Hamsanandini, M. Chandraprasad, S. Ashok Kumar, G. Hegde. Natural biowaste of Groundnut shell derived nanocarbons: Synthesis, characterization and its in vitro antibacterial activity. *Nano-Struct. Nano-Objects* **2017**, 12, 84-90. https://doi.org/10.1016/j.nanoso.2017.09.009
- A. Wu, X. Li, J. Yang, C. Du, W. Shen, J. Yan. Upcycling waste lard oil into vertical graphene sheets by inductively coupled plasma assisted chemical vapor deposition. *Nanomaterials* **2017**, 7, 318. <a href="https://doi.org/10.3390/nano7100318">https://doi.org/10.3390/nano7100318</a>
- <sup>206</sup> K. Prasad, C. D. Bandara, S. Kumar, G. P. Singh, B. Brockhoff, K. Bazaka, K. Ostrikov. Effect of Precursor on Antifouling Efficacy of Vertically-Oriented Graphene Nanosheets. *Nanomaterials* **2017**, 7, 170. <a href="https://doi.org/10.3390/nano7070170">https://doi.org/10.3390/nano7070170</a>
- <sup>207</sup> A. Kumar, A. Aljumaili, O. Bazaka, E. P. Ivanova, I. Levchenko, K. Bazaka, M. Jacob. Functional nanomaterials, synergism and biomimicry for environmentally benign marine antifouling technology. *Mater. Horiz.* **2021**, Accepted Manuscript. https://doi.org/10.1039/D1MH01103K
- W. Kuang, H. Yang, C. Ying, B. Gong, J. Kong, X. Cheng, Z. Bo. Cost-effective, environmentally-sustainable and scale-up synthesis of vertically oriented graphenes from waste oil and its supercapacitor applications. *Waste Dispos. Sust. Ener.* **2021**, 3, 31–39, <a href="https://doi.org/10.1007/s42768-020-00068-3">https://doi.org/10.1007/s42768-020-00068-3</a>
- O. Baranov, I. Levchenko, S. Xu, J. W. M. Lim, U. Cvelbar and K. Bazaka. Formation of vertically oriented graphenes: what are the key drivers of growth? *2D Mater.* **2018**, 5, 044002. <a href="https://doi.org/10.1088/2053-1583/aad2bc">https://doi.org/10.1088/2053-1583/aad2bc</a>
- P. Vinchon, X. Glad, G. Robert Bigras, R. Martel, L. Stafford. Preferential self-healing at grain boundaries in plasma-treated graphene. *Nat. Mater.* **2021**, 20, 49–54. https://doi.org/10.1038/s41563-020-0738-0
- M. Pierpaoli, M. Ficek, P. Jakóbczyk, J. Karczewski, R. Bogdanowicz, Self-assembly of vertically orientated graphene nanostructures: Multivariate characterisation by Minkowski functionals and fractal geometry, *Acta Mater.* 2021, 214, 116989. <a href="https://doi.org/10.1016/j.actamat.2021.116989">https://doi.org/10.1016/j.actamat.2021.116989</a>
- N. Bundaleska, A. Dias, N. Bundaleski, E. Felizardo, J. Henriques, D. Tsyganov, M. Abrashev, E. Valcheva, J. Kissovski, A. M. Ferraria, A. M. Botelho do Rego, A. Almeida, J. Zavašnik, U. Cvelbar, O. M. N. D. Teodoro, Th. Strunskus, E. Tatarova. Prospects for microwave plasma synthesized N-graphene in secondary electron emission mitigation applications. *Sci. Rep.* 2020, 10, 13013. <a href="https://doi.org/10.1038/s41598-020-69844-9">https://doi.org/10.1038/s41598-020-69844-9</a>
- E. Tatarova, A. Dias, J. Henriques, M. Abrashev, N. Bundaleska, E. Kovacevic, N. Bundaleski, U. Cvelbar, E. Valcheva, B. Arnaudov, A. M. B. doRego, A. M. Ferraria, J. Berndt, E. Felizardo, O. M. N. D. Teodoro, Th. Strunskus, L. L. Alves, B. Gonçalves. Towards large-scale in free-standing graphene and N-graphene sheets. *Sci. Rep.* 2017, 7, 10175. <a href="https://doi.org/10.1038/s41598-017-10810-3">https://doi.org/10.1038/s41598-017-10810-3</a>
- <sup>214</sup> I. Levchenko, J. Fang, K. Ostrikov, L. Lorello, M. Keidar. Morphological characterization of graphene flake networks using Minkowski functionals. *Graphene* **2016**, 5, 25-34. <a href="https://doi.org/10.4236/graphene.2016.51003">https://doi.org/10.4236/graphene.2016.51003</a>
- <sup>215</sup> J. Fang, I. Levchenko, S. Kumar, D. Seo, K. Ostrikov. Vertically aligned graphene flakes on nanoporous templates: morphology, thickness, and defect level control by pre-treatment. *Sci. Technol. Adv. Mater.* **2014**, 15, 055009. https://doi.org/10.1088/1468-6996/15/5/055009
- N. Z. Janković, D. L. Plata. Engineered nanomaterials in the context of global element cycles. *Environ. Sci.: Nano* **2019**, 6, 2697-2711. https://doi.org/10.1039/C9EN00322C
- <sup>217</sup> T. Yamada, A. Maigne, M. Yudasaka, K. Mizuno, D. N. Futaba, M. Yumura, S. Iijima, K. Hata. Revealing the secret of water-assisted carbon nanotube synthesis by microscopic observation of the interaction of water on the catalysts. *Nano Lett.* **2008**, 8, 4288–4292. <a href="https://doi.org/10.1021/nl801981m">https://doi.org/10.1021/nl801981m</a>

- <sup>218</sup> M. Mittal, R. Chaudhary. Experimental study on the water absorption and surface characteristics of alkali treated pineapple leaf fibre and coconut husk fibre. *Int. J. Appl. Eng. Res.* **2018**, 13, 12237-12243.
- M.-A. Perea-Moreno, F. Manzano-Agugliaro, Q. Hernandez-Escobedo, A.-J. Perea-Moreno. Peanut shell for energy: properties and its potential to respect the environment. *Sustainability* **2018**, 10, 3254. <a href="https://doi.org/10.3390/su10093254">https://doi.org/10.3390/su10093254</a>
- Y. A. Negash, D. E. Amare, B. D. Bitew, H. Dagne. Assessment of quality of edible vegetable oils accessed in Gondar City, Northwest Ethiopia. *BMC Research Notes* **2019**, 12, 793. <a href="https://doi.org/10.1186/s13104-019-4831-x">https://doi.org/10.1186/s13104-019-4831-x</a>
- O.-P. Lehtinen, R. W. N. Nugroho, T. Lehtimaa, S. Vierros, P. Hiekkataipale, J. Ruokolainen, M. Sammalkorpi, M. Österberg. Effect of temperature, water content and free fatty acid on reverse micelle formation of phospholipids in vegetable oil. *Colloids Surfaces B* **2017**, 160, 355-363. https://doi.org/10.1016/j.colsurfb.2017.09.050
- A. Wu, X. Li, J. Yang, C. Du, W. Shen, J. Yan. Upcycling waste lard oil into vertical graphene sheets by inductively coupled plasma assisted chemical vapor deposition. *Nanomaterials* **2017**, 7, 318. <a href="https://doi.org/10.3390/nano7100318">https://doi.org/10.3390/nano7100318</a>
- T. Purkait, G. Singh, M. Singh, D. Kumar, R. S. Dey. Large area few-layer graphene with scalable preparation from waste biomass for high-performance supercapacitor. *Sci. Rep.* **2017**, 7, 15239. <a href="https://doi.org/10.1038/s41598-017-15463-w">https://doi.org/10.1038/s41598-017-15463-w</a>
- M. Tabarsa, B. ZareNezhad. An eco-friendly air—water plasma surface treatment technique for improving the stability of graphene oxide nanosheets in aqueous solutions. *Mater. Today Commun.* 2021, 26, 101940. <a href="https://doi.org/10.1016/j.mtcomm.2020.101940">https://doi.org/10.1016/j.mtcomm.2020.101940</a>
- A. Alsaeedi, Y. Show. Synthesis of nano-carbon by in-liquid plasma method and its application to a support material of Pt catalyst for fuel cell. *Nanomater. Nanotechnol.* **2019**, 9, 1–6. <a href="https://doi.org/10.1177/1847980419853159">https://doi.org/10.1177/1847980419853159</a>
- S. Han, D. Mao, H. Wang, H. Guo. An insightful analysis of dimethyl phthalate degradation by the collaborative process of DBD plasma and Graphene-WO<sub>3</sub> nanocomposites. *Chemosphere* **2022**, 291, 132774. <a href="https://doi.org/10.1016/j.chemosphere.2021.132774">https://doi.org/10.1016/j.chemosphere.2021.132774</a>
- <sup>227</sup> B. E. Stein, O. Auciello, M. J. Arellano-Jimenez, B. R. Perez. Fungal Mycelium Conversion into Ultrananocrystalline Diamond via Microwave Plasma Pyrolysis. *ACS Sustain. Chem. Eng.* **2022**, 10, 3211–3218 <a href="https://doi.org/10.1021/acssuschemeng.1c07253">https://doi.org/10.1021/acssuschemeng.1c07253</a>
- J. Poore, T. Nemecek. Reducing food's environmental impacts through producers and consumers. *Science* **2018**, 360, 987-992. https://doi.org/10.1126/science.aaq0216
- J. Aschemann-Witzel. Waste not, want not, emit less. Science 2016, 352, 408-409. https://doi.org/10.1126/science.aaf2978
- <sup>230</sup> FAO, Food Wastage Footprint, Impacts on Natural Resources Technical Report **2013**. <a href="http://www.fao.org/3/i3347e/i3347e.pdf">http://www.fao.org/3/i3347e/i3347e.pdf</a>
- <sup>231</sup> D. K. Nandakumar, Y. Zhang, S. K. Ravi, N. Guo, C. Zhang, S. C. Tan, Solar energy triggered clean water harvesting from humid air existing above sea surface enabled by a hydrogel with ultrahigh hygroscopicity. *Adv. Mater.* **2019**, 31, 1806730. https://doi.org/10.1002/adma.201806730
- <sup>232</sup> S. K. Ravi, D. J. K. Swainsbury, V. K. Singh, Y. K. Ngeow, M. R. Jones, S. C. Tan. A mechanoresponsive phase-changing electrolyte enables fabrication of high-output solid-state photobioelectrochemical devices from pigment-protein multilayers. *Adv. Mater.* **2018**, 30, 1704073. https://doi.org/10.1002/adma.201704073
- R. Teimuri-Mofrad, R. Hadi, H. Abbasi. Synthesis and characterization of ferrocene-functionalized reduced graphene oxide nanocomposite as a supercapacitor electrode material. *J. Organometall. Chem.* **2019**, 880, 355-362. <a href="https://doi.org/10.1016/j.jorganchem.2018.11.033">https://doi.org/10.1016/j.jorganchem.2018.11.033</a>
- <sup>234</sup> W. Qian, T. Song, M. Ye, H. Zhang, C. Feng, G. Lu, X. Huang. Graphene oxide/ferrocene-containing polymer/gold nanoparticle triple nanocomposite. *Nanomaterials* **2019**, 9, 310. <a href="https://doi.org/10.3390/nano9020310">https://doi.org/10.3390/nano9020310</a>
- <sup>235</sup> S. Kumar, I. Levchenko, K. Ostrikov, J. A. McLaughlin. Plasma-enabled, catalyst-free growth of carbon nanotubes on mechanically-written Si features with arbitrary shape. *Carbon* **2012**, 50, 325-329. <a href="https://doi.org/10.1016/j.carbon.2011.07.060">https://doi.org/10.1016/j.carbon.2011.07.060</a>
- K. Yi, Z. Jin, S. Bu, D. Wang, D. Liu, Y. Huang, Y. Dong, Q. Yuan, Y. Liu, A. T. S. Wee, D. Wei. Catalyst-Free Growth of Two-Dimensional BCxN Materials on Dielectrics by Temperature-Dependent Plasma-Enhanced Chemical Vapor Deposition. ACS Appl. Mater. Interfaces 2020, 12, 33113–33120. https://doi.org/10.1021/acsami.0c08555
- A. Y. Pak, K. B. Larionov, E. N. Kolobova, K. V. Slyusarskiy, J. Bolatova, S. A. Yankovsky, V. O. Stoyanovskii, Yu. Z Vassilyeva, V. E. Gubin. A novel approach of waste tires rubber utilization via ambient air direct current arc discharge plasma. *Fuel Proc. Technol.* 2022, 227, 107111. https://doi.org/10.1016/j.fuproc.2021.107111
- R. Ikram, B. M. Jan, W. Ahmad. Advances in synthesis of graphene derivatives using industrial wastes precursors; prospects and challenges. *J. Mater. Res. Technol.* **2020**, 9, 15924-15951. https://doi.org/10.1016/j.jmrt.2020.11.043

<sup>&</sup>lt;sup>239</sup> Z. Wang, J. Yu, X. Zhang, N. Li, B. Liu, Y. Li, Y. Wang, W. Wang, Y. Li, L. Zhang, S. Dissanayake, S. L. Suib, L. Sun. Large-scale and controllable synthesis of graphene quantum dots from rice husk biomass: A comprehensive utilization strategy. *ACS Appl. Mater. Interfaces* **2016**, 8, 1434–1439. https://doi.org/10.1021/acsami.5b10660

P. A. Deyris, P. Adler, E. Petit, Y. M. Legrand, C. Grison. Woody species: A new bio-based material for dual Ca/Mg catalys is with remarkable Lewis acidity properties. *Green Chem.* **2019**, 21, 3133-3142. <a href="https://doi.org/10.1039/C9GC00770A">https://doi.org/10.1039/C9GC00770A</a>

<sup>&</sup>lt;sup>241</sup> C. Grison, Y. T. Ki. Ecocatalysis, a new vision of green and sustainable chemistry. *Curr. Opin. Green Sust. Chem.* **2021**, 29, 100461. <a href="https://doi.org/10.1016/j.cogsc.2021.100461">https://doi.org/10.1016/j.cogsc.2021.100461</a>